

**NOVEL PRECLINICAL TARGETS AND THERAPIES
FOR TREATMENT OF OSTEOARTHRITIS**

by

Padma Pradeepa Srinivasan

A dissertation submitted to the Faculty of the University of Delaware in partial fulfillment of the requirements for the degree of Doctor of Philosophy in
Biological Sciences

Fall 2014

© 2014 Padma Pradeepa Srinivasan
All Rights Reserved

UMI Number: 3685142

All rights reserved

INFORMATION TO ALL USERS

The quality of this reproduction is dependent upon the quality of the copy submitted.

In the unlikely event that the author did not send a complete manuscript and there are missing pages, these will be noted. Also, if material had to be removed, a note will indicate the deletion.



UMI 3685142

Published by ProQuest LLC (2015). Copyright in the Dissertation held by the Author.

Microform Edition © ProQuest LLC.

All rights reserved. This work is protected against unauthorized copying under Title 17, United States Code



ProQuest LLC.
789 East Eisenhower Parkway
P.O. Box 1346
Ann Arbor, MI 48106 - 1346

**NOVEL PRECLINICAL TARGETS AND THERAPIES
FOR TREATMENT OF OSTEOARTHRITIS**

by

Padma Pradeepa Srinivasan

Approved: _____
Robin W. Morgan, Ph.D.
Chair of the Department of Biological Sciences

Approved: _____
George H. Watson, Ph.D.
Dean of the College of Arts and Sciences

Approved: _____
James G. Richards, Ph.D.
Vice Provost for Graduate and Professional Education

I certify that I have read this dissertation and that in my opinion it meets the academic and professional standard required by the University as a dissertation for the degree of Doctor of Philosophy.

Signed:

Catherine Kirn Safran, Ph.D.
Professor in charge of dissertation

I certify that I have read this dissertation and that in my opinion it meets the academic and professional standard required by the University as a dissertation for the degree of Doctor of Philosophy.

Signed:

Randall L. Duncan, Ph.D.
Member of dissertation committee

I certify that I have read this dissertation and that in my opinion it meets the academic and professional standard required by the University as a dissertation for the degree of Doctor of Philosophy.

Signed:

Kenneth L. van Golen, Ph.D.
Member of dissertation committee

I certify that I have read this dissertation and that in my opinion it meets the academic and professional standard required by the University as a dissertation for the degree of Doctor of Philosophy.

Signed:

Gary H. Laverty, Ph.D.
Member of dissertation committee

I certify that I have read this dissertation and that in my opinion it meets the academic and professional standard required by the University as a dissertation for the degree of Doctor of Philosophy.

Signed:

Liyun Wang, Ph.D.
Member of dissertation committee

ACKNOWLEDGMENTS

I would like to start by thanking my advisor Dr. Catherine Kirn-Safran, who has been such an amazing person, guide, and employer. Over the years, you have transformed me into an independent and skilled scientist. Thank you for your support, endless optimism and a great balance throughout this journey. I hope to inherit all that I have learnt from you and I promise that I will make you proud for mentoring me as your first doctoral student.

Dr. Randy Duncan, thank you for being my committee head and making me visualize the big picture in research and life. Words cannot express the respect and admiration I have for you. I am indebted to the confidence and knowledge I gained through the years right from your physiology course, which I would take again just for the adrenaline rush and the mental stimulation of the take-home exams.

Dr. Liyun Wang, thank you for installing the mechanical aspect in me and for all the collaborative help you have rendered from the beginning. You have been a great friend and I am always inspired by your energy and compassion. Dr. Ken van Golen, I love your everlasting enthusiasm and passion for research. The research rotation in your lab was an amazing tour in research and I appreciate your thoughtfulness for rendering me authorship for my contribution during the time. Dr. Gary Laverty, I am very grateful to you for all your logical big picture questions in my prelim and committee meetings. I hope to acquire your composed nature and critical thinking.

Dr. Melinda Duncan, I would not be here if not for the opportunity and the trust you had in me. You were always there for me during the confusing stages and you have helped me make the right decision every single time. All that you have done means a lot to me and I am very proud to be your birthday twin.

I would also like to thank Dr. Anja Nohe, Dr. Erica Selva, Dr. Diane Herson, Dr. Christopher Price, Dr. Robert Sikes, Dr. Jia Song, Dr. Salil Lachke, Dr. Xinqiao Jia, Dr. Kirk Czymmek, Dr. Jeffery Caplan and Dr. John McDonald for their support and advises during the journey. Thanks to the OLAM staffs and amazing departmental office staffs especially Betty Cowgill, Tina Fontana and Doreen Anderson for their timely assistances. I cherish all the moments spent with my friends and fellow lab mates in UD especially Sarah, Dylan, Nadia, Billy, Hemanth, Vimal, Ashu, Mary, Ben, Jonathan, Xiaohan, Kerry, Jay, Casey, Katie, Amanda, Lauren, Sona, Aasma, Pratima, Amal, Archana, Mallika, Vishnu, Surabhi, Rachel, Sona, Aasma, Pratima for all the support, fun and cherishing moments.

Not visiting parents, family and friends in India for six years was the difficult part but thanks to all of you and the Biology department for making me feel at home. Dad and Mom and Sathya, you all knew from the beginning that I am capable of achieving this – I thank you for your eternal love and constant support. I am reserving the last for the best- my husband, I would not have come this far without you. All this pride and appreciation belongs to you and I feel very lucky to have a mom, dad and a best friend in you. I am dedicating this work to my four month-old miracle, Arya. Thank you for all the happiness you have brought into my life and your great cooperation while I finished up this writing.

TABLE OF CONTENTS

LIST OF FIGURES	x
ABSTRACT	xviii

Chapter

1	GENERAL INTRODUCTION	1
1.1	Articular Cartilage and the Associated Structures.....	1
1.2	Development of Cartilage.....	8
1.3	Mechanical Aspect of Bone and Cartilage Loading.....	10
1.4	Osteoarthritis	13
1.5	Pathogenesis of OA	15
1.6	Current Interventions for OA	20
2	INJECTABLE PERELCAN DOMAIN 1-HYALURONAN MICROGELS POTENTIATE THE CARTILAGE REPAIR EFFECT OF BMP2 ON MURINE MODEL OF EARLY OSTEOARTHRITIS	23
2.1	Abstract.....	23
2.2	Introduction	25
2.3	Methods	29
2.3.1	Preparation of PlnD1-HA Microgels.....	29
2.3.2	Intra-articular Injections	32
2.3.3	Histological Scoring	33
2.3.4	Immunohistochemistry	33
2.3.5	Quantitative Real-Time PCR.....	34
2.3.6	Statistical Analysis	35
2.4	Results	37
2.4.1	Effect of BMP2-loaded PlnD1-HA Microgels on Damaged Articular Cartilage in Mice.....	37
2.4.2	Effect of PlnD1-HA/BMP2 Microgels on Articular Cartilage Transcript Levels.....	43
2.4.2.1	Cartilage Synthesis Markers.....	43
2.4.2.2	Cartilage degradative enzymes and marker of hypertrophy.....	45
2.4.3	Comparative Analysis of ECM Protein Distribution in PlnD1- HA/BMP2 treated Knees	45

2.4.3.1	Type II collagen Immunoreactivity	45
2.4.3.2	Aggrecan Immunoreactivity	49
2.4.4	PlnD1-HA Microgels Prolong BMP2 Cartilage Repair Activity <i>in vivo</i>	51
2.5	Discussion.....	53
3	INHIBITION OF T-TYPE VOLTAGE SENSITIVE CALCIUM CHANNEL REDUCES LOAD-INDUCED OA IN MICE AND SUPPRESSES THE CATABOLIC EFFECT OF BONE MEHCANICAL STRESS ON CHONDROCYTES.....	59
3.1	Abstract.....	59
3.2	Introduction	61
3.3	Methods	64
3.3.1	<i>In vivo</i> Load Induced Mouse Model of OA.....	64
3.3.2	Histological Analysis of the Knee Joints.....	68
3.3.3	Cell Culture	68
3.3.4	Fluid Shear Stress (FSS) Conditions	70
3.3.5	Quantitative RT-PCR	70
3.3.6	Immunohistochemistry	71
3.3.7	Western Blotting.....	72
3.3.8	Statistical Analysis	73
3.4	Results	74
3.4.1	Cav3.2 T-VSCC KO Mice Display Reduced Cartilage Damage Relative to WT Controls Following Repetitive Knee Loading ...	74
3.4.2	T-VSCC is Required for the Anabolic Response of Osteoblasts to FSS	78
3.4.3	T-VSCC Inhibition Reverses the Chondrocyte Hypertrophy Induced by the Conditioned Media (CM) from FSS Osteoblasts.....	82
3.5	Discussion.....	87
4	INVESTIGATING THE THERAPEUTIC POTENTIAL OF INHIBITING LEPTIN FOR OSTEOARTHRITIS.....	95
4.1	Abstract.....	95
4.2	Introduction	97
4.3	Methods	100

4.3.1	Cell Culture	100
4.3.2	Fluid Shear Stress (FSS).....	101
4.3.3	ELISA.....	101
4.3.4	Destabilization of Medial Meniscus (DMM) - Surgical Model of OA.....	102
4.3.5	Anti-leptin Intra-articular Injections.....	104
4.3.6	Histological Staining and Scoring	104
4.3.7	Statistical Analysis	105
4.4	Results	106
4.4.1	Leptin has a Pro-inflammatory Effect on Chondrocytes.....	106
4.4.2	Characterization of the Primary Osteoblasts Response to FSS .	109
4.4.3	Conditioned Media (CM) from Mechanically Stimulated Primary Osteoblasts Induces the Expression of Markers of Hypertrophy by Primary Chondrocytes.....	111
4.4.4	Mechanically Stimulated Primary Osteoblasts Secrete Leptin .	113
4.4.5	Effect of Intra-articular Injections of Leptin Inhibitor Following Mouse Model of Post-traumatic OA.....	115
4.5	Discussion.....	117
5	GENERAL DISCUSSION.....	123
5.1	Growth Factor Therapy with BMP2 for OA	126
5.2	Targeting Subchondral Bone <i>via</i> T-VSCC Inhibition for OA.....	128
5.3	Discovery of Novel Targets and Biomarkers for OA: Subchondral Bone Derived Cytokines	131
5.4	The Potential Use of Leptin Inhibitor as a Therapeutic for OA	133
5.5	Studying the Association of T-VSCC Signaling and Leptin Secretion.	135
5.6	Final Conclusions	136
	REFERENCES	138
	Appendix	151
	PERMISSIONS	151

LIST OF FIGURES

- Figure 1.1: Composition of cartilage components. Water accounts for the major space. Other components include the chondrocytes, proteoglycans, collagens and minor non collagenous proteins. Adapted from [1]..... 6
- Figure 1.2: Schematic diagram of the cartilage ECM showing the chondrocytes along with the ECM components like the proteoglycan (predominantly aggrecan), collagen type II, collagen IX and other non collagenous components. Adapted from [11]..... 7
- Figure 1.3: Schematic diagram contrasting the normal joint structures and the changes in OA like the cartilage degeneration, subchondral sclerosis and synovial inflammation. Adapted from [1] 19
- Figure 2.1: Injectable PlnD1-HA microgels visualized following hydration in saline buffer. Scale bar represents 20 μm 31
- Figure 2.2: Histological sections of mouse knees processed 7 days post repair or control treatments and stained with Safranin-O and Fast Green. Knees treated with PlnD1-HA/BMP2 showed a normal smooth articular cartilage appearance (B) and showed no OA damage when compared with papain-damaged knees treated with either saline (C), PlnD1-HA (D), HA (E), or BMP2 (F). Proteoglycan depletion indicated by a loss of Safranin-O staining is marked by asterisks. An increase in chondrocyte clusters was observed in the proteoglycan-depleted region of articular cartilage of PlnD1-HA-treated knees (see arrows in D). Such clusters are absent in BMP-2 treated knees where articular cartilage fissures and delamination is observed (see arrowheads in F). No obvious difference is seen between control knees (A) injected twice with saline (in place of papain and the repair treatment) and the papain-injected knees treated with PlnD1-HA/BMP2 microgels (B). T, tibia; F, femur; m, meniscus 40
- Figure 2.3: Box and whisker plot showing the median (central line), 25-75 percentile (boxes) and the entire range of scores obtained 7 days after treatment of saline or papain-damaged knees (n=5 for control saline; n=9 for all the other groups). ** indicates $p < 0.001$ when compared to PlnD1-HA/BMP2. No statistical difference is seen between the scores obtained in control knees injected with saline twice and the papain-injected knees treated with BMP2-loaded PlnD1-HA particles ($p=0.824$) 41

Figure 2.4: Box and whisker plot showing the median, 25 to 75 percentile and the entire range of scores among the saline and papain treated knees (A, n=7 for each group). No box is seen for the papain injection condition because over 80% of the articular surfaces correspond to a score of 0.5. ** indicates $p < 0.001$ ($p = 1.25 \times 10^{-8}$ in saline vs. papain). Representative histological sections of day 0 mouse knees processed 7 days after initial saline (B) or papain (C) intra-articular injections and prior to treatment via a second intra-articular injection. T, tibia; F, femur; m, meniscus 42

Figure 2.5: Effect of the combined administration of BMP2 and PlnD1-HA particles on mRNA levels of articular cartilage ECM components and ECM-modifying enzymes. Fold changes in mRNA levels are shown for knees treated with BMP2-loaded PlnD1-HA particles relative to knees treated with growth factor free particles (PlnD1-HA) on days 1 and 7 following intra-articular injections. mRNA levels of the $\alpha 1$ chain of type II collagen (COL2a1), aggrecan (ACAN), perlecan (HSPG2) and xylosyltransferase 1 (XYLT1) were significantly increased in knees treated with PlnD1-HA/BMP2 compared with control knees whereas the opposite was seen with matrix degrading enzymes (MMP13, MMP3, and ADAMTS5) and the $\alpha 1$ chain of type X collagen (COL10a1). Each sample was run in triplicate, the represented mean fold changes are the results of two biological replicates, and error bars represent standard deviations. Fold changes equal or higher to 2 (above the dashed line in A) and equal or lower to 0.5 (below the dashed line in B) are considered statistically significant using the comparative delta-delta Ct method 44

Figure 2.6: The extent of the type II collagen signal (green) is diminished in the articular cartilage of saline (D) versus PlnD1-HA/BMP2 (C) -treated knees after 7 days of treatment. For each group, consecutive coronal knee sections were stained with Safranin O/Fast Green (A, B) and immunostained with an antibody specifically directed against type II collagen (green in C, D). A and B are the adjacent histological stains for C and D, respectively. DRAQ5™ was used as nuclear stain (blue in C, D). Growth plate (GP) cartilage served as an internal positive control for type II collagen immunodetection. Asterisks indicate the presence of a healthy articular cartilage of high cellularity in the superficial layer of PlnD1-HA/BMP2-treated knees. F, Femur; T, Tibia; m, meniscus. Scale bars represent 100 μ m 48

Figure 2.7: Articular cartilage of knees treated with PlnD1-HA/BMP2 showed increased expression of aggrecan relative to control (PlnD1-HA or saline) knees after 7 days of treatment. For each group, consecutive coronal knee sections were stained with Safranin O/Fast Green (A-C) and immunolabeled with an antibody specifically directed against aggrecan (D-F). The aggrecan-specific immune signal (green) was noticeably increased in knees treated with PlnD1-HA/BMP2 (D and G) when compared with control knees treated with PlnD1-HA (E and H) or saline (F and I). A, B, C are the adjacent histological stains for D, E and F, respectively. DRAQ5™ was used as nuclear stain (blue in D-F). Growth plate (GP) cartilage served as an internal positive control for aggrecan immunodetection in osteoarthritic knees that displayed severe depletion of proteoglycans at their articular cartilage surface (see arrows in panel D-F). Scale bars represent 100µm for either A-F or G-I. F, Femur; T, Tibia, m, meniscus..... 50

Figure 2.8: Box and whisker plot showing the median (central line), 25 to 75 percentile (boxes) and the entire range of scores obtained 14 days after treatment of papain-damaged knees (A, n=9 for each group). ** indicates $p < 0.001$ when compared to PlnD1-HA/BMP2. Representative histological sections from papain-damaged mouse knees processed 7 days post repair (B, PlnD1-HA/BMP2) or control (C, PlnD1-HA; D, saline) treatments and stained with Safranin-O and Fast Green. Proteoglycan depletion in the superficial articular cartilage layer is marked by an asterisk. Femur; T, Tibia, m, meniscus .. 52

Figure 3.1: In-vivo loading system used to experimentally induce knee OA and compare progression of disease severity between T-VSCC and WT control knees. (A) Radiograph of mouse knee joint during loading using the Bose ElectroForce loading apparatus, (B) loading cycle waveform including durations for each phase of the cycle, (C) loading regimen: Five loading episodes were performed over a period of eight days followed by a 26-day period of non loading prior to sacrifice (week 5) and histological processing 67

Figure 3.2: Decrease of OA damage in the loaded right T-VSCC KO vs. WT controls following in vivo knee loading. A: boxes and whiskers graph showing the median (central line), 25-75 % (box) and the entire range (whiskers) of histological OA scores obtained three weeks after final loading in the four compartments (MT-Medial Tibia, MF- Medial Femur, LT-Lateral Tibia, LF- Lateral Femur) of loaded wild type control and T-VSCC KO mouse knees. B and C are coronal knee sections stained with Safranin O and Fast green from either a WT or a T-VSCC KO loaded knee, respectively. Arrow in B indicates a focal lesion caused by loading in the lateral knee compartment of a WT mouse knee. * = $p<0.05$, ** = $p<0.01$ and *** = $p<0.005$; n=10 for wild type and n=7 for T-VSCC KO mice..... 76

Figure 3.3: OA scores in unloaded knees of T-VSCC KO vs. WT controls following in vivo knee loading. Box and whiskers graph showing the median (central line), 25-75 % (box) and the entire range (whiskers) of histological OA scores obtained three weeks after final loading in the four compartments (MT-Medial Tibia, MF- Medial Femur, LT- Lateral Tibia, LF- Lateral Femur) of left unloaded wild type control and T-VSCC KO mouse knees. * $p<0.05$; n=10 for wild type and n=7 for T-VSCC KO mice..... 77

Figure 3.4: The fluid shear stress (FSS)-induced expression of the early shear response marker cyclooxygenase 2 is inhibited in MC3T3-E1 cells with the addition of T-VSCC-specific inhibitor, NNC55-0396. A: quantitative PCR analysis shows that the marked increase in Cox2 (Ptgs2) mRNAs observed two hours following FSS relative to the static untreated (Static UT) control condition is significantly inhibited in the presence of NNC55-0396. The conditions are FSS untreated (FSS UT), FSS treated with NNC55-0396 (FSS NNC), static treated with NNC55-0396 (static NNC). Error bars represent standard error of mean of the biological duplicates and * indicates $p<0.05$ between FSS UT and FSS NNC, ** = $p<0.01$ between FSS UT and static NNC. B: western blot analysis performed under the same conditions described in A indicates that the FSS-induced increase of COX2 protein is decreased to control levels in the presence of NNC55-0396. Vinculin was used as a loading control 80

Figure 3.5: The fluid shear stress (FSS)-induced expression of the late shear response gene osteopontin is inhibited in the presence of the T-VSCC-specific inhibitor, NNC55-0396, in MC3T3-E1 cells. Quantitative PCR analysis shows that the increase in osteopontin (Spp1) mRNAs observed 20 hours following FSS relative to the static untreated (Static UT) control condition is significantly inhibited in the presence of NNC55-0396. The conditions are FSS untreated (FSS UT), FSS treated with NNC 55-0396 (FSS NNC), static treated with NNC 55-0396 (static NNC). Error bars represent standard error of mean of the biological duplicates and *** = $p < 0.005$ between FSS UT and FSS NNC or FSS UT and static NNC..... 81

Figure 3.6: The early OA-like phenotype of chondrocytes treated with sheared osteoblast conditioned media is attenuated when treated with conditioned media derived from osteoblast sheared in the presence of the T-VSCC inhibitor, NNC55-0396. A: quantitative PCR showing the relative fold changes in mRNA levels of collagen X (Col10a1), alkaline phosphatase (Alpl), Matrix Metalloproteinase 13 (Mmp13), aggrecan (Acan), and collagen II (Col2a1) in primary mouse chondrocytes following seven days of treatment with conditioned media (CM) collected from MC3T3-E1 cells subjected to FSS alone (FSS UT), FSS with NNC55-0396 (FSS NNC) or static with NNC55-0396 (Static NNC) when compared with untreated control chondrocytes maintained under static conditions (Static UT). Error bars represent standard error of mean of the biological duplicates and * = $p < 0.05$, ** = $p < 0.01$ 84

Figure 3.7: Real time PCR analysis showing the relative fold changes in the mRNA levels of cartilage genes in primary mouse chondrocytes following FSS and NNC55-0396 treatment. Primary mouse chondrocytes were grown in monolayer and collected 20 hours after FSS alone (FSS UT), FSS with NNC55-0396 (FSS NNC) or maintained under static conditions with NNC55-0396 (Static NNC) compared with the untreated static control condition (Static UT). Cyclooxygenase 2 (ptgs2), collagen X (Col10a1), matrix metalloproteinase 13 (Mmp13), aggrecan (Acan), collagen II (Col2a1), and alkaline phosphatase (Alpl) The error bars represent standard error of mean of the biological duplicates..... 85

- Figure 3.8: The early OA differentiation induced by FSS in primary chondrocytes is prevented in the presence of the T-VSCC inhibitor, NNC55-0396. Primary mouse chondrocytes grown in micromasses or as monolayers and stained with Alcian blue (A-B), Alizarin red (E-H) or collagen X antibody (I-L), respectively. Staining was performed following seven days of treatment with CM collected from MC3T3-E1 cells subjected to FSS alone (FSS UT), FSS with NNC55-0396 (FSS NNC), static with NNC55-0396 (static NNC) or control media obtained from MC3T3-E1 cells maintained under static conditions (Static UT). Whereas no significant difference is observed among the conditions with Alcian blue, the Alizarin red and collagen X stainings (green-collagen X, blue- Draq5 nuclear stain) showed an obvious increase in calcium deposits (F) and collagen X-specific signal (J) among chondrocytes treated with CM from FSS UT and compared with chondrocytes treated with CM from FSS NNC and both static conditions (Static UT and Static NNC)..... 86
- Figure 3.9: Quantitative PCR analysis showing the changes in Cyclooxygenase 2 (Ptgs2) mRNAs in WT and KO osteoblasts following FSS. The primary osteoblasts were either maintained static or were subjected to FSS for 2 hours and the relative mRNA levels were calculated relative to the static WT control condition. Error bars represent standard error of mean of the biological duplicates..... 93
- Figure 4.1: Experimental course of anti-leptin therapy: Intra-articular injection of either saline (n=5) or leptin inhibitor (n=4) was given three times at a weekly interval on day 1 of weeks 5, 6 and 7 after the DMM surgery. The mice were euthanized in the 8th week for OA analysis 103
- Figure 4.2: Real-time PCR analysis showing the relative fold changes in the mRNA levels of cartilage matrix degrading enzymes after leptin treatment. Primary mouse chondrocytes were collected after 24 hour of treatment with leptin at different doses (1, 10, 50 and 100 nM) and compared with the untreated control condition. Matrix metalloproteinase 13 (Mmp13), Adamts 5, collagen type X (Col10a1). The error bars represent standard error of mean of the biological replicates 107

- Figure 4.3: Alcian blue and alizarin red stainings of the primary chondrocytes grown as micromasses and monolayers respectively following leptin treatment. Leptin treatment (10nM) for 7 days induced a decrease in glycosaminoglycan (B) among the chondrocytes compared with untreated control cells (A). Alizarin red staining show that the leptin treatment increased the calcium deposits in the chondrocytes (D) compared to the untreated chondrocytes (C)..... 108
- Figure 4.4: Quantitative PCR analysis (A) and western blot (B) showing a marked increase in Cox2 (Ptgs2) mRNA among the primary osteoblasts 2 hours following FSS compared to the static control. There was no significant increase in the levels of the late response gene osteopontin (Spp1). Error bars represent standard error of mean of the biological duplicates. B: Western blot analysis indicates that FSS also induced an increase in COX2 at the protein level relative to static controls. Vinculin was used as a loading control 110
- Figure 4.5: Quantitative PCR analysis showing the fold changes in the mRNA levels of cartilage components in primary mouse chondrocytes following seven days of treatment with conditioned media (CM) collected from primary osteoblasts subjected to FSS compared with control chondrocytes treated with CM collected from static osteoblasts. Aggrecan (Acan), collagen type II (Col2a1), transcription factor Runx2, collagen type X (Col10a1) and metalloproteinase 13 (Mmp13). Error bars represent standard error of mean of the biological duplicates 112
- Figure 4.6: Leptin levels measured in the conditioned media (CM) of the primary mouse osteoblasts following FSS. CM from primary osteoblasts were collected 30 minutes following 2 hour FSS and the leptin levels were estimated using an ELISA approach. Leptin levels were normalized to the total protein levels in the CM quantified using BCA analysis. There was a 1.7 fold increase in leptin levels in the FSS CM compared to the static CM. The error bars represent the standard error of mean of the biological triplicates 114
- Figure 4.7: Boxes and whiskers graph showing the median (central line), 25-75 % (box) and the entire range (whiskers) of histological OA scores obtained in the control saline and leptin inhibitor treated mice. Statistical analysis between the groups showed no significant difference. p value is 0.233; n=5 for saline group and n=4 for leptin inhibitor group 116

Figure 5.1: Schematic summary of the dissertation chapters: Novel targets and therapeutics for OA: 1- Chapter 2- Sustained delivery of BMP2 using HA PlnD1 vehicle increases synthesis of matrix components and reduce the matrix degrading enzymes and the OA progression. 2- Chapter 3 - T-VSCC can be targeted to inhibit the early OA phenotype induced by the subchondral bone derived cytokines 125

ABSTRACT

Osteoarthritis (OA) is the most common chronic degenerative joint disorder characterized by loss of articular cartilage, fibrosis of the synovial lining, and osteophyte or new bone formation. In spite of being the principal cause of disability in the aging population, the pathology and molecular mechanisms underlying the disease etiology are not fully understood. Consequently, there are no successful pharmacological interventions which can reverse or prevent the degeneration of articular cartilage. Evidently, thorough understanding of the disease pathology at the cellular level is mandatory to develop disease-modifying drugs for OA. This dissertation is aimed at understanding the role of various biochemical factors involved in the pathogenesis of OA and targeting them to develop novel interventions. Towards achieving this goal, my first approach show that the controlled release of a heparan sulfate binding growth factor, Bone Morphogenetic Protein 2 (BMP2) using perlecan-modified biomaterials can induce anabolic changes in cartilage of mice with early OA. Such growth factor therapy needs to be initiated early in the disease process, as BMP2 becomes ineffective in the later stages of OA due to the secretion of BMP antagonists by the chondrocytes with degenerative phenotype. Nevertheless, the clinical manifestation and diagnosis of OA mostly occurs in the later stages when the patients develop pain which is associated with osteophyte formation and subchondral bone sclerosis. To this end, my next approach was to target the subchondral bone changes in OA.

Studies show that abnormal metabolic activity of subchondral bone in response to increased mechanical loading can lead to loss of articular cartilage integrity and

thinning. Recent work showed that mechanotransduction in bone is partially mediated through voltage sensitive calcium channel (VSCC) and mice deficient in $Ca_v3.2$ ($\alpha1H$), the pore forming subunit of T-VSCC have reduced response to mechanical loading and decreased bone remodeling properties. I used this $Ca_v3.2$ T-a VSCC knockout (KO) mouse to demonstrate that reduced mechanosensitivity in subchondral bone is beneficial in preventing load-induced OA. I demonstrate that mechanotransduction from osteoblasts *via* T-VSCC induces local metabolite secretion that stimulates osteoarthritic changes in chondrocytes and propose that targeting calcium channels in joints would slow/prevent progression of OA.

Irrespective of the chronological origin of cartilage and subchondral bone changes in OA, it is evident from several studies that soluble factors released from subchondral osteoblasts induce catabolic pathways in the adjacent cartilage. Here, I identify leptin as a catabolic factor expressed by the mechanically stimulated osteoblasts with a pro-inflammatory action on the chondrocytes. Subsequently, I explore the therapeutic potential of inhibiting osteoblast-derived leptin activity in a post-traumatic mouse model of OA.

Through this dissertation work I demonstrate novel potential targets and therapeutics that can be used at early and later stages of OA. With the increasing prevalence of OA, the application of these strategies can help improve the quality of life in OA patients and reduce the health care expenditure associated with knee replacement surgeries.

Chapter 1

GENERAL INTRODUCTION

1.1 Articular Cartilage and the Associated Structures

Articular cartilage is the connective tissue that surrounds the diarthroidal joint surfaces and is essential for the weight bearing capacity of the joint. Chondrocytes form the extracellular component of the hyaline articular cartilage matrix and unlike other tissues in the body with major physiological function; the cellular fraction comprised of chondrocytes represents only 3% of the articular cartilage tissue. Yet, chondrocytes are the only viable players in cartilage and perform the major anabolic function of synthesizing the extracellular matrix (ECM) around them. Water is the major component of cartilage ECM and accounts for about 70-80% of the total cartilage volume (Fig 1.1). The main organic components of the cartilage ECM are proteoglycans and collagens that provide the cartilage with its innate shock absorbing ability. The predominant fibrillar structure present in articular cartilage ECM is composed of collagen type II and aggrecan is the primary proteoglycan that draws water in the tissue. Collagen type II and aggrecan account for 12% and 9% of cartilage wet weight, respectively [1].

Collagen type II is classified as fibril-forming collagen and is composed of triple helical collagen fibrils rich in proline tripeptides. The triple helical structure and heavy crosslinking renders high stability to the collagen network. Collagen type II is characterized by hydroxylysine, glucosyl and galactosyl residues. Collagen type II

provides the tensile strength to the cartilage and limits the expansion of the aggrecan molecules thereby regulating the compressive stiffness of the tissue. Other minor fibrillar components are collagen type XI and type IX that function as regulators of fibril formation and crosslinking of the collagen network, respectively. The binding capacity and networking property of collagen helps in the delivery and retention of drugs and growth factors [1-3].

Aggrecan is composed of a central core protein with highly sulfated glycosaminoglycan side chains consisting of keratan and chondroitin sulfate. Each aggrecan unit is, in turn, attached to hyaluronic acid by link protein. The heavy negative charges of these aggrecan molecules trap water which gets expelled when joints are exposed to compressive forces but regains its original place once the forces are removed. Such expansion provides the elasticity to cartilage and is regulated by the collagen fibrillar network which provides the property of compressive stiffness [1]. Together, these properties are crucial for the shock absorption and dissipation of forces applied to the joint.

Other minor components include leucine-rich proteoglycans such as decorin, biglycan and fibromodulin. They play an essential role in regulating chondrocyte function and ECM organization. Perlecan is the main heparan sulfate proteoglycan that binds and modulate heparin-binding growth factors activity, thereby reducing their solubility and degradation by matrix-degrading enzymes. The other non-collagenous proteins that are not unique to cartilage are COMP (Cartilage oligomeric matrix protein), biglycan, matrilin I, anchorin II, thrombomodulin, chondroadherin, fibronectin and membrane proteins like syndecan, CD44 and integrins (Fig.1.2) [1].

Being avascular, aneural and alymphatic, cartilage has a very slow metabolic rate and the nutrition is mainly provided through simple diffusion from synovial fluid. The pore size of the ECM is about 6nm and the diffusion of the nutrients depends on its size, charge and molecular composition. The turnover rate of the ECM components in cartilage is low with longer half-lives. Proteoglycans like aggrecan have a turnover period of about 25 years and the half-life of collagen type II has been estimated to range several decades to 400 years [4-6].

Based on the ECM components and organization, articular cartilage has different zones: superficial, middle, deep and calcified. The superficial layer comprises 10 – 20% of the cartilage thickness and protects the deeper layers from the shear forces by being in contact with the synovial fluid. The collagen fibrils are arranged parallel to the articular surface and the chondrocytes are flat and relatively high in number. The middle or the transitional zone forms 40 – 60% of cartilage volume and bridges the superficial and deep layer. In this zone, the collagen fibrils are arranged obliquely and the chondrocytes are fewer in number and appear spherical in shape. The deep zone forms about 30 – 40% of cartilage with perpendicularly arranged collagen fibrils and highest proteoglycan content. This organization enables this zone to provide the greatest resistance to the compressive forces. The calcified zone can be distinguished from the deep zone by a tide mark and this zone anchors the deep zone to the subchondral bone. The chondrocytes in this zone are scarce and have a hypertrophic appearance [4].

The ECM of the articular cartilage is again classified into three regions based on its ECM composition and organization with respect to chondrocytes. The pericellular matrix surrounds the chondrocytes and contains proteoglycans,

glycoproteins and non-collagenous proteins. It forms a thin layer and is proposed to have a role in the signal transduction of chondrocytes. The territorial layer is the outermost layer and provides resistance to mechanical forces. This layer is thicker than the pericellular layer and contains fine collagen fibrils. The third inter-territorial layer is the thickest and lies between the other two layers. This layer has abundant proteoglycan and randomly arranged thick collagen fibrils. The biomechanical material properties of the cartilage is mostly dependent on this layer [4].

Articular cartilage functions in close association with other joint structures- subchondral bone, meniscus, synovial lining and joint capsule. Unlike the cartilage, the synovial lining and the subchondral bone are highly vascularized and innervated. The synovial membrane is composed of two layers of cells: the inner layer close to the joint space named intima and the outer layer, sub-intima that extends to form the joint capsule. Two type of cells form the synovial lining: type A macrophage-like cells and type B synovial cells. The macrophage-like cells aids in phagocytosis and inflammation. The type B cells secrete the synovial fluid rich in hyaluronic acid that is essential for the lubrication of the joints [7]

Subchondral bone is a term that collectively represents the calcified cartilage that lies below the tidemark, the cortical lamella and the underlying trabecular bone. It provides support to the adjacent articular cartilage that lies embedded onto the irregular subchondral bone surface. The steep difference in the stiffness between the various layers ranging from articular cartilage to trabecular bone helps provide a better transformation for the shear forces applied to the joint. Thus, the subchondral bone participates in the absorption of the mechanical stress and acts as a structural girder. The density and mineralization varies across the subchondral bone and greater

thickness is found in areas dealing with greater mechanical stimulation and shear forces. Such areas are also found to have increased vascularity [8].

Unlike cartilage, bone is a dynamic unit and the main fibrillar component of the calcified cartilage and cortical plate are collagen type X and collagen type I, respectively. Bone is constantly remodeled by the tight regulation between the osteoblasts/osteocytes, the bone cells responsible for bone formation and the osteoclasts, the bone resorbing cells. Osteoblasts and their terminally-differentiated osteocytes, are cells of mesenchymal origin and osteoclasts are derived from macrophage-monocyte lineage. Bone remodeling occurs in response to mechanical stimuli in four stages: activation, resorption, reversal and formation. Activation involves the recruitment of the osteoclast from circulation for the resorption of the bone ECM *via* acidification and release of proteases. After this step, the osteoclasts undergo apoptosis leaving an empty space where osteoblasts start forming a new mineralized bone matrix and this reversion from bone resorption to bone formation is termed as the reversal phase [9, 10].

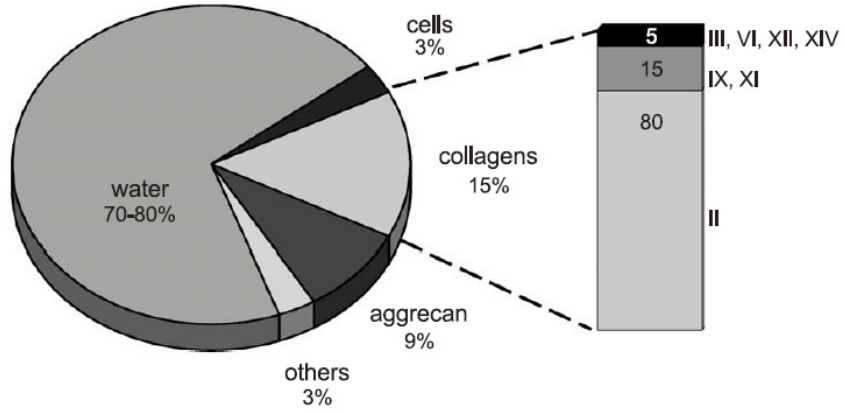


Figure 1.1: Composition of cartilage components. Water accounts for the major space. Other components include the chondrocytes, proteoglycans, collagens and minor non collagenous proteins. Adapted from [1]

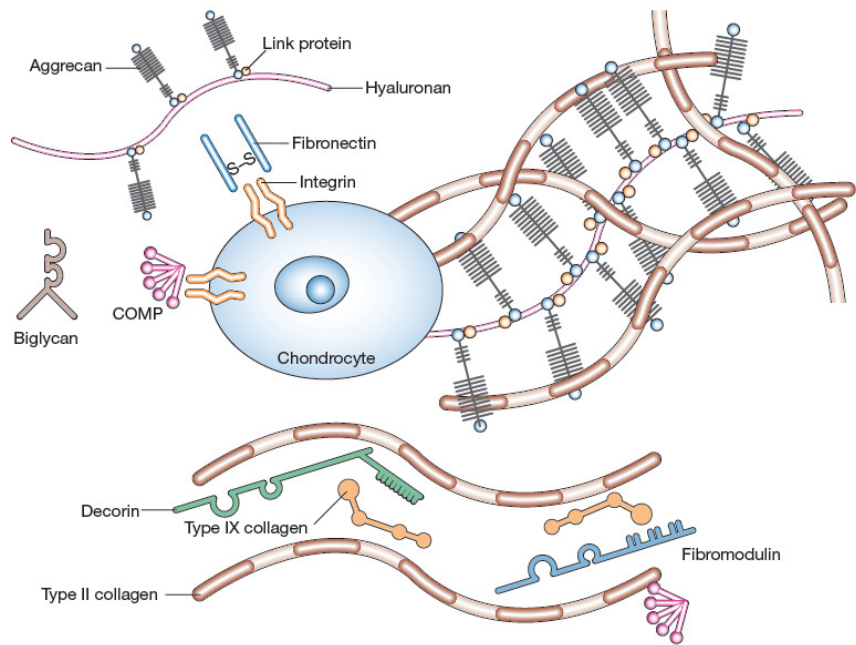


Figure 1.2: Schematic diagram of the cartilage ECM showing the chondrocytes along with the ECM components like the proteoglycan (predominantly aggrecan), collagen type II, collagen IX and other non collagenous components. Adapted from [11]

1.2 Development of Cartilage

The formation of the skeletal system also called skeletogenesis occurs in four primary phases: it begins with the migration of the mesenchymal stem cells to the site of origin; this is followed by the epithelial-mesenchymal interaction. The third step is the aggregation or the condensation of the mesenchymal cells [12]. The final phase is the differentiation into chondrocytes or osteoblasts. The process by which the cartilage is formed from the mesenchymal condensation is termed chondrogenesis. The chondrocytes differentiate from the chondroprogenitor cells of mesodermal origin and secrete the ECM containing collagen type II, XI and IX. Cartilage acts as the template for the development of long bones in the process called endochondral ossification. During this process, the chondrocytes differentiate and become hypertrophic. These chondrocytes are marked by a high expression of alkaline phosphatase and collagen type X. Eventually these chondrocytes undergo apoptosis before the mineralization and bone matrix deposition [13]. Such longitudinal bone growth occurs from the hypertrophic chondrocytes found in the bottom most layer of the epiphyseal growth plate. Above the hypertrophic layer is the proliferating layer, consisting of rapidly dividing chondrocytes arranged along the long axis of the bone. The top most layer of the growth plate consists of the slowly dividing resting cells that act as the local stem cells reserve [14].

The entire process of chondrogenesis and endochondral ossification requires an orchestration of several transcription and growth factors in addition to epigenetic factors. SOX9 is the most important transcription factor required for the chondrogenesis and specific synthesis of collagen type II from chondrocytes. Bone morphogenetic proteins (BMPs) are known to control the action of SOX9 and

chondrogenesis. Hypertrophic differentiation of the chondrocytes requires the action of transcription factor core binding factor 1, runx2 (also known as Cbfa-1). Runx2 belongs to runt domain transcription factor family and is required for the commitment to osteoblastic lineage. Runx2 activates the Indian hedgehog genes (Ihh) and secretion of collagen type X that is characteristic of prehypertrophic and hypertrophic chondrocytes, respectively. An inverse relation exists between the SOX9 and runx2 activity and SOX9 is known to down regulate runx2 expression. The terminally differentiated chondrocytes secrete vascular endothelial growth factor (VEGF) and MMPs to induce vascular invasion and degradation of the cartilage ECM respectively [13, 15].

The proliferating chondrocytes also express other growth factors like fibroblast growth factor (FGF), Wnts, TGF β , BMPs and insulin like growth factors are also known to play an essential role in the chondrogenesis. Fgf receptor 3 and 1 are known to be expressed by the proliferating mesenchymal cells and the hypertrophic chondrocytes respectively [16]. TGF β and BMPs along with runx2 control the Wnt/ β catenin pathway that is essential for the commitment of the mesenchymal cells to osteoblastic lineage and bone formation [13, 15]

1.3 Mechanical Aspect of Bone and Cartilage Loading

It is well established that bone is a dynamic tissue and mechanical stimulation is essential to maintain normal bone mass [17]. Obvious scenarios that illustrate the bone mechanosensitivity include the loss of bone mass in the microgravity and the gain of bone mass following exercise. According to Wolff's law, bone adapts its shape to accommodate the shear forces enforced on them [18].

The subchondral bone remodeling following mechanical loading is brought about by mechanotransduction, a process in which the mechanical signals transmitted from the cell surface to the nucleus are converted into biochemical and cellular events [19]. The strain and forces created during physical activity cause fluid flow along the bone cell bodies and the lacunocanalicular space which, in turns, produce fluid shear, stimulating osteoblasts and osteocytes to secrete various active metabolites like prostaglandins, nitric oxide (NO) and interleukins [20, 21]. These gene products and metabolites are established markers of the bone anabolic response to mechanical load and are capable of stimulating bone formation and inhibiting bone resorption. Identically, cytokines secreted by the subchondral osteoblasts following altered joint loading are known to initiate OA pathways in the adjacent cartilage tissue [22]. This complex mechanism of bone mechanotransduction and downstream actions require the function of various focal adhesions [23], G-protein coupled receptors [24] and ion channels (mechanosensitive and voltage-sensitive) [25, 26].

A rapid increase in calcium is the first response of bone cells subjected to fluid shear [27, 28] and voltage-sensitive calcium channels (VSCC) are major regulators of intracellular calcium concentration in bone cells. Fluid shear causes the opening of mechanosensitive calcium channels leading to a rapid calcium influx that alters the

membrane potential and acts as a stimulus to open the VSCC. This increase in intracellular calcium concentration is essential for activating the downstream signaling and secretion of anabolic markers of bone formation like prostaglandins and NO [29].

The mechanical load subjected to the joint during the day-to-day activities is a combination of strain, hydraulic pressure, fluid shear stress and electrochemical gradients. The strain levels on the bone could be roughly estimated to be 0.3% (3000 microstrain) and this is much lesser than that on the cartilage which experiences a strain of about 30% [30]. The application of compressive forces on bone obliterates bone resorption reducing the osteoclasts number and increases bone formation through the bone anabolic markers [30, 31]. The fluid shear forces on the bone cells could originate either from the fluid movement in the circulatory system or from the mechanical loading itself and the physiological amount of shear forces that the joint experiences could range between 0.8 to 3 Pa (1Pa= 10 dynes/cm²) [30, 32].

Similar to bone, cartilage also has been shown to respond to the mechanical stimulation using various animal models. Higher mechanical load cause degradation whereas regular loading is essential to maintain a healthy chondrocyte phenotype [33]. The cartilage is also subjected to various forms of mechanical forces including stresses, pressures and strains from normal day-to-day activities. Activities such as walking subjects 2-5 times the body weight at the hip joint. Such activity is estimated to induce 2-3 MPa of local forces. Climbing stairs can amount to 10-20 MPa of local stresses to the hip joint [34, 35].

The structural organization and chondrocyte response in cartilage are important to maintain and distribute the mechanical forces subjected to the joint. These components are compromised when there is abnormal loading on the joint resulting in

OA formation. For example, a shift occurs in the synthesis of collagen molecules from type II to type I. The resulting ECM has increased water content and is incapable of withstanding the compressive forces on them [35]. Increased shear forces following trauma is known to alter the chondrocyte metabolism eventually leading to matrix degradation.

Studies show a strong association between abnormal mechanical loading and OA development. Continuous exercise has demonstrated increase in proteoglycan content and thickness of cartilage, whereas complete loss of loading result in atrophy of cartilage with decrease in proteoglycan content. Also, strenuous exercise can have deleterious effect and cause cartilage degradation [36-40]. Even though abnormal shear forces on weight bearing joints can accelerate their degeneration and OA progression, increased contact stress at the cartilage interfaces is thought to play an important role in post-traumatic OA [41]. Studies following Anterior Cruciate Ligament Transaction (ACLT), a model of post-traumatic OA show that the alterations in the joint mechanics and increased articular contact stress on the joint can all contribute to the genesis of OA [42, 43].

1.4 Osteoarthritis

OA is a heterogeneous progressive disease of the synovial joints. It is the leading cause of chronic disorder among the older adults in the United States and also the most common form of arthritis [44]. The incidence of the disease increases with age and it has been projected that about 67 million people in the United States will acquire arthritis-related disability by 2030. This would include one-third of the working population, creating a greater burden in the lifestyle and health care costs [45]. According to the Framingham Cohort study (USA), 25% of adults in their 60s and 50% of adults over 80 years of age had radiographic changes of OA [46].

OA is a disease of multifactorial origin with various risk factors including older age, female gender, genetic inheritance, history of trauma and obesity. Age is the strongest risk factor for OA and OA affects 50% and 85% of the population over 65 years and 75 years of age, respectively [47]. Presentation, incidence and prevalence rates vary with gender. The most common form of OA presentation in men is hip OA and that in women are hand and knee OA. Other risk factors for the OA etiology include race, geographic factors, chondrocalcinosis, occupational knee bending, hormonal status, bone density, muscle weakness, metabolic factors and physical labor. OA of the knee is the most common presentation causing functional limitations in 13% and 17% of Americans aged 55 to 64 years and 65 to 74 years, respectively; and the two major risk factors for knee OA are obesity and trauma [46, 47].

OA can be classified as idiopathic or primary form when an actual cause is not known and secondary when there is a predisposing underlying cause for its genesis. Primary OA is the most common form of OA affecting 60% of men and 70% of women over 65 years of age due to “wear and tear” [47]. As the etio-pathology of

primary OA is not fully understood, there are no successful disease-modifying agents (DMA) to reverse disease progression leaving total joint replacement surgery as the only option to relief pain in advanced OA patients.

1.5 Pathogenesis of OA

OA is a chronic degenerative disease involving all the joint tissue characterized by gradual loss of the cartilage, subchondral bone sclerosis and synovial inflammation (Fig 1.3). The main initiating factor is the repeated mechanical injury as OA mainly involves the weight bearing joints. The initial stages of OA are marked by an increase in proliferation of chondrocytes (chondrons) to lay out new ECM including collagen type II fibrils and proteoglycans. This synthesis along with increased growth factors production by chondrocytes is an attempt to overcome the insult and initiate repair. However, with continued mechanical insult, this synthesis becomes inadequate and the degradation of ECM takes over leading to irreversible OA. Thus, OA develops when there is an imbalance between the synthesis and degradation of the cartilage matrix by the chondrocytes.

The matrix-degrading enzymes found in cartilage include a wide range of cytokines and matrix metalloproteinases (MMPs). In addition to chondrocytes, subchondral bone cells and synovial macrophages also act as sources of these catabolic enzymes in OA. Interleukin 1 β is the main pro-inflammatory cytokine in OA that is capable of inhibiting the *de novo* synthesis of ECM components and inducing the secretion of various other catabolic enzymes including various inducible nitric oxide synthase and phospholipase A2. TNF alpha, a hallmark of late OA is the other important cytokine capable of inducing cartilage degradation and acts in a similar way to and in synergism with interleukin 1 β . As a consequence, anti-cytokine therapies against interleukin 1 β and TNF alpha have been the focus for the development of OA therapeutics and have shown some success in animal models of OA [48].

The other matrix-degrading enzymes of cartilage ECM include aggrecanases or ADAMTS (A disintegrin and metalloproteinase with thrombospondin type 1 motif) and the MMP family. MMPs are further classified into stromelysins, gelatinases and collagenases. These proteases are secreted by chondrocytes and each of them degrades specific ECM components. For instance, the stromelysin MMP3 along with aggrecanases 1 and 2 (ADAMTS4 and 5) are specific against aggrecan. MMP13 is the major collagenase that is capable of degrading collagen type II and MMP2, 9 are gelatinases that further cleave the degraded collagen fibrils [7]. Other pro-inflammatory factors that are up-regulated in OA are interleukin 6, 8, 17, 18, nitric oxide and eicosanoids.

The earliest microscopic changes are characterized by roughening of the cartilage, followed by fibrillations and gradual loss of the cartilage thickness until exposure of the subchondral bone. At the molecular level, this is accompanied by the loss of aggrecan and loosening of the collagen network. This apparently results in the release of the water molecules bound by the aggrecan leading to hyperhydration causing the swelling and softening of the cartilage macroscopically. In addition, to the depletion and degradation of the existing ECM components, the expression of new molecules like collagen type X, tenascin, collagen type IIa and III characteristic of osteoarthritic cartilage takes place [1, 49].

The degraded breakdown products from cartilage ECM are released into the synovial fluid and are phagocytized by the synovial macrophages. These macrophages, in turn, release more cytokines like interleukin 1 β that are capable of activating other proteases to further degrade the cartilage. This process continues in a vicious cycle leading to further degradation of cartilage ECM. The resulting synovial

inflammation is accompanied by synovial hypertrophy and hyperplasia. Thus, synovial inflammation plays a vital role in the OA pathogenesis. Accompanied by increased innervation, synovial inflammation is considered to be a main cause of patient reported pain in OA. Also, the products from synovial inflammation are gaining recognition as biomarkers for OA and these include serum C-reactive protein, COMP, collagen type II breakdown propeptides, and hyaluronic acid [7].

Another important hallmark of OA is the formation of osteophytes, which is characteristic of later stages of the disease process. Osteophytes are the new bone spurs that are formed at the joint margins as an attempt to repair and compensate for the degenerating cartilage, the lost surface area, and the subsequent joint instability. The molecular mechanism underlying their formation is unknown but the increased biomechanical stimuli are considered to stimulate the mesenchymal cells in the synovium and periosteum to undergo secondary chondrogenesis under the influence of growth factors like TGF β and BMPs. Although mature osteophytes have structure and composition similar to the articular hyaline cartilage, their functional compensation is questionable because of their occurrence in non-weight bearing areas. However, understanding the molecular mechanisms leading to the formation of such intrinsic regenerative tissue seems important for development of repair strategies [1].

Subchondral bone acts as an integral part of joint mechanics and plays an active role in the pathogenesis of OA. Even though the presence of subchondral bone changes and osteophytes in OA is irrefutable; it is still debated as to whether the subchondral bone changes actually precede the cartilage changes. Human subject studies show an increasing association between increased bone mineral density and OA. Mechanical stress to the joint are thought to initiate bone changes leading to

abnormal bone remodeling causing sclerosis, bone marrow necrosis and trabecular abnormalities [7].

The process of bone remodeling starts with the subchondral bone resorption by osteoclasts that secrete matrix-degrading enzymes like cathepsin K and MMP13 (Matrix Metalloproteinase 13). This resorption is followed by new bone formation or sclerosis that is characterized by the increase of bone anabolic markers like osteocalcin and osteopontin and growth factors like IGF-1,-2 and TGF β 1. The newly formed bone is disorganized with variations in the shape and structure of the subchondral bone [9].

Thus, the later stages of OA are marked by sclerosis with increased mineral density and stiffness resulting in a remodeled bone that is less effective in dissipating the mechanical load applied to the joint. All this poses an additional mechanical trauma to the already challenged cartilage accelerating its degeneration. Microcracks form in the calcified layer of the articular cartilage extending to the trabecular bone and this allows communication between the cartilage, subchondral bone and the joint space. The synovial fluid seeping in through these microcracks lead to the formation of intra-osseous pseudocysts [8].

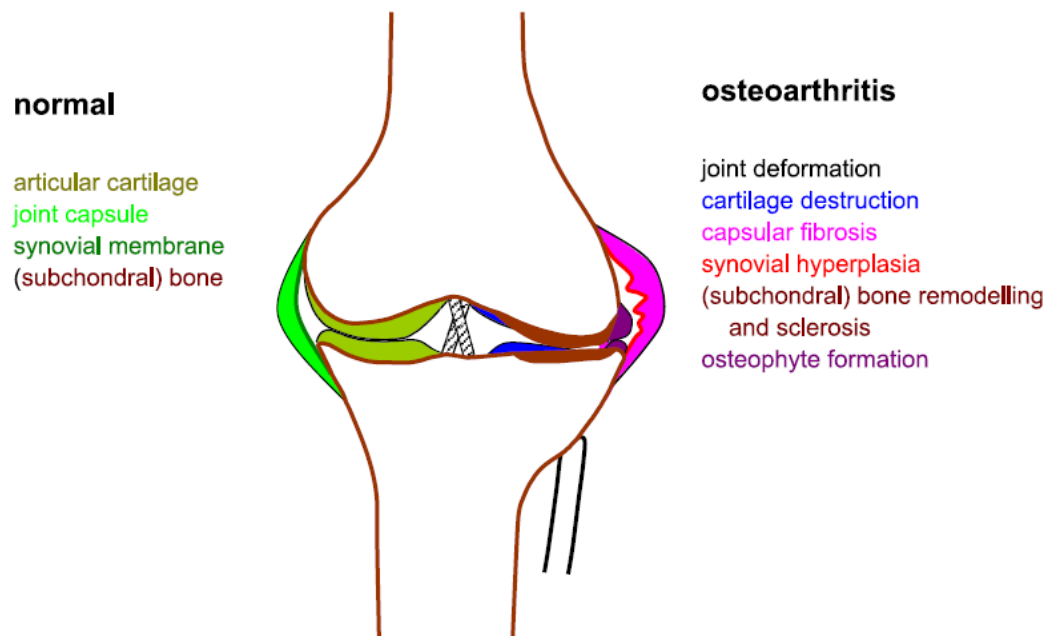


Figure 1.3: Schematic diagram contrasting the normal joint structures and the changes in OA like the cartilage degeneration, subchondral sclerosis and synovial inflammation. Adapted from [1]

1.6 Current Interventions for OA

The current treatment for OA is mainly aimed at reducing the patient's pain and increasing the mobility of the joints. Acetaminophen is the drug of choice for pain relief in mild to moderate OA pain but is less preferred due to its lower compliance and efficacy compared to NSAIDs. The major side effects caused by acetaminophen are hepato-renal toxicity. Non-steroidal Anti-inflammatory drugs (NSAIDs) are the most commonly prescribed pain killers for moderate to severe OA despite of its well established gastrointestinal side effects. These side-effects can range from dyspepsia, nausea, abdominal pain to bleeding and perforation of gastric mucosa. This demands caution with patients at risk of gastric ulcer and a co-administration of proton pump inhibitors. The non-selective NSAIDs inhibit cyclooxygenase 1 and 2 (COX1 and 2) that are required for the synthesis of eicosanoids especially prostaglandins. Selective COX2 inhibitors are available with no gastric side effects that are due to the COX1 inhibition; however these drugs pose a disadvantage of causing serious cardiovascular, hepatic and hemodynamic side effects. Nephrotoxicity can occur with both non-selective and selective COX2 inhibitors [47, 50].

Tramadol, a centrally acting weak opioid analgesic is considered when there is no improvement with acetaminophen and NSAIDs are contraindicated. Similarly other opioid therapy is given for severe pain not relieved with NSAIDs and tramadol. Topical application of capsaicin cream and NSAIDs are available for use as monotherapy or as an adjunct for hand and knee OA. Intra-articular injections of steroids are recommended for acute pain due to inflammation and joint effusion. Intra-articular hyaluronan is also widely used to relieve pain and it is thought to function by replacing the viscoelastic property of synovial fluid and lubricating the joint.

However, the need for repeated injections due to short-term relief is a disadvantage [47].

Other commonly used treatment modality is the recommendation of food supplements like glucosamine and chondroitin sulfate combinations that supposedly provide building units for cartilage repair. However, the actual outcome and efficacy of these nutraceuticals are questionable [50].

Agents like MMP inhibitors such as doxycycline and minocycline, bisphosphonates, calcitonin, diacerein, genetic therapy have reached new horizons in preclinical studies as disease modifying osteoarthritic drugs (DMOAD). Cytokine inhibitors and TNF alpha antagonists have also been studied in animal models of OA [51, 52]. Protein kinase pathways including the c-Jun N-terminal kinase, p-38 mitogen activated protein kinase (MAPK) and stress-activated protein kinase that are activated in chondrocytes are also potential novel therapeutic targets [47, 48].

The non-pharmacological physical measures for OA are achieved through exercise, weight reduction in case of obese patients, yoga, orthotic devices, thermal packs, quadriceps strengthening exercises and acupuncture. However, the importance of combining these physical measures in addition to pharmacological agents is largely overlooked. With majority of OA patients being overweight, weight reduction and exercises continue to be an essential strategy for a successful management particularly for knee and hip OA [50, 51]. Weight reduction alone has been proposed to reduce 25-48% of knee OA in women over 50 years of age [53].

Surgical and invasive approaches are considered when there is no adequate improvement of pain relief and quality of life with pharmacological interventions alone or in combination with physical measures. The various available surgical

options range from arthroscopic irrigation, osteotomy and arthroplasty. Arthroscopic irrigation or lavage is considered with patients having meniscal injuries and loose bodies. Osteotomy is preferred over arthroplasty in order to preserve the joint structure in case of young adults with unilateral involvement and symptomatic hip dysplasias. Joint replacement or arthroplasty for the knee and hip OA are reserved when other approaches fail to provide adequate improvement [50].

Chapter 2

INJECTABLE PERLECAN DOMAIN 1-HYALURONAN MICROGELS POTENTIATE THE CARTILAGE REPAIR EFFECT OF BMP2 ON MURINE MODEL OF EARLY OSTEOARTHRITIS

2.1 Abstract

The goal of this study was to use bioengineered injectable microgels to enhance the action of bone morphogenetic protein 2 (BMP2) and stimulate cartilage matrix repair in a reversible animal model of osteoarthritis (OA). A module of perlecan (PlnD1) bearing heparan sulfate (HS) chains was covalently immobilized to hyaluronic acid (HA) microgels for the controlled release of BMP2 *in vivo*. Articular cartilage damage was induced in mice using a reversible model of experimental OA and was treated by intra-articular injection of PlnD1-HA particles with BMP2 bound to HS. Control injections consisted of BMP2 free PlnD1-HA particles, HA particles, free BMP2 or saline. Knees dissected following these injections were analyzed using histological, immunostaining and gene expression approaches. Our results show that knees treated with PlnD1-HA/BMP2 had lesser OA-like damage compared to control knees. In addition, the PlnD1-HA/BMP2-treated knees had higher mRNA levels encoding for collagen type II, proteoglycans, and xylosyltransferase 1, a rate-limiting anabolic enzyme involved in the biosynthesis of glycosaminoglycan chains, relative to control knees. This finding was paralleled by enhanced levels of aggrecan in the articular cartilage of PlnD1-HA/BMP2 treated knees. Additionally, decreases in the mRNA levels encoding for cartilage-degrading enzymes and collagen type X were seen relative to controls. In conclusion, PlnD1-HA microgels constitute a formulation improvement compared to HA for efficient *in vivo* delivery and stimulation of

proteoglycan and cartilage matrix synthesis in mouse articular cartilage. Ultimately, PlnD1-HA/BMP2 may serve as an injectable therapeutic agent for slowing or inhibiting the onset of OA after knee injury.

2.2 Introduction

Articular cartilage is a viscoelastic tissue essential for the absorption of shocks and normal distribution of loads. Because of its non-vascularized, non-innervated and sparsely cell populated nature, this tissue displays poor regenerative capacity [54]. Recently, growth factor therapy has emerged as a novel strategy for enhancing chondrogenic differentiation and repairing functional cartilage [55-57]. The heparan sulfate binding growth factor (HBGF) bone morphogenetic protein 2 (BMP2), which plays a critical role in the establishment of normal cartilage during development, also was found to enhance the differentiated phenotype of mesenchymal stem cells in culture [12, 58, 59]. In addition, several studies indicate that BMP2 expression is elevated in damaged and/or mechanically-challenged cartilage during the early stages of OA.

BMP2 is an osteoinductive protein that belongs to the large TGF- β superfamily. RhBMP2 is a glycosylated, disulphide-bonded dimeric protein that can be produced in large scale by cell culture [60]. The mature active form of BMP2 results from cleavage at RXXR consensus sites and is a carboxy terminal dimer composed of 110-140 amino acids. BMPs act through type 1 and II serine-threonine kinase receptors. Binding of the BMP to the type 1 receptor induces intracellular association between type I and II receptor. This is followed by the phosphorylation of the type II and type 1 receptors. R-Smads that bind to the activated type I receptor are phosphorylated and released to further bind with Smad 4. This R-Smad/Smad 4 complex then translocates to the nucleus to stimulate transcription of the target genes [61]. Notably, BMP2 is FDA approved for clinical use and is delivered through biodegradable collagen sponges. Currently, BMPs can be delivered by the various

forms of carriers including synthetic polymers, natural origin polymers, inorganic materials and composites [62].

During the initial stages of OA, there is an increase in BMP2 levels that is believed to enhance reparative processes and reactivate morphogenetic pathways including synthesis of extracellular matrix (ECM) components [63, 64]. During OA disease progression, the weakened synthetic machinery of chondrocytes eventually becomes unable to compensate for the degradation of ECM components leading to degenerative OA. Therefore, it is apparent that supplementing BMP2 at the initial stages of OA may have a significant inhibitory effect on the development of OA [56]. Nonetheless, even with the high chondrogenic potency of BMP2, the biggest challenge lies in developing an efficient delivery system to counteract its short half-life and rapid degradation *in vivo* [65, 66]. The BMP2 secreted from the chondrocytes *in vivo* can meet with one of the three fates: they start exerting their anabolic action, or degraded by the BMP specific antagonists/inhibitors or become sequestered in the matrix components that are released slowly to the target cells [61]. Perlecan is one such naturally occurring proteoglycan found in cartilage that can help bind the locally released growth factors and can regulate their activity [67, 68].

Perlecan/HSPG2 is a large heparan sulfate proteoglycan (HSPG) that represents an essential component of cartilage ECM [68-71]. It belongs to the secreted or extracellular class of HSPG and occurs in various tissues including the basement membrane and interstitial matrix of cartilage, bone and uterus. It plays an important role in embryo implantation and placentation during development. It is also essential to maintain normal homeostasis by regulating various processes like the endothelial cell adhesion, cell proliferation and growth factor binding [68]. The NH₂-terminal

portion of perlecan (domain 1 or PlnD1) carries HS chains that bind HBGFs and enhance interaction with their signal transducing receptors [67, 68, 72, 73]. Thus, PlnD1 can act as a depot for BMP2 storage and controlled release, protect it from proteolytic degradation and potentiate its biological activity [74, 75]. Previous studies demonstrate that PlnD1 can be successfully used *in vitro* to modulate the chondrogenic bioactivity of BMP2 [76]. However, because of its own diffusion and susceptibility to degradation, PlnD1 only can be effectively used as a HBGF reservoir for *in vivo* cartilage repair if immobilized through conjugation to a larger biocompatible carrier. For this reason, a HBGF delivery system was developed by conjugating PlnD1 to hyaluronic acid (HA)-based microgels (PlnD1-HA) for the controlled realize of the condrogenic growth factor, BMP2 [55].

HA is a natural component of articular cartilage that functions as a matrix organizer by interacting with other matrix molecules such as aggrecan [77]. HA-based macromolecules are commonly used in the clinic as viscosupplements to enhance joint mobility and provide temporary relief of knee pain by increasing the viscosity and elasticity of synovial fluid [78]. However, HA alone does not promote the regeneration of cartilage ECM and is traditionally not administered in combination with active cartilage repair agents. Thus, increased physical activity after palliative HA injections often results in long term adverse effects and accelerates disease progression.

Here, I used PlnD1-HA microgels as the carrier for the controlled and slow release of BMP2 into the knee cavity of mice. We tested the efficiency of this system on articular cartilage using the papain-induced model of early OA [79]. The goal of this study was to determine the potential benefits of PlnD1 added to HA in

potentiating BMP2 activity for the attenuation of early cartilage damage in an experimental model of reversible OA.

2.3 Methods

2.3.1 Preparation of PlnD1-HA Microgels

Recombinant human BMP2 (R&D Systems, Minneapolis, MN) stock was prepared at a concentration of 10 μ g/ml in saline containing 4mM HCl and 0.1% (w/v) mouse albumin (Innovative Research, Novi, MI). Recombinant mouse PlnD1 was expressed by stably transfected kidney cells and purified using an immunoaffinity chromatography approach following established protocols [73, 80]. Post-translational modification of PlnD1 by heparan sulfate (HS) was verified by observing a change in its electrophoretic mobility following heparinase I, II, and III and chondroitinase AC treatments [73]. Because the absence of HS results in loss of BMP-2 binding activity only PlnD1 decorated by HS chains was used in this study [76].

The need for PlnD1 bioconjugation to a HA carrier to increase *in vivo* retention in the articular knee cavity, was tested previously by injecting intra-articularly Alexa 568-labeled PlnD1. Bioconjugation of PlnD1 to HA was performed as described [55]. The presence of glycosaminoglycan modifications was controlled by staining the microgels with Alcian blue. Additionally, the selective binding capacity and release of BMP2 were measured using an ELISA assay as described [55]. Finally, PlnD1-HA microgel bioactivity was evaluated *in vitro* using a micromass culture system as described [55]. Once the PlnD1-HA microgels passed all these control quality tests, they were extensively rinsed in 70% (v/v) ethanol and saline, pelleted by centrifugation at 3,000 rpm, and resuspended in sterile saline (Fig. 2.1) at a concentration of 6mg/ml. Approximately 1 mg of PlnD1-HA microgels was combined

with 250ng of BMP2. Both PlnD1-HA control and PlnD1-HA/BMP2 mixtures were preincubated for an hour at room temperature on a rocking platform prior to performing the intra-articular injections.

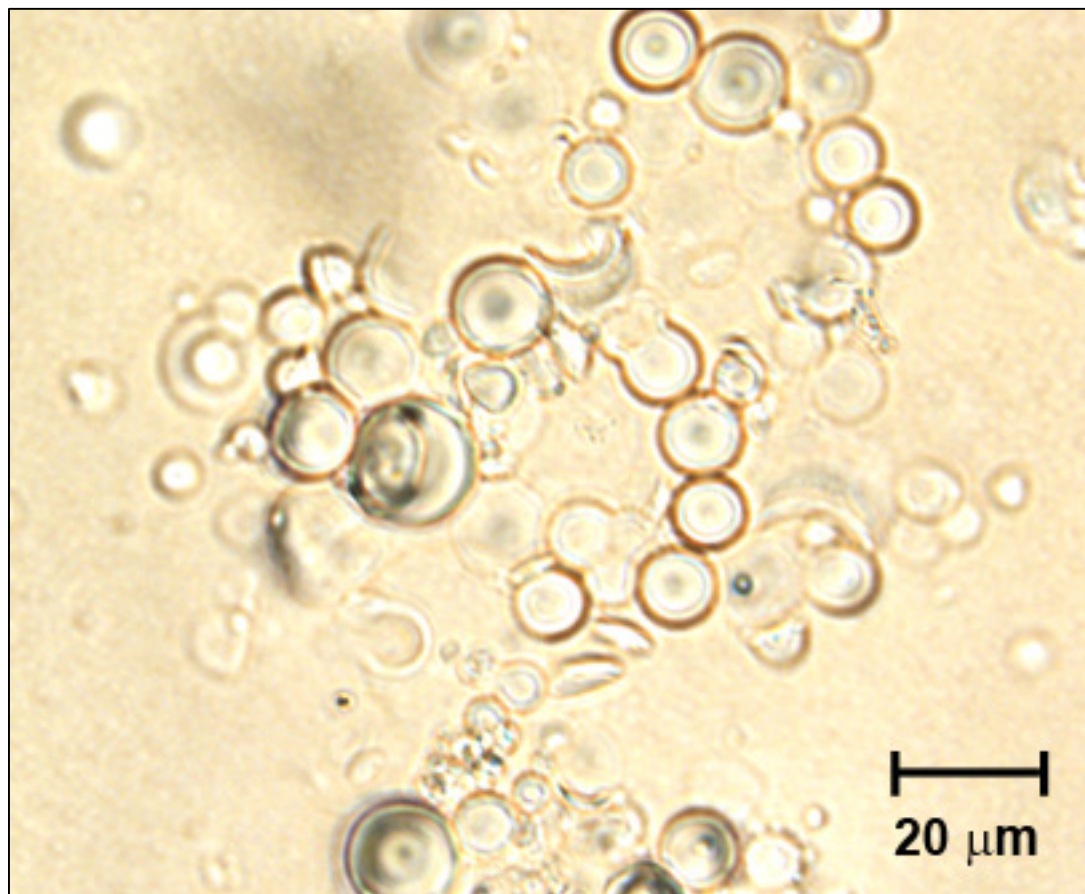


Figure 2.1: Injectable PlnD1-HA microgels visualized following hydration in saline buffer. Scale bar represents 20 μm .

2.3.2 Intra-articular Injections

Early OA-like damage was induced by injecting intra-articularly 6 μ l of a 1% (w/v) papain solution prepared in a saline solution containing 5mM L-cysteine in the knee of 10-11 week-old C57BL6/J mice. Mice were anaesthetized using mask inhalation of isoflurane for faster induction and recovery. The knee was shaved and a skin incision was made along the medial aspect of the flexed knee using a scalpel # 11. After visualizing the white glistening ligament, another incision was made medial to the ligament and the 6 μ l solution was injected slowly using a precision Hamilton syringe (50 μ l) fitted to a 30 1/2 gauge needle. All mice were given subcutaneous injections of buprenorphine (0.05-1mg/kg at surgery and after 6-12 hours as needed) and Baytril® (2mg/kg at surgery) for pain and to prevent infection, respectively.

After waiting 7 days for the OA-like damage to develop, the various test treatments were administered and the knees were allowed to recover for 7 or 14 days, after which the efficiency of each treatment condition to counteract the effects of papain was evaluated following animal sacrifice. Previous *in vitro* characterization of our delivery system demonstrated that nearly 70% of the initially bound BMP2 was released from PlnD1-HA microgels after 14 days of incubation [55]. Based on this observation, it was assumed that the majority of the bound BMP2 will be released from carrier microgels after a 14-day *in vivo* incubation period. In the initial study, the usefulness of PlnD1-HA particles plus BMP2 to limit joint damage was compared with growth factor-free PlnD1-HA particles or saline at day 7 post-treatment. In subsequent studies, HA particles or BMP2 alone served as additional control groups, and the knees were dissected 7 days after the treatment injections. Because knee damage induced by HA or BMP2 did not differ significantly from saline controls at

day 7, only PlnD1-HA or saline injections served as controls for day 14 histological scorings. All procedures involving animals were performed in accordance with protocols approved by the IACUC at the University of Delaware.

2.3.3 Histological Scoring

Knees were fixed in 10% (v/v) formalin and decalcified in a 10% (v/v) formic acid solution. 6 μ m-thick frontal sections were either stained histologically using a standard Safranin O and Fast Green staining procedure or immunostained (see below) [81]. The stringent conditions used prior and during knee sectioning did not permit us to visualize retention of the microgels in the knee cavity after histological processing. Scoring was done in the four compartments of the knee using a modified semi-quantitative scoring scale as described [82]. Briefly, the scores attributed in this study are: score 0 = normal cartilage, score 0.5 = loss of Safranin O staining with a normal articular surface, score 1 = small fibrillations or roughened articular surface, and score 2 = fibrillations extending into the superficial lamina. For each knee analyzed, 12-15 slides encompassing the entire joint were blinded and scored by two independent observers.

2.3.4 Immunohistochemistry

Deparaffinized knee sections were treated with Dako (Carpinteria, CA) antigen retrieval solution for 1 hour and blocked overnight with 3% (w/v) BSA and 2% (v/v)

goat serum. Primary rabbit antibody [anti-mouse aggrecan (Chemicon International Inc., Temecula, CA) or anti-mouse collagen type II (Biodesign International, Saco, ME)] was incubated for 4 hours at 37°C. After washing in PBS, sections were incubated with Alexa 488 conjugated goat anti-rabbit secondary antibody (Invitrogen, Carlsbad, CA) and DRAQ5™ (Biostatus, Leicestershire, United Kingdom) at 37°C for 1 hour, mounted, and viewed under a confocal microscope.

2.3.5 Quantitative Real-Time PCR

To examine transcriptional changes in cartilage-specific marker expression, mRNA was extracted from knee articular cartilage of both tibiae and femora of 4 papain-damaged knees treated with either PlnD1-HA/BMP2 (combined treatment) or PlnD1-HA (carrier only control) microgels. Mild decalcification was induced in 0.5M EDTA (Sigma-Aldrich, St. Louis, MO) overnight at 4°C. Articular cartilage tissue was microdissected away from subchondral bone prior to RNA extraction with the RNeasy® fibrous tissue mini kit (Qiagen, Valencia, CA) and DNAase treatment (Turbo DNA-free, Ambion Inc, Austin, TX). One µg of mRNA was used to synthesize cDNA using the iScript™ cDNA synthesis kit (BioRad, Hercules, CA) and the quantitative PCR reaction was run in triplicate. Primer sets specific for cartilage markers were purchased from SA Biosciences (Frederick, MD) and included type II and X collagens (COL2a1 and COL10a1); aggrecan (ACAN); perlecan, the major HSPG produced in the pericellular matrix of chondrocytes (HSPG2); and the isoform of xylosyltransferase found in cartilage (XYLT1). In addition, the following primers were used: 1) two aggrecan degrading enzymes, matrix metalloproteinase 3 (MMP3)

and aggrecanase-2 (ADAMTS5), and 2) one enzyme primarily responsible for type II collagen breakdown (MMP13) [83, 84]. The relative mRNA fold change in PlnD1-HA/BMP2 vs. PlnD1-HA (carrier only) treatments was compared at 1 or 7 days post-injection. These two time points were selected based upon previous *in vitro* kinetic studies of BMP2 release from PlnD1-HA microgels that occurred in two distinct phases with an initial burst occurring during the first day (10% of cumulative release) followed by a steady controlled release (3.8%/day) that reached a cumulative release of approximately 50% after seven days [55]. For this reason, mRNA analysis was conducted without delay (day 1) during the burst phase to detect transient events responsible for activation of synthesis pathways and in the middle of the steady linear release phase (day 7) before 100% release was achieved.

2.3.6 Statistical Analysis

The histological scores obtained at different time points from different knees ($n \geq 9$) were analyzed using the Kruskal-Wallis statistical test as described on Dr. John H. McDonald's website (University of Delaware, Newark, DE) [85]. Bonferroni correction was performed for multiple comparisons and p values less than 0.0083 and 0.0167 were considered significant at day 7 (6 groups) and day 14 (3 groups), respectively. For gene expression studies, each sample was run in triplicate, cycle threshold (CT) values were obtained for each gene of interest and were corrected with that of GAPDH. The relative mRNA fold change was calculated using the $2^{-\Delta\Delta CT}$ formula as described [86] and was considered significant if the fold increase or

decrease was above 2 or below 0.5, respectively. The mean values of two biological replicates (total of 8 knees) were reported.

2.4 Results

2.4.1 Effect of BMP2-loaded PlnD1-HA Microgels on Damaged Articular Cartilage in Mice

The efficacy of the various treatments in counteracting the damage produced by papain was evaluated by histological scoring (Figs. 2-2 and 2-3). Seven days post-treatment, PlnD1-HA/BMP2 injected knees had significantly lesser OA-like damage than the knees treated with PlnD1-HA ($p= 1.1 \times 10^{-5}$, Fig. 2.3) or the knees treated with saline ($p= 1.3 \times 10^{-5}$, Fig. 2.3). The majority of coronal knee sections obtained 7 days after a single injection of PlnD1-HA/BMP2 microgels showed a smooth and thick articular cartilage surface with chondrocytic clusters of normal appearance surrounded by intense Safranin-O staining (Fig. 2.2B). This result was seen in around 90% of the animals tested (8 out of 9 injected knees). Remarkably, severe damage induced by papain including proteoglycan loss and initial delamination of the superficial layer that were observed prior to treatment (day 0, Fig. 2.4) were entirely reversed by a single intra-articular injection of PlnD1-HA/BMP2 microgels when analyzed at day 7 post-treatment (Fig. 2.2B). In addition, the morphology of PlnD1-HA/BMP2 treated knees at day 7 was not distinguishable from control knees that were injected twice with a saline solution in place of papain at day minus 7 and in place of the treatment at day 0 (Fig. 2.2A-B and Fig. 2.3, $p= 0.824$).

In contrast, control saline (Fig. 2.2C) and PlnD1-HA (Fig. 2.2D) treatments of papain-damaged knees resulted in obvious proteoglycan depletion and small fibrillations in approximately 80% (7/9 knees) and 70% (6/9 knees) of the individuals tested, respectively. Additional control treatments consisting of an injection of either

HA or BMP2 microgels in the absence of PlnD1 did not reverse proteoglycan loss (Fig. 2.2E-F, in 7/9 and 8/9 knees respectively). Papain-damaged knees treated with HA (Fig. 2.2E, with fibrillation in 4/9 knees) had a significantly higher OA score compared to knees treated with PlnD1-HA/BMP2 (Fig. 2.2B) indicating the lack of chondrogenic repair activity (Fig. 2.3, $p= 2.78 \times 10^{-6}$). The same observation was made following BMP2 treatment (Fig. 2.3, BMP2 vs. PlnD1-HA/BMP2; $p= 3.2 \times 10^{-7}$) where scores were slightly more severe and cartilage fibrillation occurred in 7/9 knees (see arrows in Fig. 2.2F). Interestingly, chondrocyte clusters were seen near the joint surface in the eroding proteoglycan-depleted region of PlnD1-HA treated knees relative to control treatments (see arrows in Fig. 2.2D).

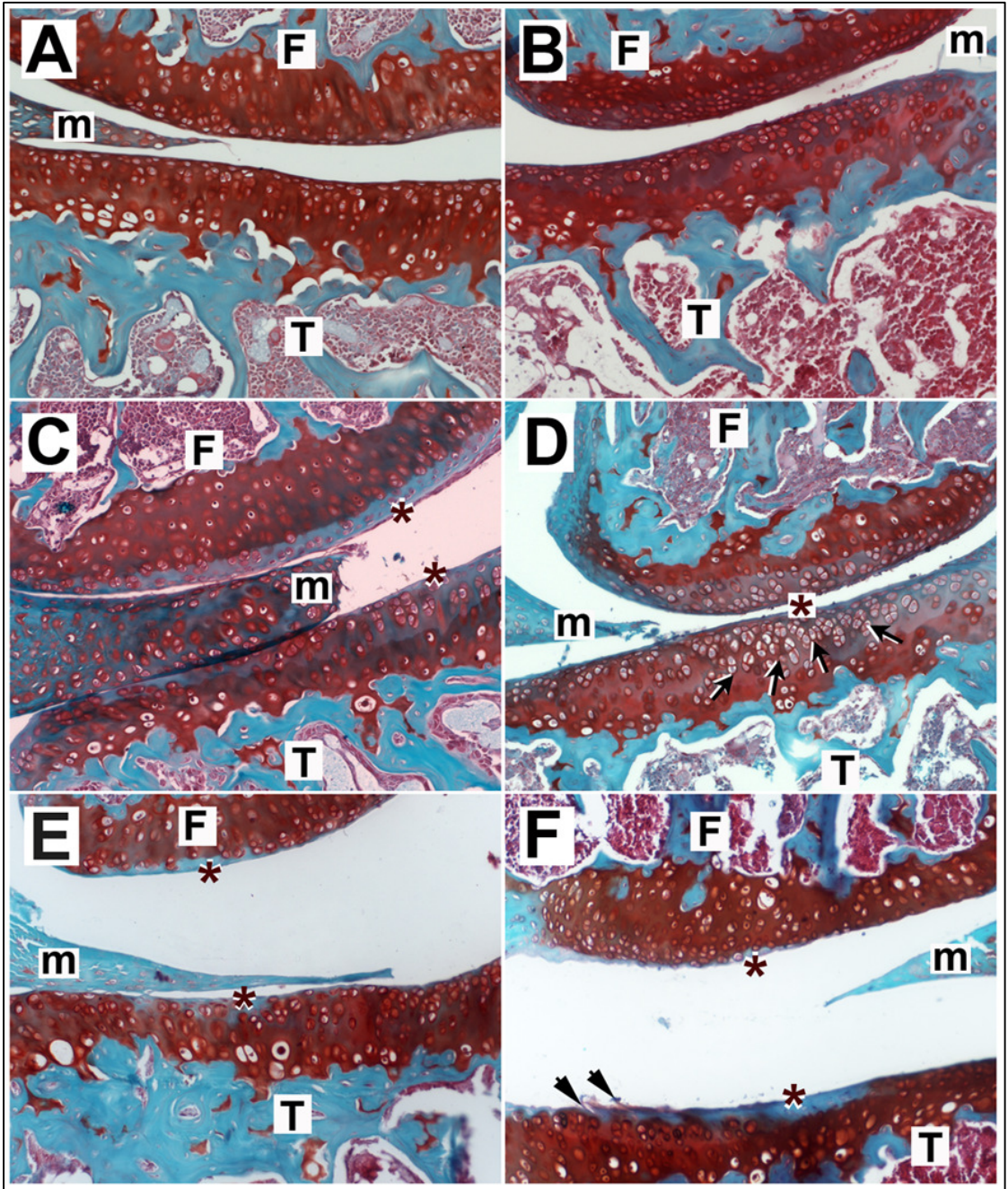


Figure 2.2: Histological sections of mouse knees processed 7 days post repair or control treatments and stained with Safranin-O and Fast Green. Knees treated with PlnD1-HA/BMP2 showed a normal smooth articular cartilage appearance (B) and showed no OA damage when compared with papain-damaged knees treated with either saline (C), PlnD1-HA (D), HA (E), or BMP2 (F). Proteoglycan depletion indicated by a loss of Safranin-O staining is marked by asterisks. An increase in chondrocyte clusters was observed in the proteoglycan-depleted region of articular cartilage of PlnD1-HA-treated knees (see arrows in D). Such clusters are absent in BMP-2 treated knees where articular cartilage fissures and delamination is observed (see arrowheads in F). No obvious difference is seen between control knees (A) injected twice with saline (in place of papain and the repair treatment) and the papain-injected knees treated with PlnD1-HA/BMP2 microgels (B). T, tibia; F, femur; m, meniscus

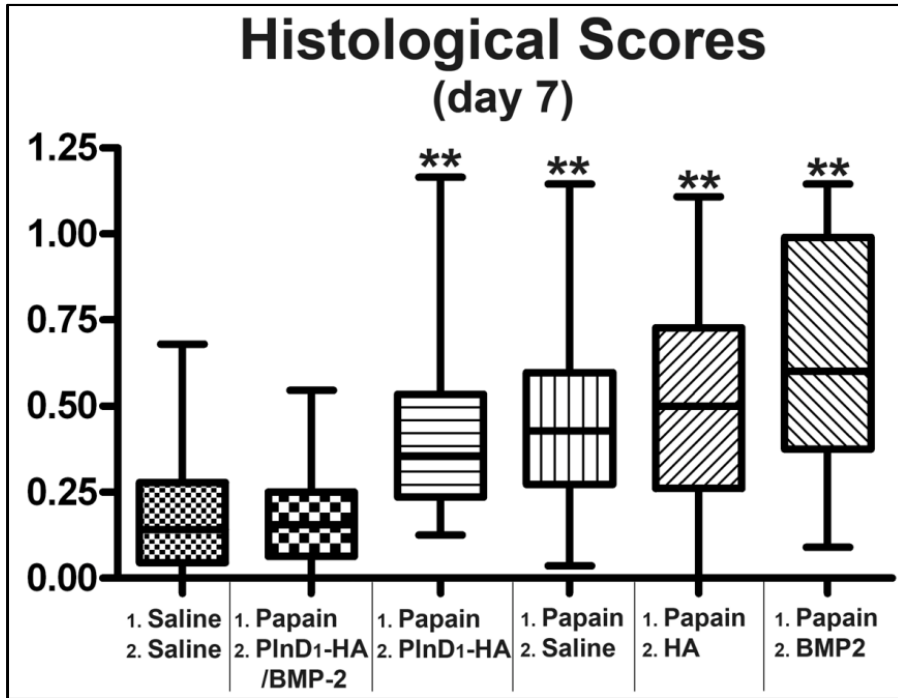


Figure 2.3: Box and whisker plot showing the median (central line), 25-75 percentile (boxes) and the entire range of scores obtained 7 days after treatment of saline or papain-damaged knees (n=5 for control saline; n=9 for all the other groups). ** indicates p<0.001 when compared to PlnD1-HA/BMP2. No statistical difference is seen between the scores obtained in control knees injected with saline twice and the papain-injected knees treated with BMP2-loaded PlnD1-HA particles (p=0.824).

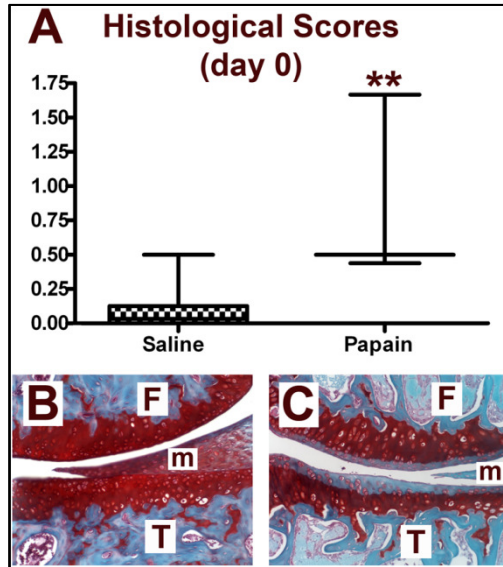


Figure 2.4: Box and whisker plot showing the median, 25 to 75 percentile and the entire range of scores among the saline and papain treated knees (A, n=7 for each group). No box is seen for the papain injection condition because over 80% of the articular surfaces correspond to a score of 0.5. ** indicates $p < 0.001$ ($p = 1.25 \times 10^{-8}$ in saline vs. papain). Representative histological sections of day 0 mouse knees processed 7 days after initial saline (B) or papain (C) intra-articular injections and prior to treatment via a second intra-articular injection. T, tibia; F, femur; m, meniscus

2.4.2 Effect of PlnD1-HA/BMP2 Microgels on Articular Cartilage Transcript Levels

2.4.2.1 Cartilage Synthesis Markers

Transcripts levels of ECM components were measured in articular cartilage of papain damaged knees treated with either PlnD1-HA/BMP2 or growth factor free control PlnD1-HA particles (Fig. 2.5A). As early as one day post-treatment, the mRNA level for the alpha1 chain of the major fibrillar component of cartilage, type II collagen (COL2a1), was slightly, but significantly, increased 2-fold in cartilage extracted from knees treated with PlnD1-HA/BMP2 relative to control knees. This positive effect continued with time and a 6-fold increase in type II collagen mRNA levels was seen at day 7 post-treatment in PlnD1-HA/BMP2 treated knees when compared to control samples.

Transcript levels of the major cartilage proteoglycan, aggrecan, were about 2.5-fold greater in PlnD1-HA/BMP2 versus control knees at day 7. We also examined the mRNA levels of perlecan itself, the most abundant HSPG present in cartilage. The relative mRNA level of perlecan was significantly higher in the PlnD1-HA/BMP2 treated knees relative to control knees at day 7. The relative levels of transcripts encoding for the enzyme that initiates glycoaminoglycan chain extension by adding the first sugar group to proteoglycans, xylosyltransferase 1 (XYLT1) [87] also was measured. PlnD1-HA/BMP2 treated knees demonstrated an increase in mRNA encoding for this enzyme in the early post-treatment phase (day 1). The increase remained significant at day 7 when compared to control knees.

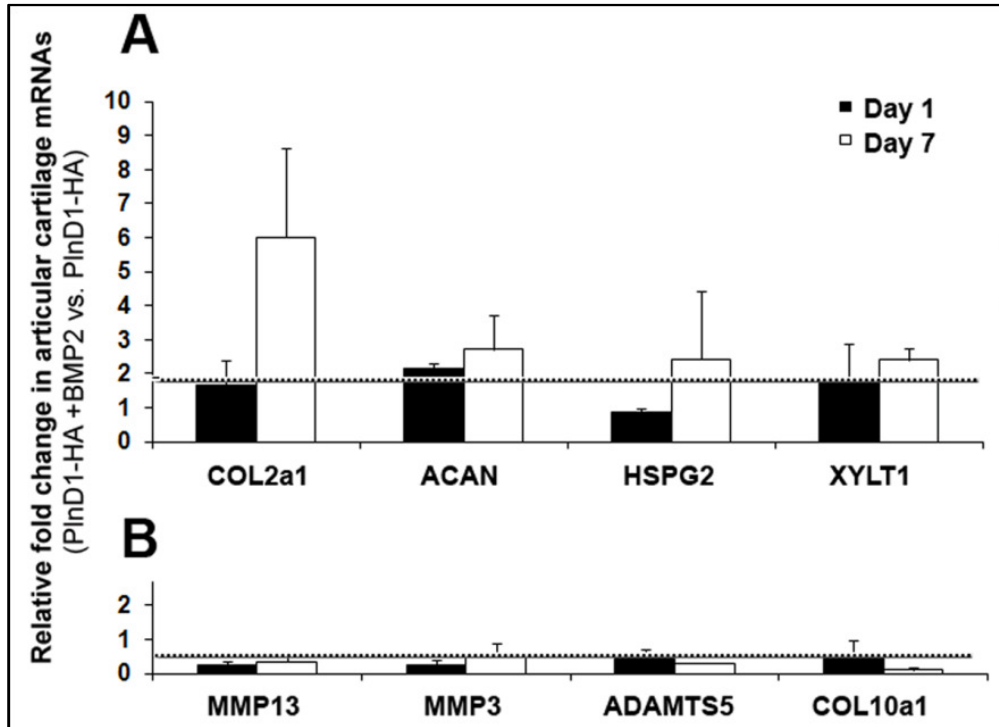


Figure 2.5: Effect of the combined administration of BMP2 and PlnD1-HA particles on mRNA levels of articular cartilage ECM components and ECM-modifying enzymes. Fold changes in mRNA levels are shown for knees treated with BMP2-loaded PlnD1-HA particles relative to knees treated with growth factor free particles (PlnD1-HA) on days 1 and 7 following intra-articular injections. mRNA levels of the $\alpha 1$ chain of type II collagen (COL2a1), aggrecan (ACAN), perlecan (HSPG2) and xylosyltransferase 1 (XYLT1) were significantly increased in knees treated with PlnD1-HA/BMP2 compared with control knees whereas the opposite was seen with matrix degrading enzymes (MMP13, MMP3, and ADAMTS5) and the $\alpha 1$ chain of type X collagen (COL10a1). Each sample was run in triplicate, the represented mean fold changes are the results of two biological replicates, and error bars represent standard deviations. Fold changes equal or higher to 2 (above the dashed line in A) and equal or lower to 0.5 (below the dashed line in B) are considered statistically significant using the comparative delta-delta Ct method.

2.4.2.2 Cartilage degradative enzymes and marker of hypertrophy

We also measured the mRNA levels of degrading enzymes responsible for the breakdown of cartilage ECM components and type X collagen (COL10a1), a marker for chondrocyte hypertrophy and pathological calcification of articular cartilage (Fig. 2.5B). The mRNA levels of both MMP3 and MMP13 were decreased significantly in the knees treated with PlnD1-HA/BMP2 compared to the control knees at day 1 and day 7 after treatment injections. The mRNA levels of ADAMTS5 were also significantly decreased at both day 1 and day 7 between the PlnD1-HA/BMP2 treated and control knees. The level of transcripts encoding for the α 1 chain of type X collagen, was significantly decreased by nearly 5-fold at day 7 in PlnD1-HA/BMP2 treated vs. PlnD1-HA injected knees.

2.4.3 Comparative Analysis of ECM Protein Distribution in PlnD1-HA/BMP2 treated Knees

2.4.3.1 Type II collagen Immunoreactivity

Potential changes in the expression pattern of the major fibrillar component, type II collagen, was assessed by comparing immunostained sections of papain-damaged knee sections harvested 7 days after treatment with either BMP2-loaded PlnD1-HA particles or saline (Fig. 2.6). There was no obvious difference in the intensity of the type II collagen-specific signal detected at the joint interface of PlnD1-HA/BMP2-treated knees (Fig. 2.6C) and the articular cartilage remaining in knees

treated with saline or control PInD1-HA particles (Fig. 2.6D). Thus, the global decrease of signal seen in control knees relative to PInD1-HA/BMP2 can be attributed to a decrease in the amount of articular cartilage tissue present in this region. Conversely, the presence of healthy articular cartilage in the superficial layer of PInD1-HA/BMP2-treated knees was accompanied by a concomitant increase in the overall extent of collagen type II-positive tissue when compared to control conditions (compare C and D in Fig. 2.6).

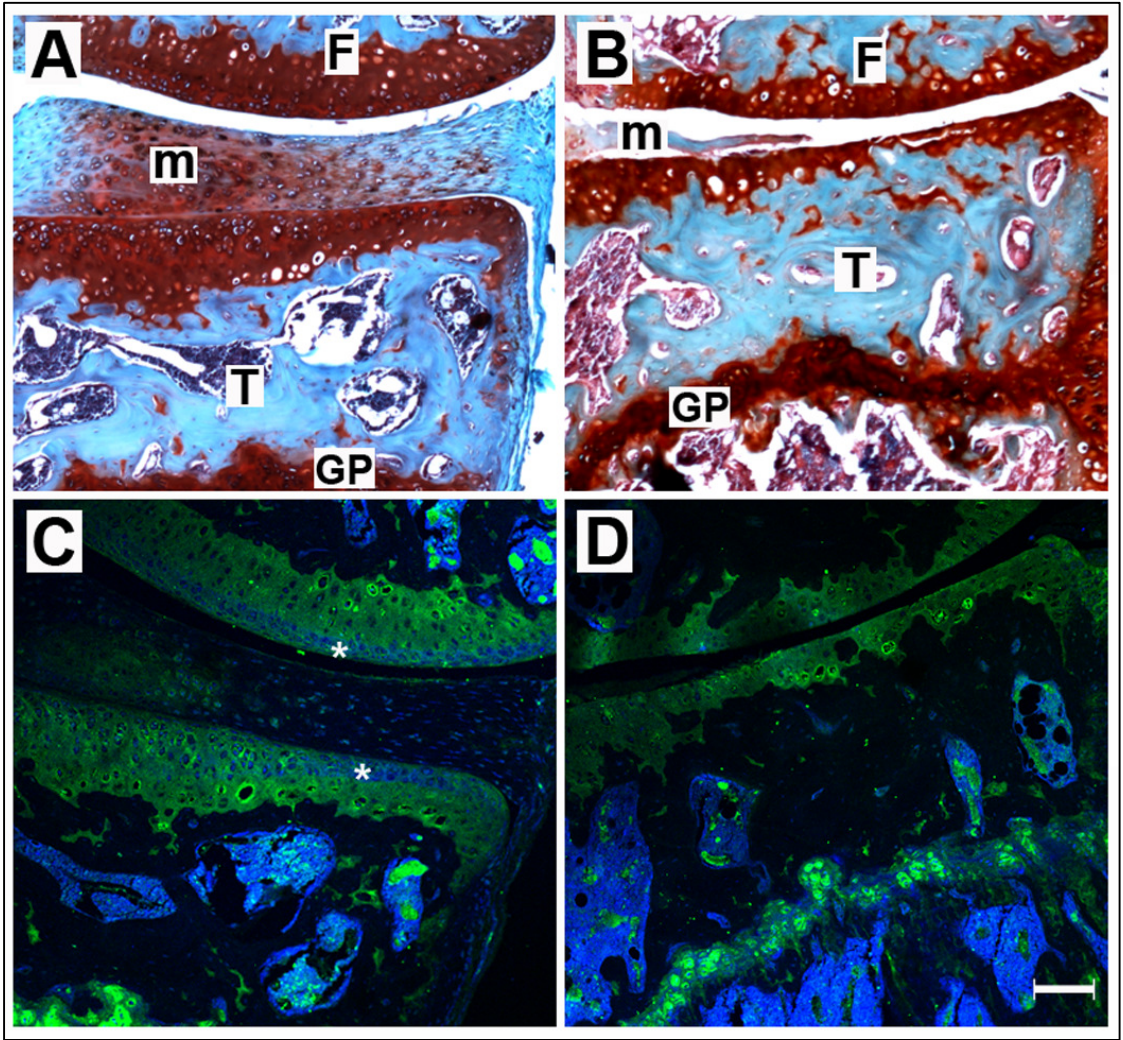


Figure 2.6: The extent of the type II collagen signal (green) is diminished in the articular cartilage of saline (D) versus PlnD1-HA/BMP2 (C) - treated knees after 7 days of treatment. For each group, consecutive coronal knee sections were stained with Safranin O/Fast Green (A, B) and immunostained with an antibody specifically directed against type II collagen (green in C, D). A and B are the adjacent histological stains for C and D, respectively. DRAQ5™ was used as nuclear stain (blue in C, D). Growth plate (GP) cartilage served as an internal positive control for type II collagen immunodetection. Asterisks indicate the presence of a healthy articular cartilage of high cellularity in the superficial layer of PlnD1-HA/BMP2-treated knees. F, Femur; T, Tibia; m, meniscus. Scale bars represent 100µm.

2.4.3.2 Aggrecan Immunoreactivity

To correlate the higher levels of aggrecan transcripts in PlnD1-HA/BMP2 treated articular cartilage with corresponding protein expression, we performed immunolabeling of treated knees with an antibody directed against the aggrecan molecule (Fig. 2.7). The articular cartilage of knees treated with PlnD1-HA/BMP2 (Fig. 2.7D and G) showed higher expression of aggrecan than control knees treated with PlnD1-HA (Fig. 2.7, compare D and G to E and H) or saline (Fig. 2.7, compare D and G to F and I). In contrast, aggrecan signal in growth plate cartilage remained unchanged among all three experimental conditions and was used as a positive control for antibody immunoreactivity (Fig. 2.7D-F).

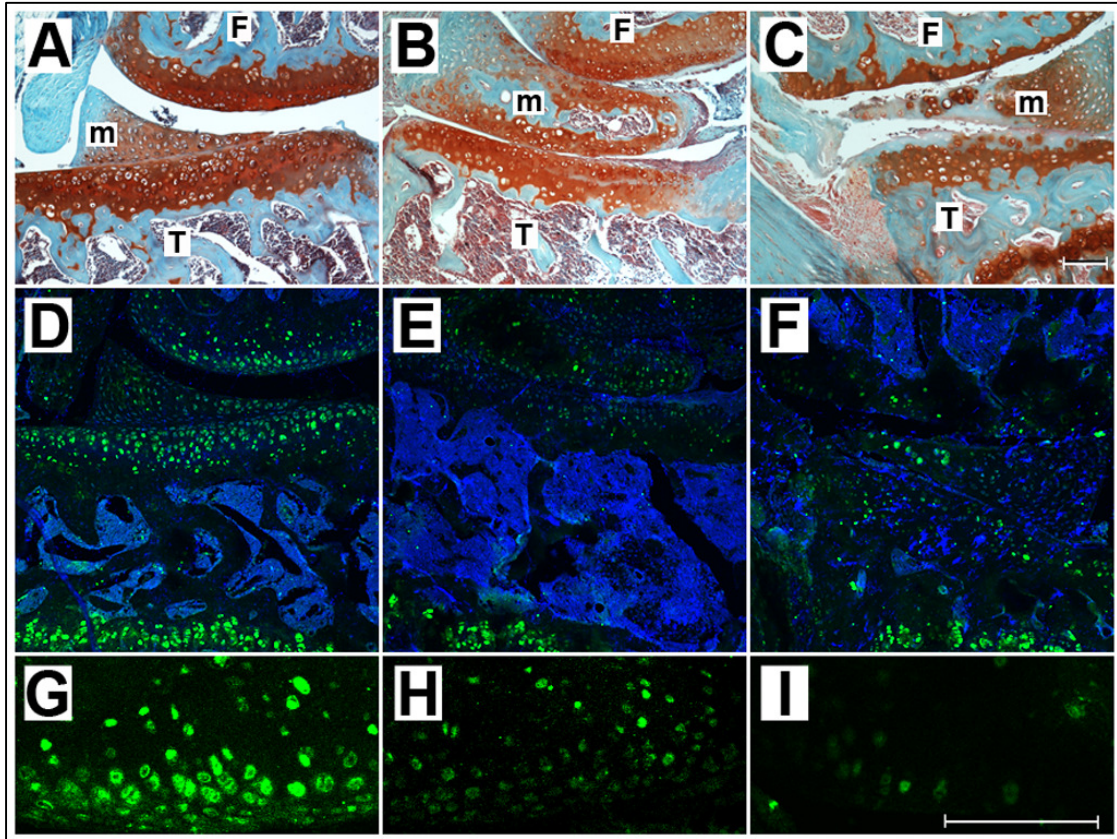


Figure 2.7: Articular cartilage of knees treated with PlnD1-HA/BMP2 showed increased expression of aggrecan relative to control (PlnD1-HA or saline) knees after 7 days of treatment. For each group, consecutive coronal knee sections were stained with Safranin O/Fast Green (A-C) and immunolabeled with an antibody specifically directed against aggrecan (D-F). The aggrecan-specific immune signal (green) was noticeably increased in knees treated with PlnD1-HA/BMP2 (D and G) when compared with control knees treated with PlnD1-HA (E and H) or saline (F and I). A, B, C are the adjacent histological stains for D, E and F, respectively. DRAQ5™ was used as nuclear stain (blue in D-F). Growth plate (GP) cartilage served as an internal positive control for aggrecan immunodetection in osteoarthritic knees that displayed severe depletion of proteoglycans at their articular cartilage surface (see arrows in panel D-F). Scale bars represent 100µm for either A-F or G-I. F, Femur; T, Tibia; m, meniscus

2.4.4 PlnD1-HA Microgels Prolong BMP2 Cartilage Repair Activity *in vivo*

To determine if PlnD1-HA microparticles can prolong the chondrogenic effect of BMP2 on articular cartilage over a longer period of time, we compared the histological appearance of papain-damaged knees dissected 14 days after a single intra-articular injection of either PlnD1-HA/BMP2, PlnD1-HA, or saline (Fig. 2.8B-D). The analysis of the histological scores showed that PlnD1-HA/BMP2-treated knees had lesser OA-like damage than the knees of the two control groups (Fig. 2.8A). Although increased, these scores followed the same trends as the scores obtained after 7 days of treatment and PlnD1-HA/BMP2-treated knees still displayed significantly less damage than knees treated with either PlnD1-HA or saline ($p=6.10^{-9}$ and $p=0.005$, respectively).

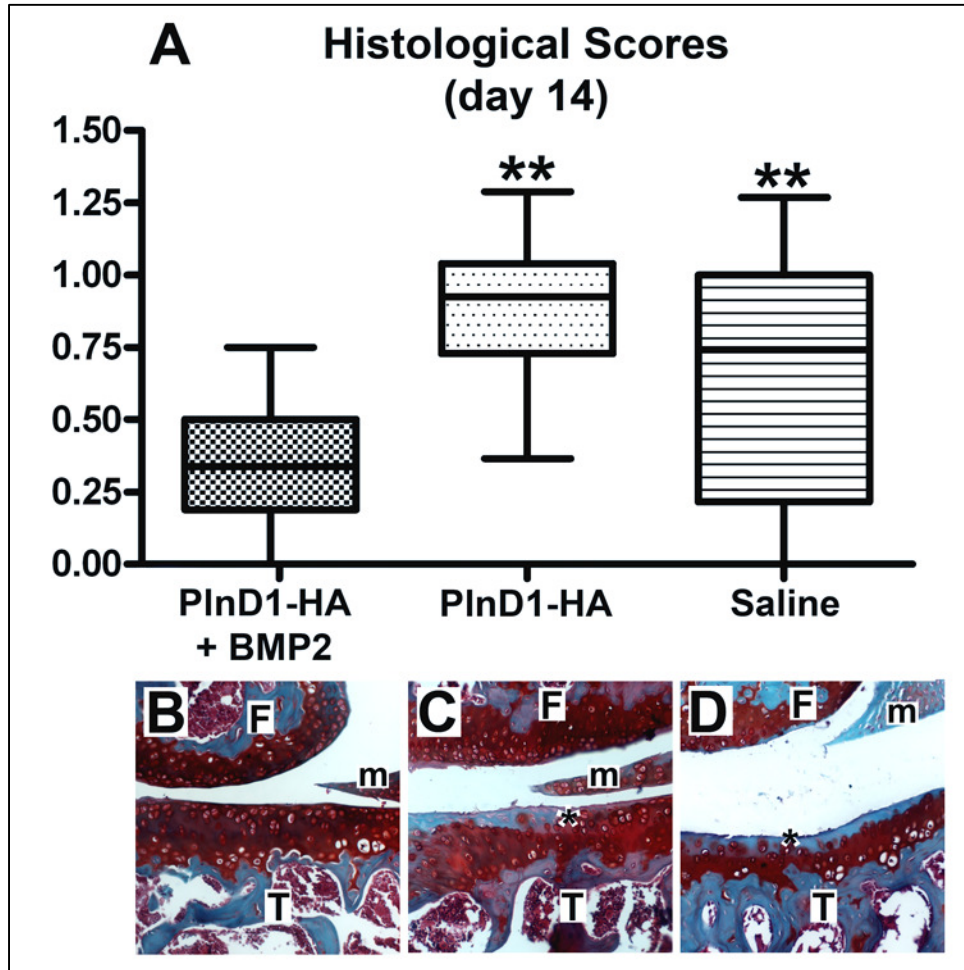


Figure 2.8: Box and whisker plot showing the median (central line), 25 to 75 percentile (boxes) and the entire range of scores obtained 14 days after treatment of papain-damaged knees (A, n=9 for each group). ** indicates $p < 0.001$ when compared to PlnD1-HA/BMP2. Representative histological sections from papain-damaged mouse knees processed 7 days post repair (B, PlnD1-HA/BMP2) or control (C, PlnD1-HA; D, saline) treatments and stained with Safranin-O and Fast Green. Proteoglycan depletion in the superficial articular cartilage layer is marked by an asterisk. F, femur; T, Tibia; m, meniscus

2.5 Discussion

Despite its established anabolic effect during chondrogenesis and pathogenesis of OA, BMP2 usefulness in cartilage repair has been limited due to its short *in vivo* half-life and known side effects when administered at high doses [55, 88]. Indeed, when injected under its soluble form into the knee cavity it rapidly loses its bioactivity due to clearance through systemic passive diffusion/clearance, and/or inhibition via specific BMP antagonists and proteases [65, 66, 89]. Additionally, burst induction from repetitive high dose injections or sustained overexpression through adenoviral genetic insertion of TGF β family members are known to result in adverse side effects on adjacent joint tissues including induction of an inflammatory response, synovial fibrosis, and formation of *de novo* osteophytes at sites of tendon insertions or at the periosteal joint margins [88, 90, 91].

Consistent with previous reports, the single administration of soluble BMP2 in the current study neither induced side effects like expansion of the synovial membrane/subchondral bone sclerosis/osteophyte formation nor enhanced cartilage repair. For this reason, PlnD1 bearing HS chains was bioconjugated to a biocompatible carrier (HA microgel) to potentiate/prolong BMP2 action after injection in mouse knee cavities. In our system, binding of BMP2 to HS chains could serve two roles as it both protects BMP2 from being degraded and may enhance its opportunity to bind with cellular receptors through the formation of functional ternary complexes in a similar fashion to that described for FGF2 [92, 93]. Although it is not well understood if the folded core protein portion of PlnD1 itself plays a direct role in the modulation of BMP2 activity, it is important for: 1) covalent conjugation to the carrier microgels due to the presence of surface lysines and 2) proper spacing of at least two

appropriately spaced surface HS chains that facilitate the controlled release of BMP2 [55]. Recently, another member of the TGF β superfamily, Activin A, was found to specifically bind to perlecan via HS chains interactions that regulate its localization within tissues [94]. Although Activin A binds HS of perlecan via its cleavable N-terminal pro-region, BMP-2 and BMP-4 were reported to interact with proteoglycans in a HS-dependent fashion through a highly conserved region of their mature NH₂-terminal portion [95]. This form of non-covalent highly specific binding is important in retaining the growth factor bioactivity that could easily be compromised through covalent chemical bonds and is likely to increase its half-life, as demonstrated by prolonged *in vitro* and *in vivo* effects [55]. Indeed, injection of BMP2 in combination with PlnD1-HA microgels carrying HS chains in papain-damaged knees significantly improved histological scores when compared to all other treatments including free BMP2.

The significant score improvement observed in PlnD1-HA/BMP2 treated knees observed at day 7 was still evident, albeit diminished, 14 days post-injection. These results extend previous *in vitro* findings that PlnD1-HA potentiates BMP2 and helps in spatial and temporal presentation of BMP2 for approximately two weeks [55]. It can be speculated that the release kinetics of BMP2 from PlnD1-HA microparticles are governed by the equilibrium between the endogenous BMP2 released from the degrading cartilage matrix and those bound to the PlnD1-HA particles. Such dynamic model would support stimulation of repair pathways and prevention of interaction between active BMP2 molecules and their natural antagonists. While this idea requires further investigation, it is clear from the data obtained during a two-week period that PlnD1-HA microgels injected in the absence of BMP2 are not responsible for knee

damage worsening and that injection of these microgels in combination with BMP2 induces an anabolic response in articular cartilage.

Comparative analysis of mRNA levels in articular cartilage following treatment with PlnD1-HA microgels in the presence or absence of BMP2 indicates that BMP2 release from these biomaterials rapidly increases the relative level of transcripts encoding for both aggrecan and its modifying enzyme (XYLT1) during cartilage repair processes [87]. These initial transcriptional events soon were followed by a significant increase in the relative levels of both type II collagen and perlecan mRNAs. The fact that BMP2 efficiently delivered via PlnD1-HA microgels increased the steady state of mRNA encoding for ECM components, strongly implies that the repair mechanisms involved under our experimental conditions primarily consist of de novo synthesis of cartilage matrix by resident chondrocytes. In addition, the small but significant decrease of the relative mRNA levels encoding for MMP3 and MMP13 upon PlnD1-HA/BMP2 treatment suggests that our BMP2 delivery system also may reduce early OA onset by inhibiting articular cartilage matrix degradation. This data contrasts with other reports in which BMP2 stable overexpression via adenoviral integration leads to an initial catabolic response by chondrocytes and boosts matrix turnover [56]. Thus, the lack of catabolic effect accompanied by increased matrix synthesis under our treatment conditions indicates that controlled delivery of BMP2 induces a seemingly exclusive anabolic effect that may protect new and resident cartilage against further destruction by MMPs. Consistent with our results, *in vitro* studies conducted in chondrocyte progenitors demonstrated that the close homolog of BMP2, BMP4, can strongly down-regulate MMP3 and MMP13 gene expression [96]. In comparison, the relatively low but significant decrease of MMP3 and MMP13 gene

expression obtained under our experimental conditions may be attributed to the low amount of chondrocytic stem cells present in adult articular cartilage.

The significant and continuous increase in aggrecan transcript levels during the course of the experiments is accompanied by a transcriptional inhibition of ADAMTS5, the aggrecan-specific protease [83]. Whereas up-regulation of *Adamts5* gene expression is a well-accepted indicator of early disease progression, moderate down-regulation of ADAMTS5 transcripts during the initial phase post injection actually may be important for normal cartilage turnover and the creation of space for organized deposition of newly synthesized ECM components [56]. Finally, reduction of both MMP13 and type X collagen mRNA levels in treated versus control knees indicated that the global reparative effect of PInD1-HA/BMP2 biomatrices on articular cartilage do not activate developmental program associated with cartilage growth plate terminal differentiation [83, 89]. Altogether, our gene expression data shows that BMP2 delivered through PInD1-HA triggers both anabolic (by increasing the transcription of proteoglycans and type II collagen) and protective responses (by lowering matrix degradation).

The replenishment of proteoglycans such as aggrecan with large negatively charged polysaccharide chains is essential for the restoration of the viscoelastic properties of normal functional hyaline cartilage with ability to resist compressive loads [83]. Therefore, our aggrecan expression data strongly favors a reversion of the early OA damage induced by papain. While *Col2a1* gene expression was significantly upregulated, signal specific for type II collagen protein remained unchanged in proteoglycan-depleted regions of the articular cartilage superficial layer. During early OA, the loss of aggrecan is initiated at the joint surface and progresses to the deeper

zones before degradation of the collagen fibrillar meshwork [83]. Similarly, the original collagen matrix might not have been destabilized under our experimental conditions and the lack of obvious change in the intensity of type II collagen-specific signal among treatments is likely due to the difficulty of visualizing *de novo* expression above baseline levels [83]. This idea is supported by the fact that the type II collagen triple helix is remarkably stable (half-life in cartilage ≥ 100 years) [97].

In summary, we demonstrated that single injection of BMP2 complexed to PlnD1/HA-based microgels in papain-damaged knees can increase the mRNA levels of articular cartilage matrix components, reverse proteoglycan loss and cartilage erosion, and inhibit cartilage degradative pathways and hypertrophy. Although our experimental design allowed us to study the early effects of bioactive microgels, one of the limitations of this study is that papain is a reversible model of OA that prevents the exploration of the long term effect of single or multiple injections of active microgels. Indeed, self-repair mechanisms occur and replenishment of proteoglycans become visible around one month post-papain injection [79]. Importantly, our data shows that BMP2 only promotes a strong and sustained anabolic response on compromised cartilage when delivered in a controlled manner that mimics its natural mode of release from the cartilage matrix. Thus, covalent modification of HA with bioactive molecular complexes of native cartilage may constitute a new promising therapeutic option to control the anabolic response of articular cartilage chondrocytes and block degradative processes in patients susceptible to develop OA at relatively young age. Problems associated with knee injury in young patients exposed to intense daily activities (athletes, military trainees, etc.) include the formation of fibrocartilage at sites of injury followed by progressive degeneration and development of severe OA

[98]. Future studies will investigate if multiple injections of BMP2-releasing PlnD1-HA microgels can help preserve the normal structure of hyaline cartilage and slow disease progression in more severe instability-induced models of knee OA. In conclusion, the current study shows for the first time that the PlnD1-conjugated, HA-based microgels can enhance BMP2 bioactivity *in vivo* and are promising injectable materials for the targeted delivery of HBGFs without the initiation of side effects often seen following repetitive administration of growth factors.

Chapter 3

INHIBITION OF T-TYPE VOLTAGE SENSITIVE CALCIUM CHANNEL REDUCES LOAD-INDUCED OA IN MICE AND SUPPRESSES THE CATABOLIC EFFECT OF BONE MEHCANICAL STRESS ON CHONDROCYTES

3.1 Abstract

Osteoarthritis (OA), the most common form of arthritis, is characterized by the loss of articular cartilage, increased subchondral bone remodeling, inflammation of the synovial lining and osteophyte formation. Previous studies suggest that subchondral osteoblasts release pro-inflammatory factors upon mechanical stimulation and significantly contribute to the pathology of OA. Because voltage-sensitive calcium channels (VSCC) regulate intracellular calcium, one of the earliest cellular responses in osteoblasts, we postulated that T-type VSCCs play an essential role in the subchondral bone formation response to load and that this response enhances the progression of OA. To determine the effects of T-VSCC on OA progression, we used repetitive mechanical insults to induce OA in the knees of $Ca_v3.2$ T-VSCC null and wild-type (WT) mice. Three weeks after loading, T-VSCC null mice exhibited significantly lower focal articular cartilage damage than the WT controls. To determine if this reduction in cartilage damage resulted from altered signaling in osteoblasts or chondrocytes, we selectively blocked T-VSCCs in murine osteoblastic cells (MC3T3-E1) or primary murine chondrocytes prior to exposure of fluid shear stress. We found this inhibition significantly reduced the expression of both early and late mechanoresponsive genes such as cyclooxygenase 2 and osteopontin, respectively, in osteoblasts but had no effect on gene expression in chondrocytes.

Furthermore, treatment of chondrocytes with conditioned media (CM) obtained from sheared MC3T3-E1 cells induced expression of markers of hypertrophy in chondrocytes and this was nearly abolished when MC3T3-E1 cells were pre-treated with the specific T-VSCC inhibitor. These results indicate that the subchondral bone formation resulting from OA plays a prominent role in OA progression and that the T-VSCC is essential to the release of osteoblast-derived soluble factors that are instrumental in inducing an early OA phenotype. Further these findings suggest that T-VSCC may be a valuable therapeutic target for blocking load-induced cartilage degeneration.

3.2 Introduction

Osteoarthritis (OA) is the most common form of arthritis and the leading cause of disability among older adults in the United States [44]. This degenerative disease affects the whole joint, causing not only the loss of articular cartilage but also synovial inflammation, subchondral bone sclerosis and osteophyte or bone spur formation. Although it is not entirely clear whether changes in subchondral bone precede cartilage changes or vice versa, it is widely accepted that subchondral bone sclerosis and remodeling are closely associated with OA development [99, 100].

Subchondral bone remodeling and its effects on the overlying cartilage may be the result of mechanotransduction, a process in which the mechanical signals encountered by the cell are converted into biochemical and cellular events [19]. Mechanical stimulation is important for skeletal integrity and it has been clearly established that routine exercise is essential to maintain normal bone mass [17]. Physical activity induces deformations of the bone matrix and shearing forces on osteoblasts and osteocytes, stimulating them to secrete various active metabolites including prostaglandins, nitric oxide (NO), and pro-inflammatory cytokines [20, 21]. Although such metabolites are established markers of bone anabolic responses to mechanical load and are essential for stimulating bone formation, persistent secretion of soluble factors such as cytokines by subchondral osteoblasts following altered joint loading may be responsible for initiating OA-like changes in the adjacent cartilage tissue [22].

A rapid increase in intracellular calcium level is the earliest recorded biochemical response following mechanical stimulation in the osteoblasts and chondrocytes [27, 28]. Voltage-sensitive calcium channels (VSCC) have been shown

to be important in altering intracellular calcium concentration in osteoblasts via calcium influx elicited by membrane depolarization [29] and are known to play an essential role in regulating intracellular processes, including cytokine signaling [101, 102]. VSCCs are multimeric protein complexes with pore forming ($\alpha 1$) and auxiliary ($\alpha 2\delta$ and β) subunits and are classified into high voltage activated (long lasting or L-VSCC) and low voltage activated (transient or T-VSCC). Based on the $\alpha 1$ subunit, L-VSCC is further divided into four isoforms ($Ca_v1.1$, $Ca_v1.2$, $Ca_v1.3$ and $Ca_v1.4$) and T-VSCC into three isoforms ($Ca_v3.1$, $Ca_v3.2$, $Ca_v3.3$) [103, 104]. Interestingly, the transiently active $Ca_v3.2$ T-VSCC isoform that requires weak membrane depolarization for activation is expressed by osteoblasts, osteocytes, and chondrocytes and is considered to be a major mediator of plasma membrane calcium permeability during osteogenesis [103].

Recent studies showed that mice carrying a null mutation for the $Ca_v3.2$ gene ($Ca_v3.2$ KO) display reduced bone formation, reduced subchondral bone remodeling, and diminished rate of mineral apposition following disuse-induced bone loss compared to wild type (WT) littermates [105]. $Ca_v3.2$ ($\alpha 1H$) transgenic mice were developed by Dr. Kevin Campbell at the University of Iowa and commercially available through the Jackson Laboratory. These mice are viable with a deletion of the $Ca_v3.2$ subunit and exhibit myocardial fibrosis and constricted coronary arterioles [102]. Here, we postulate that the T-VSCC located in the plasma membrane of osteoblasts and/or chondrocytes mediate mechanotransduction signals and plays an essential function in the initiation of osteoarthritis (OA). To test this hypothesis, we used $Ca_v3.2$ KO mice carrying a null mutation for the $Ca_v3.2$ $\alpha 1$ subunit of the T-VSCC and induced OA using a non-invasive *in vivo* knee loading model. *In vivo*

loading can induce a number of mechanical stimuli on cells present in the joint tissue including; compression, strain, hydrostatic pressure and fluid shear [30]. In the current study, we focus on the effects of fluid shear stress (FSS) on osteoblasts and used an *in vitro* co-culture system to show that mechanical stimulation of osteoblasts with FSS induces the release of soluble factors that have catabolic activity on chondrocytes. To distinguish the role of the T-VSCC in response to FSS in either osteoblasts or chondrocytes, we selectively inhibited T-VSCC function using a pharmaceutical blocker, NNC55-0396 [106], and studied the effects of this inhibition on chondrocytes.

3.3 Methods

3.3.1 *In vivo* Load Induced Mouse Model of OA

Male Cav3.2 T-VSCC KO mice bred on a C57BL6/J background and C57BL6/J wild-type (WT) mice were obtained from the Jackson Laboratory (Bar Harbor, ME) at 10-12 weeks of age, then subjected to non-invasive joint loading using a method similar to that described by Poulet et al. [107]. Briefly, mice were anaesthetized using inhaled isoflurane, the right lower limb was placed with the knee flexed into the joint loading apparatus, which consisted of a curved knee cup and a rigid ankle holder/support attached into a Bose LM1 TestBench mechanical testing system. Initially a compressive pre-load of 0.5 N was applied to the lower limb through the knee cup and ankle holder (Fig. 3.1A), after which a dynamic compression regimen was applied to the joint/tibiae over five alternate days. The loading regimen consisted of 80 cycles in which the waveform for a single cycle included a 0.025sec of rise time, 0.05sec peak load time, 0.025sec fall time and 4.9sec holding/resting time (Fig. 3.1B). A peak load of 8.5N was chosen based on our strain gaging analysis. The load level and duration of load applied in this regimen were shown to be sufficient to induce focal cartilage lesions that progress in their extent overtime [107], but were unlikely to induce microdamage in the underlying bone epiphysis and tibial diaphysis in healthy young animals, which is typically associated with fatigue loading [108-110].

. Using a separate set of animals, a single-element gage (EA-06-015DJ-120; Measurements Group, Inc., Raleigh, NC) was fixed on the relatively flat anterior-

medial surface (30%-50% distal to the tibial proximal end) of both tibiae from two null and three WT mice after sacrifice. The intact tibia was axially compressed with a gradually increasing load (0.9N/s from 0.2N to 9.2N) using the Bose LM1 system; the resulting voltage change was measured in real-time using Bose's data acquisition circuits. The voltage to strain calibration was done with aluminum cantilever beams using beam theory to derive strains [111]. The strain gauging analysis revealed no significant difference between the rigidity of the null versus WT tibiae (269.3+34.8 vs. 265.4+42.1 $\mu\epsilon/N$, $p>0.05$). Therefore, peak load of 8.5N was chosen because limbs of both genotypes could withstand comparable strain (2260-2290 $\mu\epsilon$) without activation of a differential woven bone response. All animal studies were performed with the approval of the Institutional Animal Care and Use Committee (IACUC) of the University of Delaware.

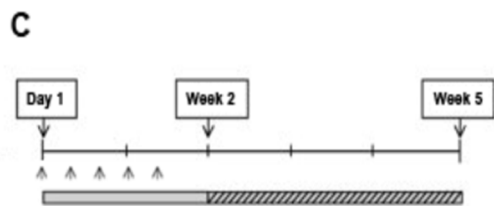
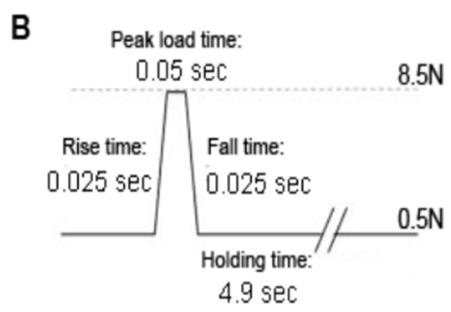
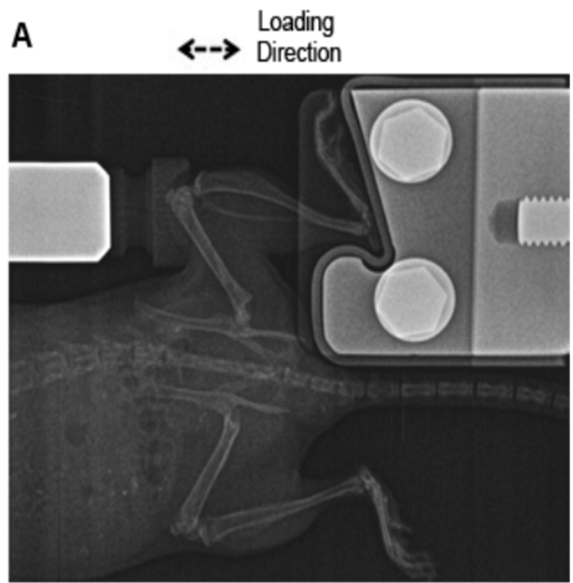


Figure 3.1: In-vivo loading system used to experimentally induce knee OA and compare progression of disease severity between T-VSCC and WT control knees. (A) Radiograph of mouse knee joint during loading using the Bose ElectroForce loading apparatus, (B) loading cycle waveform including durations for each phase of the cycle, (C) loading regimen: Five loading episodes were performed over a period of eight days followed by a 26-day period of non-loading prior to sacrifice (week 5) and histological processing

3.3.2 Histological Analysis of the Knee Joints

Mice were euthanized three weeks after the final loading bout and the soft tissue was removed. Joints were fixed in buffered-zinc formalin (Z-fix, Anatech Ltd., Battle Creek, MI) for 24hrs, then decalcified using formic acid containing EDTA (Formical-2000, Decal Chemical Corporation, Tallman, NY) for 7 days, under orbital shaking at room temperature. The knee joints were then paraffin-embedded and whole knees were sectioned to obtain coronal 6 μ m-thick sections. About 12-15 alternate slides from each knee were stained with Safranin O and Fast Green. The histologically stained slides were then scored in the four knee compartments (Medial Tibia, Medial Femur, Lateral Tibia and Lateral Femur) by two blinded scorers as described [112]. Scores were attributed as follows: 0 = normal smooth cartilage surface, 0.5 = decrease in Safranin O staining, 1 = rough cartilage surface with small fibrillations, 2 = fibrillations extending below the superficial layer, 3 = fibrillations/erosions extending < 25% of the entire cartilage thickness, 4 = fibrillations/erosions extending 25-50% and 5 = fibrillations/erosions extending 50-75% of cartilage thickness.

3.3.3 Cell Culture

To prepare primary mouse sternal chondrocytes, rib cages were obtained from 3-5 day-old pups. The extraction protocol was adapted from Dr. K.M. Lyons' lab (UCLA, CA) and passages 1 to 3 were used for experiments. Briefly, the rib cages

were serially digested using pronase (2mg/ml in 1×PBS; Roche Diagnostics, Indianapolis, IN) and collagenase P (3mg/ml in DMEM; Roche Diagnostics) for 15min in a 37°C incubator. The rib cages were rinsed in 1×PBS after each digestion and placed in collagenase P (0.3mg/ml in DMEM) solution overnight in a 37°C incubator. Next day the cells were filtered using a cell strainer and then cultured in a chondrogenic media composed of DMEM supplemented with 10% (v/v) FBS and 1% (v/v) penicillin/streptomycin, 50µg/ml ascorbic acid and 10mM β-glycerophosphate. To maintain their chondrocytic phenotype, cells were cultured either as micromasses (for mRNA extraction), pellets (for immunohistochemistry), or monolayer (for alizarin red staining). MC3T3-E1, osteoblast-like cells were grown in αMEM media supplemented with 10% (v/v) FBS and 1% (v/v) penicillin/streptomycin and subjected to FSS for 2 hours. Selective T-VSCC inhibition was achieved by pre-treating the cells with NNC55-0396 (NNC) [106] and the conditions are as follows: FSS untreated (FSS UT) or pretreated with NNC (FSS NNC) and maintained at static, untreated (static UT) or pretreated with NNC (static NNC).

Collection of cell extracts was performed after 2hrs of FSS followed by either a 2hr- or 20hr-rest period for assessment of early and late shear response genes, respectively. For indirect co-culture, chondrocyte micromasses were treated with CM of MC3T3-E1 subjected to one of the four conditions described above and collected after a 2hr-rest period. Treatment of micromasses tested the effect of osteoblast-derived factors released in response to mechanical stress *via* exocytosis and was performed for seven days to induce chondrocytic changes at both transcriptional and translational levels [22]. The direct effect of NNC and FSS on chondrocytes was also assessed under the above mentioned four conditions.

3.3.4 Fluid Shear Stress (FSS) Conditions

A rocker platform was used to induce FSS and the characteristic shear stress at the center of the flask in the horizontal position was calculated to be ~ 3.5 dynes/cm² using the mathematical formula described by Zhou et al. [113]. This system when well controlled can be used to achieve temporary oscillations in standard cell culture dishes. It also provided a sterile environment and limited further dilution of conditioned media (CM) for the indirect co-culture experiments. The cells were subjected to FSS in T-25 flasks with 5ml of culture media and the rocker was operated at a speed of 120 RPM for 2 hrs.

3.3.5 Quantitative RT-PCR

To compare the transcriptional activity of selected genes, RNA was extracted from MC3T3-E1 monolayers or primary chondrocytes cultured as micromasses using the RNeasy mini kit (Qiagen, Valencia, CA), DNase treated (Turbo DNasefree, Ambion Inc., Austin, TX), and used as a template for cDNA synthesis (cDNA synthesis kit, BioRad, Hercules, CA). The reaction mix was as follows: 12.5µl of 2×SYBR Green mix, 5µl forward and reverse primers (4µM), 0.5µl of cDNA and 7.5µl of water. PCR reactions were run in duplicates using the ABI 7300 PCR system (Life Technologies, Grand Island, NY). The obtained C_T values were normalized to

the housekeeping gene, GAPDH and fold changes were calculated using the delta C_T method as described [112].

3.3.6 Immunohistochemistry

Type X collagen immunodetection was performed on cryosections obtained from chondrocyte pellets treated with the MC3T3-E1 conditioned media (CM) for one week. The pellets were washed in 1×PBS and were fixed in 4% (v/v) paraformaldehyde in 1×PBS for 10min. The pellets were embedded in Optimum Cutting Temperature compound (O.C.T., Tissue-Tek®, Torrance, CA) prior to cryosectioning and 12µm-thick sections were obtained. The sections were rehydrated in 1×PBS and subjected to an antigen exposure step via a 0.2% (w/v) Type IV-S hyaluronidase (Sigma-Aldrich, St. Louis, MO) digest for 1hr at room temperature. The sections were then washed in 1×PBS, blocked with 2% (v/v) goat serum and 3% (w/v) BSA in 1×PBS for 1hr, and incubated for 2hr at 37°C in a humidified chamber with a rabbit polyclonal anti-collagen X antibody (1:200 dilution in blocking agent) generously provided by Dr. WA Horton (Shriners Hospital for Children, Portland, OR). Sections were then washed with 1×PBS before incubation with both Alexa 488-conjugated goat anti-rabbit secondary antibody (Invitrogen, Carlsbad, CA) (1:200) and DRAQ5™ (1:1000) nuclear stain (BioStatus Ltd., Leicestershire, UK) for one hour at 37°C in a humidified chamber. Following additional washes with 1×PBS, sections were mounted with Gel/Mount anti-fading solution (Biomedica Corp., Foster City, CA), and viewed under a LSM Zeiss confocal microscope as described [112].

3.3.7 Western Blotting

COX2 protein levels were determined in MC3T3-E1 cells using western blotting. Total cell lysates were collected 2hrs after FSS using RIPA buffer including a protease inhibitor cocktail mix (Thermo Scientific, Rockford, IL). Protein extracts were diluted 1:1 with Laemmli sample buffer containing β -mercaptoethanol and denatured at 95°C for 10min before running the extracts in a 4-12% Bis-Tris NuPage Polyacrylamide gel (1.5mm \times 10 well; Invitrogen, Carlsbad, CA) using 1 \times MES SDS Running Buffer (Invitrogen). 10 μ l See Blue Plus-2 Standard (Invitrogen) was used as a ladder control and the gel was run at 160V for 1hr. The gel was then transferred to a nitrocellulose membrane using wet transfer at 40V for 4hrs and the blots were blocked overnight at 4°C in 5% (w/v) milk in Tris-buffered saline with 1% Tween 20 (5% milk in TBS-T). The blots were then incubated with primary antibody against COX2 at a 1:1000 dilution (goat α -COX2; Santa Cruz, Dallas, TX) for 2hrs at room temperature. After three washes of 10min each in 1% (v/v) TBS-T, the blot was incubated with the donkey horseradish peroxidase anti-goat IgG antibody at a 1:10,000 dilution (Abcam, Cambridge, MA) for 1hr at room temperature. Following three additional washes of 10min each in TBS-T, detection was done using SuperSignal West Dura Chemiluminescent Substrate Pierce detection kit (Thermo Fisher Supersignal West Scientific, Rockford, IL). The experiment was repeated with three experimental replicates and ImageJ software (NIH, Bethesda, MD) was used to perform densitometric analysis.

3.3.8 Statistical Analysis

The histological scores were analyzed using a non-parametric Kruskal-Wallis test and Bonferroni correction was performed for multiple comparisons as described in [114]. Gene expression fold changes and densitometric values obtained from real time PCR and western blotting respectively were analyzed using a Student t-test. All *in vitro* experiments were performed using cell lines issued from different batches or different animals and the data are presented as the mean of at least six individual values obtained from experiments run at different times.

3.4 Results

3.4.1 Cav3.2 T-VSCC KO Mice Display Reduced Cartilage Damage Relative to WT Controls Following Repetitive Knee Loading

To determine whether a link exists between mechanical stimulation through T-VSCC activation and OA, we subjected age-matched Cav3.2 T-VSCC KO and WT mice to non-invasive repetitive knee loading for five alternate days. Histological analysis of sections of loaded knees harvested three weeks after *in vivo* loading showed that KO knees had significantly lower mean OA scores than the WT control knees (Fig. 3.2; $p=0.001$). Furthermore, the comparison of OA scores within individual knee compartments (Fig. 3.2A) showed that the loaded KO mouse sections had significantly lower OA scores in the medial femur ($p=0.012$), medial tibia ($p=0.001$), and lateral femur ($p=0.027$) than in the corresponding compartments of loaded WT control knees. The maximum OA damage was observed in the lateral femur of WT mice (see Fig. 3.2A and arrow in Fig. 3.2B). Such focal damages were primarily found in the posterior and lateral positions of WT knee especially in the lateral femur compartment where contact loading force experienced by the articular cartilage surface is maximal.

Statistical analysis of the left unloaded knee sections among the WT and KO mice showed no significant differences within the knee compartments except for medial femur ($p=0.02$). The comparison of the mean scores from all the compartments combined revealed a significant difference in OA scores between the unloaded WT and unloaded KO knees ($p=0.0027$) (Fig.3.3).

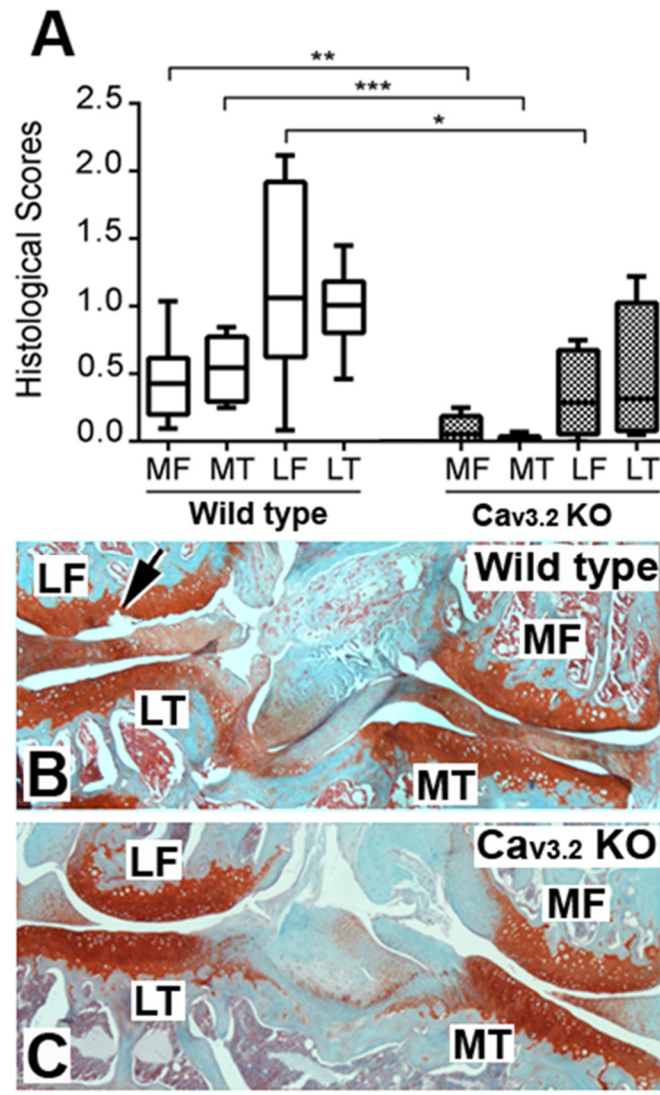


Figure 3.2: Decrease of OA damage in the loaded right T-VSCC KO vs. WT controls following in vivo knee loading. A: boxes and whiskers graph showing the median (central line), 25-75 % (box) and the entire range (whiskers) of histological OA scores obtained three weeks after final loading in the four compartments (MT-Medial Tibia, MF- Medial Femur, LT-Lateral Tibia, LF- Lateral Femur) of loaded wild type control and T-VSCC KO mouse knees. B and C are coronal knee sections stained with Safranin O and Fast green from either a WT or a T-VSCC KO loaded knee, respectively. Arrow in B indicates a focal lesion caused by loading in the lateral knee compartment of a WT mouse knee. * = $p < 0.05$, ** = $p < 0.01$ and *** = $p < 0.005$; $n = 10$ for wild type and $n = 7$ for T-VSCC KO mice

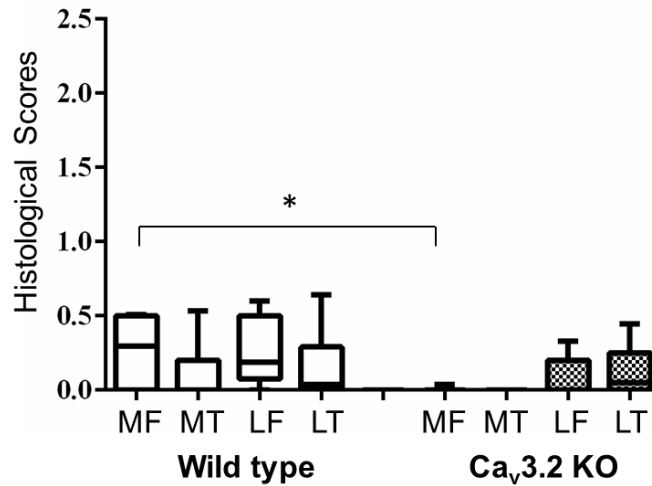


Figure 3.3: OA scores in unloaded knees of T-VSCC KO vs. WT controls following in vivo knee loading. Box and whiskers graph showing the median (central line), 25-75 % (box) and the entire range (whiskers) of histological OA scores obtained three weeks after final loading in the four compartments (MT-Medial Tibia, MF- Medial Femur, LT-Lateral Tibia, LF- Lateral Femur) of left unloaded wild type control and T-VSCC KO mouse knees. * $p < 0.05$; $n = 10$ for wild type and $n = 7$ for T-VSCC KO mice.

3.4.2 T-VSCC is Required for the Anabolic Response of Osteoblasts to FSS

To examine changes in shear-response genes indicative of an early and late anabolic response in bone, MC3T3-E1 osteoblasts were exposed to FSS for two hours and RNA was extracted either 2 or 20hrs following mechanical stimulation (Fig. 3.4A & Fig. 3.5, respectively). A nearly 50-fold increase ($p < 0.01$) was found for Ptgs2 (Cox2) mRNA levels in cells subjected to FSS (FSS UT) relative to static control cells (static UT) within 2hrs following FSS (Fig. 3.4A). This increase in Ptgs2 transcripts was accompanied by a marked increase in COX2 protein levels (Fig. 3.4B, lane 3). In addition, this early response was followed by an approximate 5-fold increase in osteopontin (Spp1) mRNA levels in FSS vs. static control cells 20hrs after FSS stimulation. Both of these increases in Ptgs2 and Spp1 mRNA levels were significantly reduced when cells were subjected to FSS in the presence of NNC (FSS NNC). In contrast, cells maintained under static conditions and subjected to NNC treatment (Static NNC) showed no significant changes in Ptgs2 or Spp1 levels when compared with static control cells (Static UT). Western blot analysis comparing COX2 protein levels among these four experimental conditions in osteoblasts showed that the COX2 protein increase in response to FSS is also attenuated to control levels by the T-VSCC blocker (Fig. 3.4B).

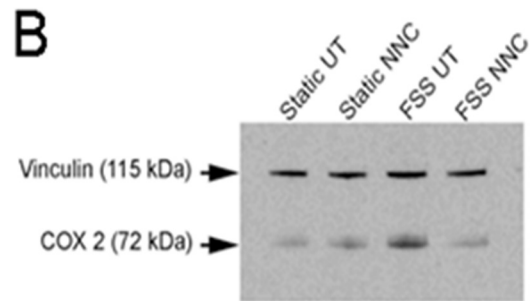
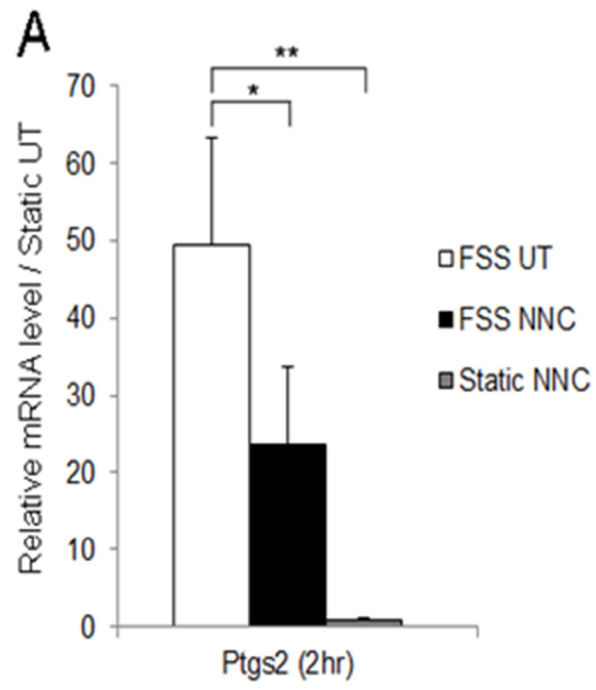


Figure 3.4: The fluid shear stress (FSS)-induced expression of the early shear response marker cyclooxygenase 2 is inhibited in MC3T3-E1 cells with the addition of T-VSCC-specific inhibitor, NNC55-0396. A: quantitative PCR analysis shows that the marked increase in Cox2 (Ptgs2) mRNAs observed two hours following FSS relative to the static untreated (Static UT) control condition is significantly inhibited in the presence of NNC55-0396. The conditions are FSS untreated (FSS UT), FSS treated with NNC55-0396 (FSS NNC), static treated with NNC55-0396 (static NNC). Error bars represent standard error of mean of the biological duplicates and * indicates $p < 0.05$ between FSS UT and FSS NNC, ** = $p < 0.01$ between FSS UT and static NNC. B: western blot analysis performed under the same conditions described in A indicates that the FSS-induced increase of COX2 protein is decreased to control levels in the presence of NNC55-0396. Vinculin was used as a loading control

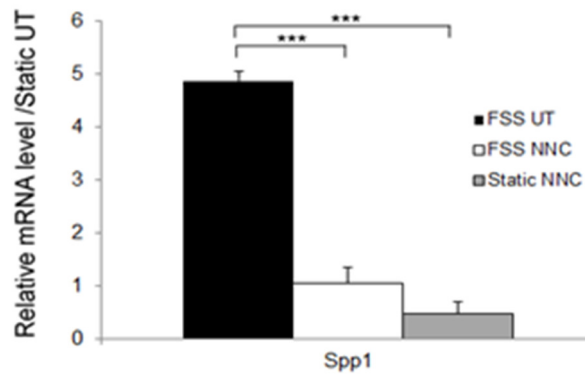


Figure 3.5: The fluid shear stress (FSS)-induced expression of the late shear response gene osteopontin is inhibited in the presence of the T-VSCC-specific inhibitor, NNC55-0396, in MC3T3-E1 cells. Quantitative PCR analysis shows that the increase in osteopontin (Spp1) mRNAs observed 20 hours following FSS relative to the static untreated (Static UT) control condition is significantly inhibited in the presence of NNC55-0396. The conditions are FSS untreated (FSS UT), FSS treated with NNC 55-0396 (FSS NNC), static treated with NNC 55-0396 (static NNC). Error bars represent standard error of mean of the biological duplicates and *** = $p < 0.005$ between FSS UT and FSS NNC or FSS UT and static NNC

3.4.3 T-VSCC Inhibition Reverses the Chondrocyte Hypertrophy Induced by the Conditioned Media (CM) from FSS Osteoblasts

To determine whether mechanically challenged osteoblasts can trigger an OA-like phenotype in chondrocytes using our *in vitro* system, we obtained osteoblast-derived CM from osteoblasts cultured under either static or FSS conditions and compared the expression profiles of primary mouse chondrocyte micromasses treated with such osteoblast-derived CMs (FSS UT vs. Static UT, Fig. 3.6). In addition, the contribution of T-VSCC function was examined by adding NNC to the medium during FSS and testing the effect of the resulting CM (FSS NNC) on chondrocytes. The CM from sheared osteoblasts (FSS UT) induced up-regulation of collagen X (Col10a1), alkaline phosphatase (Alpl), and Mmp13 mRNAs in chondrocytes relative to CM obtained from static (Static UT) control cells (Fig 3.6). In contrast, chondrocytes cultured with CM obtained from both sheared (FSS NNC) or non-sheared (Static NNC) osteoblasts cultured in the presence of NNC displayed a significant reduction in the expression of both Col10a1 and Alpl genes relative to the FSS UT condition. Although there were no significant differences in the levels of aggrecan and collagen II across the various conditions, we found a decreasing trend in the expression level of Mmp13 mRNA in chondrocytes treated with CM from FSS NNC and static NNC compared to chondrocytes treated with CM from FSS UT, obtained from osteoblasts sheared in the absence of NNC (Fig. 3.6).

The direct effect of FSS and/or T-VSCC inhibitor on primary mouse chondrocytes was tested using the same conditions described above for osteoblasts (Fig. 3.7). FSS increased the relative levels of Ptgs2 transcripts in chondrocytes when compared to static untreated (Static UT) chondrocytes, albeit to a lower extent than

what was observed in MC3T3-E1 cells. Addition of NNC to the medium during FSS decreased *Ptgs2* gene activation to near basal levels (Static UT). Interestingly, the expression of the *Mmp13* gene, a marker of cartilage matrix degradation, showed a slight elevation following shear stress, but also returned to basal levels in the presence of the T-VSCC inhibitor. In contrast, no clear direct effect was observed on either *Col10a1* or *Alpl* gene expression upon NNC administration (FSS NNC) relative to FSS alone (FSS UT) or static controls. Importantly, no detrimental effect on cartilage matrix marker gene expression such as collagen II (*Col2a1*) and aggrecan (*Acan*) was observed when chondrocytes were treated in the presence of NNC (Static NNC or FSS NNC). In fact, a small but significant ($p=0.022$) increase in *Acan* mRNA was found when FSS NNC was compared with FSS UT (Fig. 3.7).

To ascertain whether the changes in mRNA transcript levels reflect a phenotypic change in chondrocytes, we performed 1) alcian blue staining for sulfated glycosaminoglycans, 2) alizarin red staining for assessment of the presence of calcium deposits associated with a switch to hypertrophy/ectopic calcification, and 3) collagen X immunohistochemical staining for a direct measure of hypertrophy. Whereas alcian blue staining showed no noticeable difference among the four conditions tested (Fig. 3.8A-D), alizarin red and collagen X staining depicted a visibly increased staining in chondrocytes treated with CM from sheared osteoblast (Fig. 3.8F and J) compared to those treated with CM obtained from osteoblasts sheared in the presence of NNC (Fig. 3.8G-H and K-L) and the static control condition (Fig 3.8E and I).

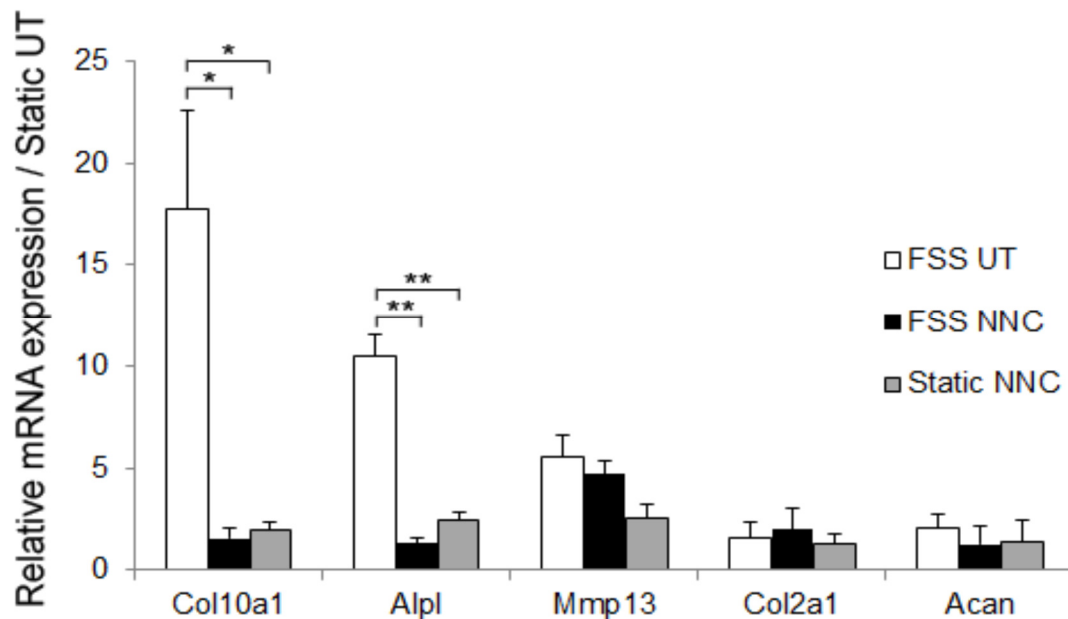


Figure 3.6: The early OA-like phenotype of chondrocytes treated with sheared osteoblast conditioned media is attenuated when treated with conditioned media derived from osteoblast sheared in the presence of the T-VSCC inhibitor, NNC55-0396. A: quantitative PCR showing the relative fold changes in mRNA levels of collagen X (Col10a1), alkaline phosphatase (Alpl), Matrix Metalloproteinase 13 (Mmp13), aggrecan (Acan), and collagen II (Col2a1) in primary mouse chondrocytes following seven days of treatment with conditioned media (CM) collected from MC3T3-E1 cells subjected to FSS alone (FSS UT), FSS with NNC55-0396 (FSS NNC) or static with NNC55-0396 (Static NNC) when compared with untreated control chondrocytes maintained under static conditions (Static UT). Error bars represent standard error of mean of the biological duplicates and * = $p < 0.05$, ** = $p < 0.01$.

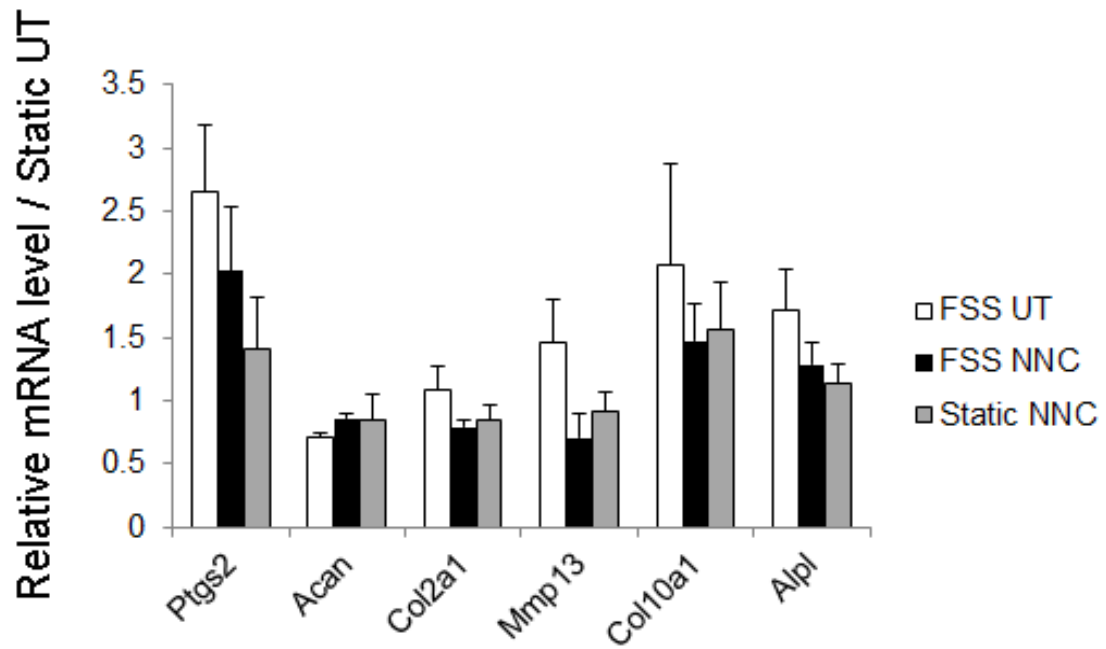


Figure 3.7: Real time PCR analysis showing the relative fold changes in the mRNA levels of cartilage genes in primary mouse chondrocytes following FSS and NNC55-0396 treatment. Primary mouse chondrocytes were grown in monolayer and collected 20 hours after FSS alone (FSS UT), FSS with NNC55-0396 (FSS NNC) or maintained under static conditions with NNC55-0396 (Static NNC) compared with the untreated static control condition (Static UT). Cyclooxygenase 2 (ptgs2), collagen X (Col10a1), matrix metalloproteinase 13 (Mmp13), aggrecan (Acan), collagen II (Col2a1), and alkaline phosphatase (Alpl). The error bars represent standard error of mean of the biological duplicates.

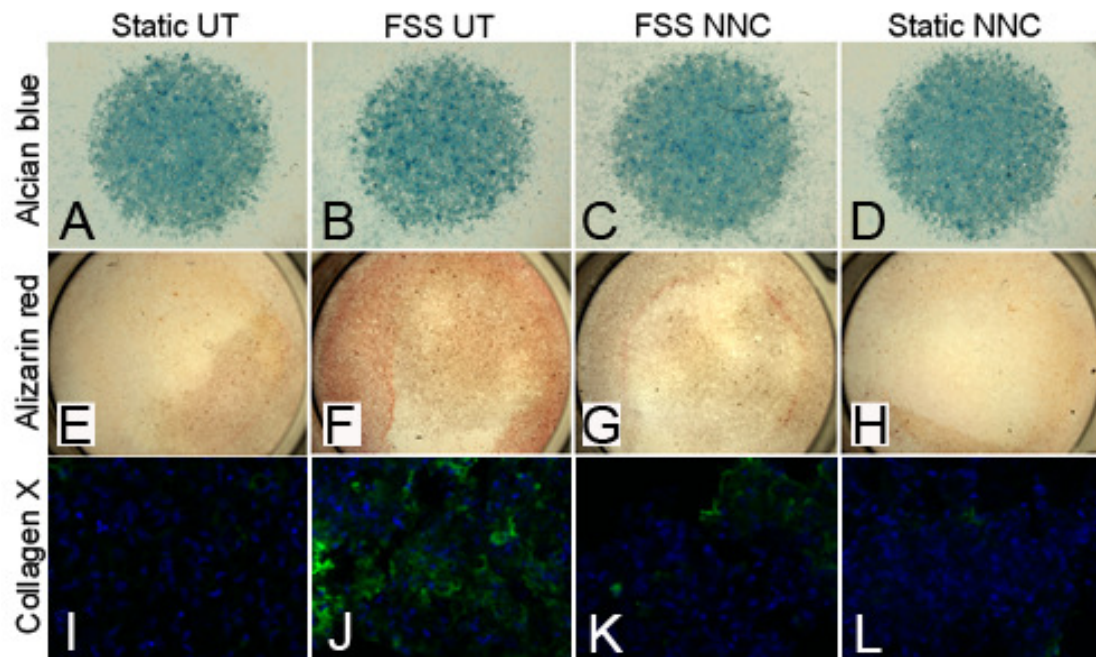


Figure 3.8: The early OA differentiation induced by FSS in primary chondrocytes is prevented in the presence of the T-VSCC inhibitor, NNC55-0396. Primary mouse chondrocytes grown in micromasses or as monolayers and stained with Alcian blue (A-B), Alizarin red (E-H) or collagen X antibody (I-L), respectively. Staining was performed following seven days of treatment with CM collected from MC3T3-E1 cells subjected to FSS alone (FSS UT), FSS with NNC55-0396 (FSS NNC), static with NNC55-0396 (static NNC) or control media obtained from MC3T3-E1 cells maintained under static conditions (Static UT). Whereas no significant difference is observed among the conditions with Alcian blue, the Alizarin red and collagen X stainings (green-collagen X, blue- Draq5 nuclear stain) showed an obvious increase in calcium deposits (F) and collagen X-specific signal (J) among chondrocytes treated with CM from FSS UT and compared with chondrocytes treated with CM from FSS NNC and both static conditions (Static UT and Static NNC).

3.5 Discussion

It is well accepted that abnormal metabolic activity associated with elevated bone mineral density and increased subchondral bone sclerosis play a key role as predictors of OA [115, 116]. Here, we propose that reduced mechanosensitivity *via* inhibition of the T-VSCC is beneficial in preventing early stage OA and used an *in vivo* gene-targeting strategy and an *in vitro* inhibitor approach to test this idea. Recent work showed that Ca_v3.2 T-VSCC KO mice exhibit reduced bone formation and bone remodeling properties following disuse-induced bone loss, suggestive of a major role for the Ca_v3.2 T-VSCC in bone mechanotransduction [105]. This phenotype indicates that the Ca_v3.2 T-VSCC null mouse model is ideal to study the *in vivo* effect of reduced mechanoresponsiveness on OA development. Although, the absence of functional Ca_v3.2 T-VSCC in these mice did not alter the overall integrity of the cartilage, Ca_v3.2 KO mice exhibited significantly less focal cartilage damage following repetitive knee loading compared to age-matched WT control mice. Since increased bone mineral density and bone turnover are strongly associated with OA, the observed results suggest that the reduced bone remodeling properties in the Ca_v3.2 KO mice might be beneficial in preventing OA pathogenesis [99, 100, 117]. Also it is interesting to note that there was a significant difference in the OA damage among the unloaded control knees in the MF compartment.

Several ion channels have been associated with the mechanical response of osteoblasts *in vitro* and bone formation *in vivo*, including the Ca_v1.2 L-type VSCC [118, 119], mechanosensitive cation-selective channel (MSCC) [118, 120] and the transient receptor potential vanilloid 4 channel (TRPV4) [121]. One that is of particular interest is the TRPV4 channel which has been found in both cartilage[122]

and bone [123]. This channel is known to be important in normal cartilage development [122, 124] and chondrocyte's response to mechanical stimulation [125]. Recent study performed in mice deficient for TRPV4 showed progressive cartilage degeneration in aging *Trpv4*^{-/-} mice relative to WT controls, indicative of its chondroprotective role [126]. Interestingly, development of spontaneous OA in *Trpv4*^{-/-} mice occurs in association with increased subchondral bone thickness and mineralization of the meniscal tissues. This is consistent with our findings seen in the *Ca_v3.2* KO mice, where decreased subchondral bone remodeling is associated with chondroprotection.

To delineate the role of the T-VSCC in osteoblast mechano-transduction of downstream signaling events, MC3T3-E1 osteoblastic cells were subjected to FSS with or without an inhibitor that prevents calcium currents by interfering with the gating of the T-VSCC pore-forming subunit. The observed reduction in the expression of stress-response genes such as COX2 and osteopontin following the inhibition of T-VSCC indicates that T-VSCC activity is essential for the anabolic bone response to load and is in agreement with decreased calcium signaling and the reduced bone formation rate observed in *Ca_v3.2* KO mice [105]. Previous studies demonstrate a positive relationship between subchondral bone volume and OA and indicate that bone adaptation to altered mechanical loading is associated with the release of bone-derived anabolic markers and cytokines [21, 127-129]. We next sought to determine whether factors released by mechanically stimulated osteoblasts can alter the chondrocyte phenotype *in vitro* and if T-VSCC inhibition in osteoblasts can attenuate the resulting pro-catabolic response on chondrocytes. The chondrocyte-osteoblast co-culture model was chosen to expand on our *in vivo* study mainly because bone and cartilage are the

primary joint tissues exposed to external compressive loading *via* direct contact between femoral condyles and the tibial plateau and osteoblasts are the primary cells responsible for subchondral bone deposition. In addition, osteoblasts and osteocytes belong to the same cell lineage and are both sensitive to mechanical loading [130, 131]. More importantly, this work supports a direct role for T-VSCC and its associated calcium response to shear stress in osteoblasts and is consistent with previous T-VSCC blocker studies performed using primary bone cell cultures and an osteocytic cell line [105, 132].

As expected, the CM obtained from shear-stressed osteoblasts induced a hypertrophic phenotype in primary mouse chondrocytes. Up-regulation of collagen X and alkaline phosphatase expression by chondrocytes is indicative of hypertrophy and premature calcification, respectively; and is associated with the initial steps of OA that are generally followed by activation of a large panel of cartilage matrix degrading enzymes including MMPs [22, 133, 134]. Thus, the current data suggest that biochemical factors released from osteoblasts in response to mechanical load induce an early OA phenotype in chondrocytes. Prasad, *et al.* showed, using the same co-culture system, that media derived from osteoblasts obtained from OA patients induced a similar hypertrophic response in normal articular chondrocytes and significantly decreased the expression of cartilage-specific genes [22]. We were not able to observe down-regulation of cartilage-specific genes using CM derived from sheared healthy osteoblasts, which may point out to signaling differences between young healthy and aged, diseased cells. Regardless, expression of both hypertrophic markers was significantly attenuated in chondrocytes treated with CM derived from sheared osteoblasts pre-treated with the T-VSCC-specific inhibitor, supporting the

involvement of T-VSCC in the hypertrophic response of chondrocytes from bone-derived factors.

The treatment of FSS osteoblasts with the T-VSCC inhibitor did not return the expression of COX2 to static control levels. Nonetheless, subsequent treatment of chondrocytes with CM obtained from FSS NNC-treated osteoblasts reduced the levels of hypertrophic genes to baseline. This is likely because other factors in addition to prostaglandins are secreted from sheared osteoblasts as a result of load-induced T-VSCC activation. Although identifying specific bone-derived factors released upon loading of subchondral bone is beyond the scope of this paper, the results presented in this study clearly show that the co-culture FSS system is an attractive experimental system for the discovery of novel metabolites with catabolic activity on chondrocytes. As seen in this study, COX2 followed by osteopontin were also increased in human OA joints along with alkaline phosphatase activity [7, 9]. Even though this raises an obvious strategy for targeting a factor such as COX2 or a specific cytokine in OA patients, the ineffectiveness of such single factor strategies is evident from the failure of the COX inhibitors in reversing the natural history of the disease. Thus, it will be more effective to block an upstream target like T-VSCC rather than the individual downstream players, as this approach would result in impaired calcium signaling and diminished secretion of multiple bone-derived factors with pro-catabolic activity on cartilage.

To determine if chondroprotection in KO mice is due to the lack of T-VSCC in bone cells or chondrocytes, we also subjected the murine primary chondrocytes to FSS with or without a T-VSCC specific inhibitor. Direct mechanical stimulation of chondrocytes produced a minimal response when subjected to the same FSS

conditions as bone cells. Even though the observed effect occurred to a much lower extent in chondrocytes than in osteoblasts, it is noteworthy to mention that the treatment with T-VSCC inhibitor had no negative side effect on cartilage matrix markers and even resulted in a slight increase in aggrecan gene expression. This suggests that the blocking of T-VSCC may in fact have some direct favorable effect on cartilage in addition to inhibition of osteoblast-induced hypertrophic differentiation. Based on the differential response of osteoblasts and chondrocytes to FSS with T-VSCC inhibition *in vitro*, we conclude that the reduced cartilage damage in T-VSCC null mice results predominantly from the lack of T-VSCC function in osteoblasts rather than in chondrocytes.

I propose that the reduced cartilage damage observed in the KO mice is a consequence of the lack of T-VSCC in the osteoblasts rather than in chondrocytes. To confirm this, further work needs to be done with conditional knockout of T-VSCC in osteoblasts. As an alternate approach I used the primary osteoblasts extracted from the T-VSCC KO and WT mice to perform the *in vitro* experiments. But the primary WT osteoblasts exhibited a much lower response to FSS unlike the MC3T3 with only a 2 fold increase in COX2 unlike the several fold increase in MC3T3. I speculate that this could be due to the desensitization of the osteoblasts during the shaking step in the extraction process itself (Methods in Chapter 4). Other obvious explanation could be that the FSS of ~ 3 dynes/cm² induced in the rocker platform was relatively lower to produce an optimal stimulation of primary osteoblasts versus MC3T3 cells. Even though the overall response to FSS was low among the WT osteoblasts, the FSS response was attenuated in the KO osteoblasts exposed to FSS (Fig. 3.9). Although not very significant this trend is similar to the results obtained with the untreated and NNC

treated MC3T3 cells. This suggests that the in vitro results observed with the T-VSCC inhibition could be attributed to the loss of the Cav3.2 subunit.

Although, T-VSCC is not the only pathway for initial calcium influx in mechanically-loaded joint tissues [132], the current work clearly reveals that T-VSCC plays a direct role in cellular events associated with mechanical regulation of bone tissue and is subsequently responsible for inducing an early OA phenotype, which may eventually lead to cartilage thinning and loss. Therefore, we believe that blocking of T-VSCC will reduce the bone changes and pro-inflammatory cytokine production which, in turn, is important to maintain cartilage integrity. The direct continuation of this work will be to test the chondroprotective effect of T-VSCC inhibitor using local intra-articular injections in preclinical models of OA. As with any intra-articular injections and drug delivery systems, rapid clearance and degradation of the injected T-VSCC inhibitor are potential problems.[62, 112] This issue can be counteracted by conjugating T-VSCC inhibitor with hyaluronan-based microgels for time-dependent controlled delivery.[112] Although disruption of T-VSCC function was found to interfere with the normal relaxation of coronary arteries [101, 102], local administration of the T-VSCC inhibitor using a slow release delivery system will prevent systemic circulation of the drug and limit risk of side effects. One advantage to using a T-VSCC inhibitor for OA emerges from its role in nociception. In particular, Cav3.2 subunit has been implicated in modulating chronic peripheral and central pain. Indeed, the target of several novel analgesic drugs is Cav3.2 T-VSCC and local injection of a T-VSCC inhibitor may therefore be an effective treatment for OA and an alternative for systemic NSAIDs.[135-137]

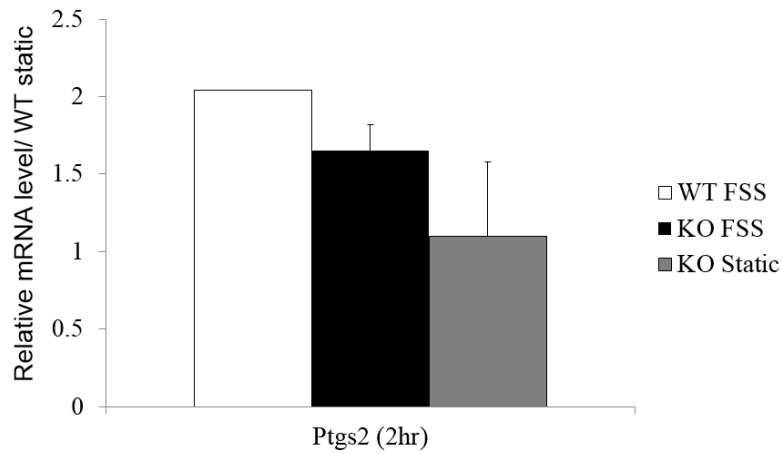


Figure 3.9: Quantitative PCR analysis showing the changes in Cyclooxygenase 2 (Ptgs2) mRNAs in WT and KO osteoblasts following FSS. The primary osteoblasts were either maintained static or were subjected to FSS for 2 hours and the relative mRNA levels were calculated relative to the static WT control condition. Error bars represent standard error of mean of the biological duplicates.

In summary, this study indicates that T-VSCC is a novel mediator of OA progression by increasing load-induced signaling between subchondral osteoblasts and articular chondrocytes. These data further suggest that the T-VSCC may be a potential target for prevention of OA progression and selective T-VSCC blockers such as NNC could be used in the treatment of load-induced OA. Future translational investigations will focus on establishing T-VSCC inhibitors as locally administered DMOAD for lessening cartilage and subchondral bone OA changes in both post-traumatic and age-related OA.

Chapter 4

INVESTIGATING THE THERAPEUTIC POTENTIAL OF INHIBITING LEPTIN FOR OSTEOARTHRITIS

4.1 Abstract

Osteoarthritis (OA) is the most common chronic degenerative disorder, yet its pathology and etiology are not completely understood. One of the major controversies is whether the subchondral bone changes precede the cartilage damage and its role in OA. Currently, there is evidence that demonstrates that stressed subchondral osteoblasts secrete pro-inflammatory substances like interleukin 6, cyclooxygenase-2 (COX-2) and prostaglandins that trigger cartilage degeneration. Here, I propose that the hormone leptin is one of the pro-inflammatory proteins secreted by the stressed OBs that stimulate the secretion of matrix-degrading enzymes from chondrocytes leading to OA. First, I show that exogenous addition of leptin to primary mouse chondrocytes stimulates the secretion of collagen X, matrix metalloproteinase 13 and Adamts5 that, in turn, are known to cause breakdown of the cartilage matrix components leading to OA. Then, I extracted primary mouse osteoblasts from calvaria and demonstrated their response to fluid shear stress (FSS) using an orbital shaker. In addition, I examined the effect of the conditioned media (CM) from the FSS-stimulated normal osteoblasts on the primary mouse chondrocytes. The CM from FSS osteoblasts increased expression of hypertrophy markers such as runx2 and collagen type X by chondrocytes compared to the CM obtained from control cells grown under static conditions. I also show that the CM of the FSS osteoblasts contains higher levels of leptin than the static CM. Therefore, I propose that leptin is one of the pro-inflammatory cytokine released from mechanically stimulated osteoblasts capable of

inducing early hypertrophic changes in the chondrocytes. Subsequently, I postulate that locally secreted leptin is a potential target to slow/prevent OA and I test the efficacy of leptin inhibitor as a therapeutic for OA in a surgical knee destabilization mouse model. The translational objective of this project is to show that intra-articular injections of leptin inhibitor can be used as a potential therapeutic for OA.

4.2 Introduction

Osteoarthritis (OA) is the leading cause of chronic disability, yet its etiology is not fully understood. There are several known modifiable and non-modifiable risk factors including age, gender, trauma, obesity. Obesity is a well-established strong modifiable risk factor for the most commonly occurring load-induced knee OA. This is because the knee joint is subjected to three to five times more mechanical load in obese individuals even with normal movements. In addition, obesity has been shown to increase the risk of developing OA on the contralateral normal side in women with OA due to altered weight loading on the non-affected side [138]. The underlying explanation for the association for OA and obesity is not just the obvious increase in mechanical loading on the joint tissue but also the elevated levels of adipokines. Leptin is an adipokine hormone with strong implications in OA and studies indicate an association between increased leptin levels and OA progression and severity [139].

Leptin is a 16 kDa non-glycosylated protein hormone of the class I cytokine superfamily. The primary function of leptin is to regulate food intake and energy expenditure. It acts centrally in the hypothalamus by inducing the secretion of the anorexigenic factor and suppressing the secretion of orexigenic factors like neuropeptide Y. In the target cells, leptin binds with the leptin receptor that belongs to the interleukin-6 cytokine family of receptors with long (OB-RL) and short isoforms (OB-RS). Leptin and leptin receptor are encoded by the genes *ob* and *db*, respectively [140].

Studies have demonstrated a strong correlation between the high leptin levels and OA and this is irrespective of whether the patient is obese or not. This is further

evident from the study performed by Griffin *et al.* (include year here) that delineates the important role played by leptin in obesity *via* increased mechanical loading. As leptin is a satiety hormone, the mice with the deletion of the *leptin* gene (*ob/ob*) and the *leptin receptor* gene (*db/db*) are morbidly obese with a 10-fold increase in adiposity, high blood glucose, and insulin levels relative to control mice [140]. Such increase in body weight is obviously expected to accelerate the development of OA. Interestingly, these mutant mice did not display a higher incidence of spontaneous OA compared with the control mice displaying a normal weight [141]. These results suggest that higher biomechanical factors alone in absence of metabolic cytokines like leptin would be insufficient to induce OA [142-144]. This idea is consistent with the observation that higher incidence of OA is seen in non-weight bearing joints of obese individuals compared to normal adults [145]. Additionally, this data supports the use of anti-leptin therapy as a novel method for slowing OA progression.

Leptin is mainly secreted by the white adipocytes and is stored in vesicles that are released through constitutive or regulated exocytosis [146]. In addition, to its major secretion from white adipose tissue, leptin has also been shown to be expressed by the other joints tissues like osteoblasts, osteocytes, chondrocytes and synovium [147, 148]. Also, shear stress induces the secretion of leptin from osteoblasts [149]. Studies show that leptin levels are high in the synovial fluid and serum of OA patients compared to the normal subjects [150, 151]. In addition, high leptin level correlates with the severity of cartilage damage and increases the expression of MMP1, MMP13 and interleukin1 β on chondrocytes [152, 153]. Overall, studies suggest that leptin has a well-established catabolic role on the cartilage and accelerates OA progression.

Based on these increased association of OA and leptin, I hypothesize that locally secreted leptin in the synovial joints is a potential therapeutic target for OA. I show that leptin has a pro-inflammatory action on primary mouse chondrocytes and mechanically stimulated osteoblasts could be a potential source. Finally, I investigate the effect of intra-articular injections of a leptin signaling inhibitor in a DMM mouse model of OA. The translational objective of this work is to use anti-leptin therapy to reverse disease progression and provide symptomatic relief in OA patients.

4.3 Methods

4.3.1 Cell Culture

Primary mouse osteoblasts were extracted from the cranium of 3-5 day-old C57BL/6J wild type pups, cleaned under microscope in 1× PBS solution and were placed in the medium containing DMEM (Invitrogen), 10% (v/v) FBS (Hyclone) and 1% Penn/Strep overnight. Next day, the calvarial halves were washed in 2ml of collagenase solution (containing 5.6 mM glucose, Mg²⁺/Ca²⁺-free PBS and type 1 collagenase [Worthington Biochemical Corporation, Lakewood, NJ] at 230 units/ml) prepared in 1×PBS and placed on a shaker at 37°C for 15 minutes to remove any residual tissues. The calvarial halves were washed again in 1× PBS and shaken for an additional 1 hour with the collagenase solution. The resulting suspension containing the osteoblasts was filtered using a cell strainer and centrifuged at 1000 RPM for 10 minutes to obtain a cell pellet. The pellet was then suspended in DMEM complete media and plated into a 6-well plate. Passages below three were used for the study and the cells were split upon reaching 80-90% confluence.

To prepare primary mouse sternal chondrocytes, rib cages were obtained from 3-5 day-old pups. The extraction protocol was adapted from Dr. K.M. Lyons' lab (UCLA, CA) and passages 1 to 3 were used for experiments. Briefly, the rib cages were serially digested using pronase (2mg/ml in 1×PBS; Roche Diagnostics) and collagenase P (3mg/ml in DMEM; Roche Diagnostics) for 15min in a 37°C incubator. The rib cages were rinsed in 1×PBS after each digestion and placed in collagenase P (0.3mg/ml in DMEM) solution overnight in a 37°C incubator. Next day the cells were

filtered using a cell strainer and then cultured in a chondrogenic media composed of DMEM supplemented with 10% (v/v) FBS and 1% (v/v) penicillin/streptomycin, 50 μ g/ml ascorbic acid and 10mM β -glycerophosphate. The chondrocytes were cultured either as micromasses or in monolayer.

4.3.2 Fluid Shear Stress (FSS)

The osteoblasts were cultured in T25 flasks and subjected to fluid shear forces on an orbital shaker platform (Stovall life sciences, Waltham, MA) at 100 rpm for 2 hours inside of a humidified incubator at 37°C and 5% CO₂. Previous studies have calculated that this system generates low magnitude shear forces of about ~1.5 dynes/cm² [154, 155]. Studies indicate that the mechanical response of the osteoblasts to fluid flow generated in the orbital shaker is similar to that obtained from an oscillatory pump [156]. In addition, this system provided advantages of sterile environment and minimal dilution of the conditioned medium (CM) for co-culture of chondrocytes.

4.3.3 ELISA

The primary mouse osteoblasts were either subjected to FSS on the orbital shaker or maintained under static conditions for 2 hours and the CM was collected after 30 minutes of rest period. The CM was concentrated 2 times and the relative leptin levels in the CM following FSS were estimated using a mouse leptin ELISA kit

(Enzo Life sciences, Farmingdale, NY) according to the manufacturer's protocol using the standards provided with the kit. The optical density was read at OD 450 and the leptin levels thus obtained were normalized to the total concentration of protein estimated by BCA (bicinchoninic acid) assay using the BCA protein assay kit (Thermo scientific)

4.3.4 Destabilization of Medial Meniscus (DMM) - Surgical Model of OA

The DMM surgery was performed on the right knee of 10-12 week-old male C57BL/6J mice as described in [157]. Briefly, a 3mm incision was made medially over distal patella and the white glistening joint capsule was opened to expose the intercondylar region. The medial meniscotibial ligament (MMTL) that anchors the medial meniscus (MM) to the tibial plateau was transected proximo-laterally leaving the medial meniscus intact. The DMM model produces insidious OA changes in the cartilage with minimal iatrogenic damage and studies demonstrates that mice develop obvious OA changes eight weeks post-surgery [157, 158]. Intra-articular anti-leptin injections (treatment injections) or saline (control injections) were administered on day 1 of the 5th, 6th, and 7th week post-DMM and the mice were euthanized at the end of 8 weeks for histological examination and scoring (Fig.4.1).

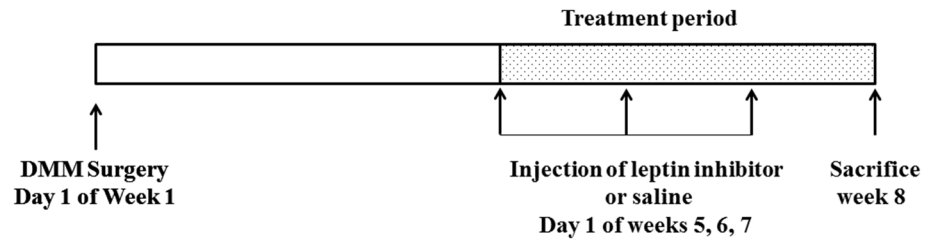


Figure 4.1: Experimental course of anti-leptin therapy: Intra-articular injection of either saline (n=5) or leptin inhibitor (n=4) was given three times at a weekly interval on day 1 of weeks 5, 6 and 7 after the DMM surgery. The mice were euthanized in the 8th week for OA analysis.

4.3.5 Anti-leptin Intra-articular Injections

Recombinant leptin Chimera (R&D Systems, Minneapolis, MN) is a leptin signaling inhibitor competing with leptin binding to its cognate receptor with an established effective dose of 0.004-0.015 μ g/ml in presence of 1 ng/ml leptin. From the previous studies, the highest leptin levels found in the human joints ranges around 20ng/ml. Therefore, the leptin inhibitor was administered at a concentration of 0.45 μ g/ml in order to target leptin levels as high as 30ng/ml.

4.3.6 Histological Staining and Scoring

The knees collected after euthanizing the mice at the end of 8 weeks post-DMM were fixed in 10% (v/v) formalin overnight and decalcified in 10% (v/v) formic acid in 1X PBS for 7 days before embedding them in paraffin blocks. Knee sections of 6 μ m thickness were obtained and about 10-15 sections from each knee were stained with Safranin O and Fast green and the OA changes were scored using the Modified Glasson et al. (2007) scoring scale by two blinded scorers (who did not have access to the identity of the sections) [157]. The mean of both the scorers for the treated (anti-leptin injected) and control (saline injected) were obtained for statistical analysis.

4.3.7 Statistical Analysis

The mean histological scores of the control and treated knees were analyzed using the Kruskal-Wallis test, a non-parametric statistical test. p values less than 0.05 were considered significant [114].

4.4 Results

4.4.1 Leptin has a Pro-inflammatory Effect on Chondrocytes

Effect of exogenous addition of recombinant mouse leptin on primary mouse chondrocytes was assessed at different concentrations (1nM, 10nM, 50nM, and 100nM). Twenty-four hours of treatment with leptin increased the gene expression levels of collagen X (Col10a1) and matrix-degrading enzymes like matrix metalloproteinase 13 (Mmp13) and aggrecanase 2 (Adamts5) (Fig. 4.2 even at the lower concentrations tested). To assess the effect of leptin (10nM) on proteoglycan content and mineralization, alcian blue and alizarin red staining were performed on the primary chondrocytes grown for seven days as either micromasses or monolayers, respectively. There was a marked decrease in the alcian blue and an increase in alizarin red among the chondrocytes treated with leptin compared to the control untreated cells (Fig. 4.3).

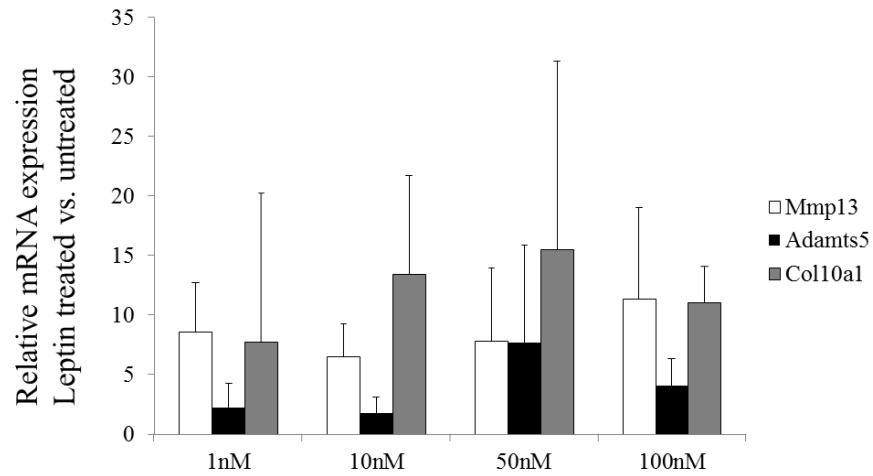


Figure 4.2: Real-time PCR analysis showing the relative fold changes in the mRNA levels of cartilage matrix degrading enzymes after leptin treatment. Primary mouse chondrocytes were collected after 24 hour of treatment with leptin at different doses (1, 10, 50 and 100 nM) and compared with the untreated control condition. Matrix metalloproteinase 13 (Mmp13), Adants 5, collagen type X (Col10a1). The error bars represent standard error of mean of the biological replicates.

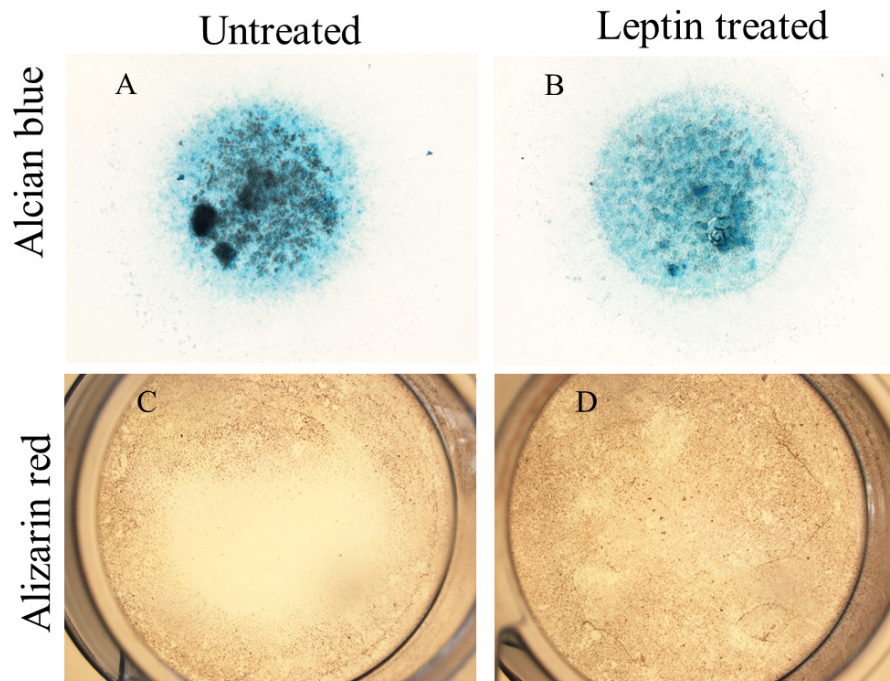


Figure 4.3: Alcian blue and alizarin red stainings of the primary chondrocytes grown as micromasses and monolayers respectively following leptin treatment. Leptin treatment (10nM) for 7 days induced a decrease in glycosaminoglycan (B) among the chondrocytes compared with untreated control cells (A). Alizarin red staining show that the leptin treatment increased the calcium deposits in the chondrocytes (D) compared to the untreated chondrocytes (C)

4.4.2 Characterization of the Primary Osteoblasts Response to FSS

Levels of the early shear response gene, *Ptgs2* also known as cyclooxygenase 2 (*Cox2*) was measured to demonstrate the response of the primary mouse osteoblasts to FSS using the orbital shaker. Osteoblasts grown in monolayers were either subjected to FSS or maintained under static conditions for 2 hours. Quantitative RT-PCR performed after 2 hours showed about an eighteen-fold increase in *Ptgs2* (*Cox2*) mRNA levels following FSS versus static condition (Fig. 4.4A). Similarly western blot analysis performed with the cell extracts obtained after 2 hours of FSS demonstrated an elevation in *Cox2* protein levels following FSS compared to static condition (Fig. 4.4B). However, there was no significant change in the levels of the late-shear response gene, osteopontin (*spp1*).

4.4.3 Conditioned Media (CM) from Mechanically Stimulated Primary Osteoblasts Induces the Expression of Markers of Hypertrophy by Primary Chondrocytes

To determine whether the primary osteoblasts subjected to a relatively low magnitude FSS are capable of inducing catabolic response on chondrocytes, a co-culture was performed as described under Chapter 3. The chondrocytes treated with the CM from FSS osteoblasts displayed an approximate 1.5-fold increase in two markers of hypertrophy: collagen type X (*Col10a1*) and Runx2 (transcription factor) compared to the static group. No noticeable change was found for the matrix-degrading enzymes Mmp13, specific for collagen type II. Also, the expression levels of the two cartilage ECM genes (*Acan* and *Col2a1*) were not significantly different among the chondrocytes treated with CM from FFS-treated osteoblasts and the static osteoblasts (Fig. 4.5).

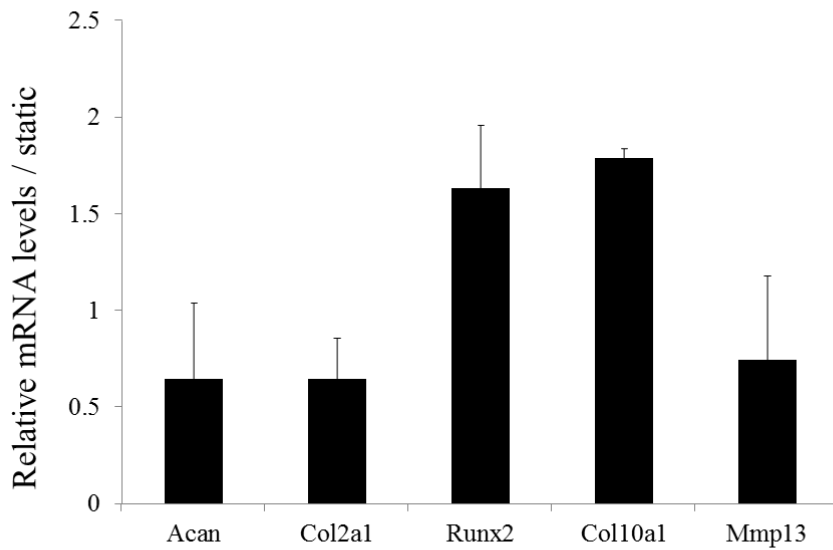


Figure 4.5: Quantitative PCR analysis showing the fold changes in the mRNA levels of cartilage components in primary mouse chondrocytes following seven days of treatment with conditioned media (CM) collected from primary osteoblasts subjected to FSS compared with control chondrocytes treated with CM collected from static osteoblasts. Aggrecan (Acan), collagen type II (Col2a1), transcription factor Runx2, collagen type X (Col10a1) and metalloproteinase 13 (Mmp13). Error bars represent standard error of mean of the biological duplicates.

4.4.4 Mechanically Stimulated Primary Osteoblasts Secrete Leptin

In order to investigate whether mechanically stimulated osteoblasts derived from bone tissue are a potential source of local leptin secretion, an ELISA assay was performed with the conditioned media (CM) collected 30 minutes following 2 hours of FSS and this was compared to the leptin levels found in the CM of the osteoblasts maintained under static conditions. There was nearly a two-fold increase in leptin levels in the osteoblasts subjected to FSS compared to static osteoblasts (Fig. 4.6).

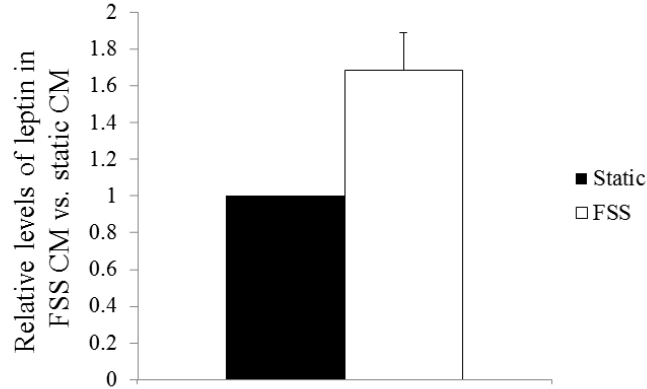


Figure 4.6: Leptin levels measured in the conditioned media (CM) of the primary mouse osteoblasts following FSS. CM from primary osteoblasts were collected 30 minutes following 2 hour FSS and the leptin levels were estimated using an ELISA approach. Leptin levels were normalized to the total protein levels in the CM quantified using BCA analysis. There was a 1.7-fold increase in leptin levels in the FSS CM compared to the static CM. The error bars represent the standard error of mean of the biological triplicates.

4.4.5 Effect of Intra-articular Injections of Leptin Inhibitor Following Mouse Model of Post-traumatic OA

To investigate the potential therapeutic effect of blocking leptin, intra-articular knee injections of a leptin antagonist were given to mice which were experimentally induced to develop OA *via* DMM surgery. The injections were given three times at a weekly interval starting at week 4 after DMM surgery and the mice were sacrificed one week after final injection. The histological scoring showed no significant difference ($p=0.233$) in the OA scores between the group treated with the leptin antagonist ($n=4$) and the control untreated group ($n=5$). The comparison between the individual compartments also showed no significant difference between the control and the treated group. However, a trend of decreased overall scores was seen in the group treated with the leptin antagonist compared with the saline treated control group (Fig. 4.7).

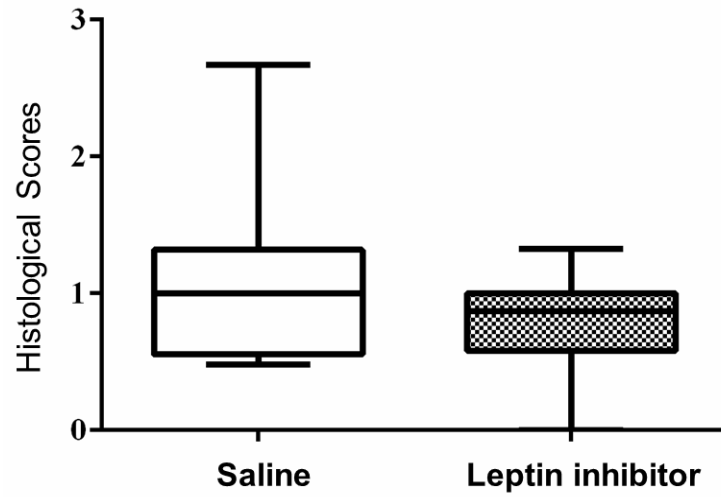


Figure 4.7: Boxes and whiskers graph showing the median (central line), 25-75 % (box) and the entire range (whiskers) of histological OA scores obtained in the control saline and leptin inhibitor treated mice. Statistical analysis between the groups showed no significant difference. p value is 0.233; $n=5$ for saline group and $n=4$ for leptin inhibitor group.

4.5 Discussion

Osteoarthritis is a highly prevalent disabling joint disease and its prevalence is expected to double by year 2020. This enormous increase is mainly attributed to obesity, the single most important and major risk factor for knee OA [51]. Although prevention and weight reduction seem to be a logical way to reduce the incidence of OA, effective therapeutic strategies need to be focused on the two causative factors - increased mechanical load itself and the increased levels of adipokines like leptin. Recent studies suggest leptin could be the metabolic link between obesity and OA [142]. Even in non-obese individuals, leptin levels are increased in the osteoarthritic cartilage, subchondral bone, and osteophytes when compared to the normal joint cartilage [151]. Interestingly, female OA patients have higher levels of free leptin in the synovial fluid than male OA patients and it is intriguing to comment that leptin could be the possible explanation for the increased incidence of OA in females [148, 159]. Also higher leptin levels were consistently observed in the synovial fluids of the OA patients compared to the normal adults [150, 160, 161]. Based on such strong associations of leptin with OA, this study aims at investigating the potential therapeutic effect of blocking leptin locally in knees of OA subjects.

Primary chondrocytes treated with leptin at various concentrations show significant elevation of the matrix-degrading enzymes (MMP13 and ADAMTS5) and the marker of hypertrophy marker, collagen type X even at the lowest leptin concentration used (1nM). This observation is physiologically relevant because the concentration of leptin in synovial fluid associated with OA has been shown to be around 20ng/ml (corresponding to ~1nM) in human subjects [160, 161]. Even at the translational level, leptin treatment decreased the new matrix deposition by the

chondrocytes as evident from the decreased alcian blue staining for polyanions in proteoglycans. Additionally, this loss of the chondrocytic phenotype was accompanied by an increase in alizarin red staining indicative of a mineralizing phenotype characteristic of early OA.

Leptin was shown to up-regulate the levels of nitric oxide synthase and nitric oxide (NO) in synergism with interleukin 1 β and interferon γ . Interleukin 1 β is the major pro-inflammatory cytokine in OA and it is well established that NO induced by leptin can also regulate the secretion of other matrix degrading enzymes and regulate apoptosis of chondrocytes thereby playing a crucial role in maintaining the cartilage ECM [162]. Also leptin induces the secretion of the matrix-degrading enzymes like MMP3 and MMP13 that are capable of breaking down aggrecan and collagen type II, respectively. As these ECM components are important to maintain the cartilage homeostasis, their breakdown results in cartilage degradation and onset of OA [152]. More importantly, leptin is also known to increase the levels of interleukin 8, another established cytokine among the human synovial fibroblasts extracted from OA subjects [163]. Taken together along with my data, it is undisputable that leptin acts as a pro-inflammatory cytokine capable of inducing OA changes in chondrocytes [164].

It is well established that mechanical loading up-regulates cytokine production from the subchondral bone cells [21] and these cytokines, in turn, are capable of inducing an OA phenotype on the adjacent cartilage. Prasadam *et al* (2010) also showed that the CM from the osteoblasts derived from OA patients was able to increase the hypertrophy markers in the chondrocytes. Here, I investigate whether healthy young osteoblasts subjected to low magnitude FSS secrete soluble factors into the CM, which in turn have a pro-inflammatory effect on chondrocytes. CM from FSS

osteoblasts increased collagen type X and runx2 mRNA levels in the chondrocytes and these markers are indicative of a hypertrophic early OA phenotype. However the elevation was not robust and this could be due to the low magnitude of FSS generated by the orbital shaker that may not have been optimal in stimulating the release of metabolites from osteoblasts. Therefore, higher magnitude FSS is expected to induce a dose and time-dependent release of soluble metabolites from chondrocytes. Clinically, this translates to the release of matrix-degrading enzymes when abnormal loads are subjected to the joints [35]

All the biological factors released from subchondral osteoblasts initiating the degenerative phenotype in the adjacent cartilage are yet to be characterized. Here, I show that leptin is one of the cytokines secreted by the mechanically stimulated osteoblasts. There was an elevation of leptin levels in the CM of osteoblasts after 30 min of FSS. Such rapid secretion is more likely to be the result from the release leptin molecules pre-packaged in storage vesicles rather than a *de novo* synthesis which would require a longer time period prior to release [146]. In addition, it was shown that subchondral osteoblasts extracted from OA joints secrete more leptin compared to normal osteoblasts and that leptin is capable of up-regulating its own secretion [147]. Based on these data, I propose that subchondral osteoblasts are a source of local leptin secretion in the joints and that the small and soluble leptin reaches the adjacent cartilage through microcracks and other communication pathways to induce the OA changes [128, 161].

In addition, local secretion of leptin in knee joints could occur from other cells as well including the adipocytes that are present in the knee infrapatellar fat pad and chondrocytes in addition to subchondral osteoblasts [159, 165]. Even though leptin is

found in higher amounts in almost every tissue of OA joints, synovium and adipocytes appear to be the major sources of leptin secretion. Subsequently, it would be interesting to see if the CM collected from the mechanically sheared normal adipocytes contain increased levels of leptin and can induce a hypertrophic phenotype in chondrocytes.

Whether local leptin secretion occurs from subchondral osteoblasts, adipocytes or the synovial lining of the joint cavity, the pro-inflammatory action of leptin on chondrocytes is well established [164]. Therefore, I postulate that blocking leptin through intra-articular leptin inhibitor injections will counteract the pro-inflammatory response initiated by leptin on chondrocytes and slow/inhibit further damage of the cartilage.

Therapeutic effect of leptin inhibition was investigated by injecting a commercially available leptin antagonist blocking leptin activity into the intra-articular cavity of mouse knees that were previously subjected to DMM surgery. This model mimics the natural sequence of molecular events that eventually lead to post-traumatic OA by altering knee biomechanics and forcing mechanical load to be focused on a relatively smaller area causing cartilage damages in the medial side [157].

The histological analysis of the knees showed no significant difference in the OA scores between the DMM knees treated with leptin antagonist and the control saline treated knees, although a trend was apparent with lesser OA scores in the knees treated with leptin inhibitor. The absence of significant difference could be due to various reasons. It could have been that the sample size was too small to demonstrate any significant differences and this can be addressed by a repeating the study to increase the statistical power. Another potential reason is the rapid clearance and

degradation of the injected leptin signaling inhibitor, as this could have abridged the protective and maximal effect of the leptin inhibitor. An effective approach to negate this possibility is to use a bioactive delivery vehicle that can aid in providing a slow prolonged release of the inhibitor thereby preventing its degradation and rapid clearance [62, 112, 166]. Also such approach to prolong the retention would reduce the need for multiple injections and increase the drug compliance. DMM is known to induce moderate to severe structural changes in the cartilage and it is possible that the chondrocytes had already reached a non-reversible degradative phenotype when the leptin inhibitor was injected. Therefore, milder OA models such as the chemically induced or load-induced models (presented under Chapters 2 &3, respectively) of OA may be valuable alternatives for studying the efficacy of leptin inhibitor in the absence of a delivery vehicle.

Pain is one of the most important debilitating factors of OA with various underlying mechanisms including nociceptive and neuropathic pathways [160]. Although there are several explanations for its etiology, obesity and body mass index (BMI) have been shown to strongly and independently correlate with the OA pain severity. Interestingly, weight loss alone did not reverse the pain implicated by the high BMI [167, 168]. This again suggests that adipokines like leptin might very well play a role in OA pain and it was shown that a low to moderate co-relation can exist between the adipokine levels in synovial fluid and OA pain [160]. Also, there is a close association between the inflammation of the adipocytes in infra-patellar fat pad and pain intensity [51]. Subsequently, it would be interesting to see if the combination of the leptin inhibition and weight loss accounts for the full reversibility of OA pain in

obesity. This combination therapy can be used as a strategy in tailoring a cause and patient-based treatment approach that can be applied for obese OA patients.

A future direction for this work could be aimed at studying the progression of OA in the leptin-deficient mice (db/db mice and ob/ob mice) following the induction of OA either by surgical or *in vivo* loading OA models. This would provide details and explanation regarding the association of OA changes in cartilage and subchondral bone and leptin. Various time points can provide details regarding the chronological order of cartilage and bone changes in OA. These studies will also provide valuable insight about the role played by biomechanical, metabolic, and genetic effects of leptin and obesity in OA [144]. Combining such studies with periodic collection of serum after inducing OA can also help identify novel biomarkers for OA, like leptin [169].

Chapter 5

GENERAL DISCUSSION

OA is a highly prevalent progressive joint disorder characterized by articular cartilage degeneration and metabolic changes in subchondral bone and the synovium. The pathogenesis of OA is complex and not fully understood. Being avascular and aneurotic, cartilage is notoriously known for its poor capacity for regeneration [170]. As early as 18th century, William Hunter stated that "ulcerated cartilage is a troublesome thing and that once destroyed, it is not repaired" [171]. In addition, the clinical diagnosis of OA mostly occurs at the later stages of OA progression, where the damage to the chondrocytes and ECM is way beyond repair. Due to these challenges there are no successful pharmacological interventions available for treating the disease. Therefore it is important to understanding the molecular mechanisms involved in the initiation and progression of the disease. Another limitation in the OA research is that the studies aimed at developing therapeutics mainly target the cartilage considering it to be the tissue causing the symptoms [51]. Since OA is a disease involving the entire joint, it is crucial to focus equal attention to the other joint structures like the subchondral bone and synovium to effectively address the disease. In this dissertation, I aim to understand the various biochemical molecular events underlying the cartilage and subchondral bone changes in OA. I uncover novel targets and therapeutics for OA by targeting the cartilage and subchondral bone that can be applied at the early and later stages of OA (Fig. 5.1). I have demonstrated the usefulness of PlnD1-HA vehicle for BMP2-controlled delivery using the mild reversible papain mouse model of OA. I also demonstrate the important role played by subchondral bone mechanotransduction through T-VSCC signaling and the

chondroprotective role of T-VSCC inhibition using a load-induced mouse model of OA. Finally, I identify leptin as one of the subchondral bone-derived metabolites that display a pro-inflammatory action on chondrocytes. Subsequently, I propose that inhibition of leptin and T-VSCC may be used as therapies for the prevention of spontaneous OA and post-traumatic OA. These novel strategies combined with sensitive biomarkers for the early detection can be effectively applied to provide non-surgical treatment to the OA patients and limit permanent debilitating joint damage.

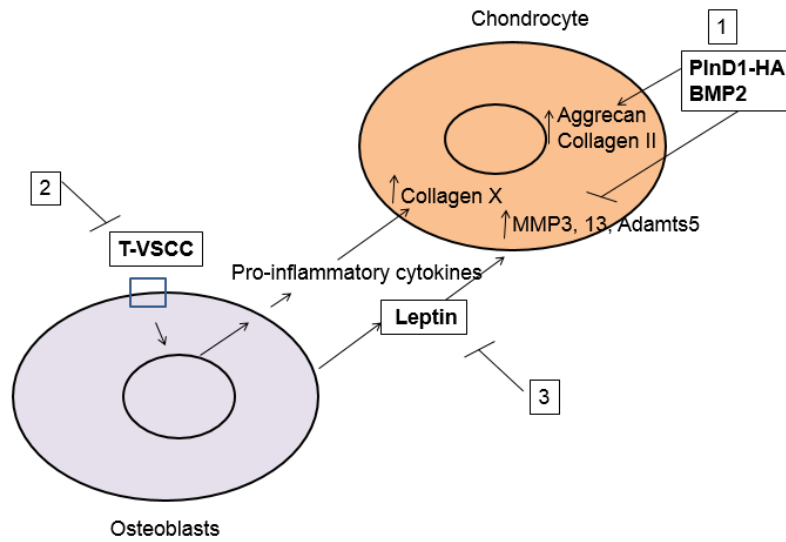


Figure 5.1: Schematic summary of the dissertation chapters: Novel targets and therapeutics for OA: 1- Chapter 2- Sustained delivery of BMP2 using HA PInD1 vehicle increases synthesis of matrix components and reduce the matrix degrading enzymes and the OA progression. 2- Chapter 3 - T-VSCC can be targeted to inhibit the early OA phenotype induced by the subchondral bone derived cytokines.

5.1 Growth Factor Therapy with BMP2 for OA

Several growth factors are implicated to have anabolic and differentiation action on cartilage like BMPs (2,4,6,7,9,13), transforming growth factor β (TGF- β), fibroblast growth factors (FGF-2,4,8) and insulin-like growth factor 1 (IGF-1). These growth factors have been shown to fine tune chondrocyte growth, differentiation, development and gene expressions. However, when these growth factors are given individually as treatment for OA in animal models, their effectiveness is not very optimal. For instance, the full differentiation and mitogenic potential of IGF-1 requires the presence of other growth factors like FGF. Also it was shown that BMP2 itself was not able to abolish the pro-inflammatory effect induced by interleukin 1 β , but such therapeutic effect is desirable to effectively safe guard the cartilage from further degradation [48]. Therefore, future work should test if this deficiency is overcome by injecting a combination of two growth factors or growth factor with cytokine inhibitor. Such therapy combinations can also catalyze the repair process when administered along with the cartilage transplants.

Polypeptide growth factors like IGF1, TGF- β 1, FGF2 were shown to regulate their own gene expression and protein production [172]. Therefore it would be interesting to study the regulation and the synergistic effect of co-administrating BMP2 and another polypeptide growth factor using the PlnD1-HA vehicle. Other interesting combinations are the two FDA-approved BMPs- BMP2 and 7. Also BMP7 have been shown to be effective in preventing cartilage degeneration using animal models of OA [173, 174]. In the study performed by [173], BMP7 was administered on a weekly basis in rats to affect the strenuous running induced OA damage. Clinically such weekly injections can amount to reduced patient compliance due to

frequent injections. This can be overcome by using a delivery vehicle like PlnD1-HA that can prolong the release of a single injection over relatively longer periods of time while preventing the degradation of the growth factors. The PlnD1-HA delivery system was able to sustain the effect of BMP2 in preventing cartilage damage for about two weeks following single injection and this effect was similar to that observed at 1 week post injection. Such sustained activity and longer injection intervals is essential to reduce the iatrogenic cartilage injuries that can result from frequent intra-articular injections. BMP7 injection was also found to up-regulate its own expression *in vivo* in rat knees that lasted for more than seven days after single injections [173]. This is a desirable effect that would complement the chondrocytes attempting to replace the cartilage matrix in OA. For all these reasons, future work should focus on administering the chondrogenic BMPs using a vehicle like the PlnD1-HA.

Growth factors can be effective in the initial stages of the OA progression by stimulating chondrocytes of normal phenotype to replace the lost matrix [48, 175]. Such growth factor therapy can prove inefficient once the chondrocytes adopt a more degradative phenotype in the later stages of OA, due to increased secretion of BMP antagonists [7, 61]. Studies show that BMP2 itself can up-regulate the expression of BMP antagonists like noggin and gremlin in cell cultures, which in turn can negate the potential actions of BMP2 [176, 177].

The PlnD1-HA has all the desirable properties expected out of a delivery system. Being native cartilage components, PlnD1 and HA has no chance to provoke an inflammatory reaction and are naturally bio-degradable. The potentiating and modulating activities of PlnD1 and HA in a time- and space-dependent manner is well established. Also the other modalities to deliver growth factors like BMPs include

entrapment, adsorption and covalent binding. Such delivery methods can produce a burst release of BMP in large quantity and this can induce ectopic bone formation rather than just cartilage formation. The PInD1-HA shows a minimal burst release with a more sustained presentation of growth factor with linear release kinetics and almost no hypertrophic effect on cartilage. Also covalent binding and entrapment can lead to loss or modification of bioactivity due to conformational changes. Such disadvantage is absent in the PInD1-HA system as the unique heparin binding capacity of perlecan domain 1 is exploited in this process. Another main challenge that must be overcome by the delivery system is the high mechanical stresses subjected to the joint on a regular basis. Again this is inherently present with the PInD1-HA as the important function of the proteoglycans and hyaluronic acid is to provide compressive stiffness to the cartilage. All these unique features render PInD1-HA a desirable biomimetic delivery vehicle for the controlled release of growth factors [55, 62, 166] .

5.2 Targeting Subchondral Bone *via* T-VSCC Inhibition for OA

There is increasing evidence that OA is a disease resulting from joint failure as a whole and the role of subchondral bone in the initiation and progression of OA is irrefutable. The subchondral bone sclerosis and osteophytes are hallmarks of late OA. As a result, the subchondral bone and its derivatives continue to be obvious targets to develop new biomarkers and therapeutics for OA.

Studies show strong association with increased bone mineral density (BMD) and abnormal bone scan with knee/hip OA in human subjects [7, 178]. Further evidence is the well-established inverse relation between osteoporosis and OA and this

again can be explained due to the presence of high bone density among the OA patients [138]. To further investigate whether the reduced mechanosensitivity helps prevent the initiation/progression of OA, I induced OA in the $Ca_v3.2$ TVSCC KO mice that was shown to exhibit reduced bone mineral apposition following unloading [105]. The reduced OA scores in the KO mice compared to the WT controls emphasize the association of chondroprotective effect and reduced bone formation properties.

The non-invasive loading mouse model of OA was described by Poulet *et al.*, 2011 and they showed that the repetitive loading regimen induced osteophyte formation and ossification of meniscus along with cartilage damage in the WT mice [107]. The T-VSCC KO mice used in my study was shown to exhibit reduced bone mineral density and this is associated with reduced cartilage damage. However either study does not demonstrate the chronological order of cartilage and bone changes in OA. To pinpoint these sequential changes, further studies need to be done at various time points with the T-VSCC KO and WT mice to compare and predict the chronologic development of bone and cartilage changes. Also, evaluation of the subchondral bone changes by immunodetection of bone anabolic markers coupled with micro-CT can yield more information regarding the concurrent bone changes occurring along with the cartilage changes.

It is well established that the T-VSCC and L-VSCC are the major regulators of intracellular calcium in the osteocytes and osteoblasts respectively. The use of T-VSCC inhibitor, NNC 55-0369 blocked the peak intracellular calcium response following shear more effectively among the osteocytes than the osteoblasts. Notably, the calcium response following shear was reduced to about half among the osteoblasts which is similar to my results observed with the COX 2 levels that was reduced to

about half following T-VSCC inhibition [105]. As osteocytes are a major cell type in the subchondral bone, it would be relevant to investigate the effect of the T-VSCC inhibition in an osteocytic cell line considering the well-known function of osteocytes in bone mechanosensation through T-VSCC. As the extraction of the primary osteocytes is very challenging, an alternative approach is to use osteocyte-like clonal cell lines such as MLO-Y4.

In order to evaluate the role of T-VSCC among the chondrocytes, the primary mouse chondrocytes were subjected to hypotonic swelling and the resulting calcium signaling response was measured. There was no significant change in the intracellular calcium response with blockage of the T-VSCC function using NNC 55-0369. Similarly there was no marked difference in the intracellular calcium peak among the primary chondrocytes extracted from WT and the T-VSCC KO mice. This suggests that T-VSCC has a more profound effect through their downstream signaling in the bone cells than the chondrocytes. However further work with conditional knockouts in the bone cells and chondrocytes will be needed to validate this finding.

I grew the chondrocytes in the monolayer in order to subject them to FSS. This is associated with several limitations. Firstly, the chondrocytes grown in monolayer does not mimic the *in vivo* distribution of chondrocytes in addition to losing their inherent biomechanical properties. This can be overcome by growing the chondrocytes in micromasses or pellets. However, it would be more appropriate to use a compressive loading system to mechanically stimulate the cells rather than FSS as compressive loading would be more physiological and closer to the *in vivo* loading experienced by the chondrocytes [179]. Also the response to FSS among the chondrocytes was much lesser compared to that of osteoblasts. This could be

explained due to the lesser magnitude of FSS (3 dynes/cm²) and/or the shorter duration used. Previous studies suggest that the use of higher FSS (20 dynes/cm²) for “prolonged period can induce the expression of OA genes [180]. Therefore future studies can be conducted with the chondrocytes grown in pellets or micromasses and using higher magnitude compressive loading to study the effect of T-VSCC function in chondrocytes.

5.3 Discovery of Novel Targets and Biomarkers for OA: Subchondral Bone Derived Cytokines

Loss of T-VSCC and its downstream function resulted in the inhibition of hypertrophic OA phenotype induced by the CM from the FSS osteoblasts. Such OA phenotype in chondrocytes is induced by the osteoblasts derived cytokines and many of them are yet to be identified. Identifying these individual soluble factors is essential to understand the missing parts of OA pathology and also to develop novel biomarkers and therapies. An effective way to identify the differential metabolites is through metabolomics approach, where the metabolites are isotopically labeled for the mass spectrometry identification. Such metabolites originating from the subchondral bone are known to communicate with the cartilage through microcracks and microfractures that occur following bone fatigue. These appear as fine hairlines and broader gaps extending between the subchondral bone plate and the calcified layer of the cartilage. It is also believed that such communication also provides nutrients to the avascular cartilage by means of vascular invasion from the medullary cavity in the bone [127]. The diffusion rate of sodium fluorescein (376 Da) was quantified to be about 0.07 and 0.26 $\mu\text{m}^2/\text{sec}$ between calcified cartilage and subchondral bone. Taken together these

studies provide evidence for both direct and indirect communication pathways between the bone and cartilage [128].

The anabolic markers of bone such as osteocalcin, osteopontin and COX2 are found increased in human OA joints along with increased alkaline phosphatase activity [7, 9]. My experiments show that the osteoblasts exposed to FSS demonstrate an increase in osteopontin and COX2 that are both known to be implicated in OA. Also the CM from the FSS osteoblasts induced an increase in alkaline phosphatase gene levels on chondrocytes. All these genes were attenuated with T-VSCC inhibition, supporting the idea that such therapy is a promising approach for chondroprotection. COX2 is an enzyme required for the synthesis of prostaglandins (PGs) and PGE2 has been shown to promote MMP production causing cartilage damage. It augments inflammatory response in the cartilage, synovium and bone cells [7]. Also, COX2 is an established subchondral bone derived cytokine with implications in OA. In addition, overload and stretch can stimulate the chondrocytes to secrete prostaglandins along with other cytokines and metalloproteinases that, in turn, decreases matrix synthesis and degrade ECM [148]. All these evidences advocate targeting COX2 for OA treatment. However, COX inhibitors like NSAIDS are already commonly prescribed for OA; yet they are found to be inefficient in reversing the natural progression of the disease. This scenario suggests that inhibition of just one subchondral bone derived inflammatory mediator may not be an effective approach, as the other cytokines can take over catabolic events. Therefore, I propose that blocking T-VSCC upstream of these cytokine-dependent pathways would be an effective strategy rather than inhibiting the individual players.

5.4 The Potential Use of Leptin Inhibitor as a Therapeutic for OA

Leptin is clearly a potential target for OA, given its well-established pro-inflammatory action and strong association with OA. However, the intra-articular injection of leptin antagonist failed to significantly reduce the OA damages following experimental induction of OA *via* knee destabilization. As discussed earlier, this could be due to the insufficient power of the study or the rapid clearance and degradation of the injected particles. Another explanation could be the late administration of the therapeutic after the onset of the irreversible cartilage changes following the DMM surgery. This possibility can be addressed by conducting further study with milder models like the papain model of OA.

Moreover, some studies propose an anabolic action for leptin on cartilage matrix. Intra-articular injection of leptin was shown to increase the synthesis of proteoglycans and growth factors like IGF-1 and TGF β [148, 181]. This could be due to a bimodal action of leptin, as higher levels of leptin has reduced anabolic effect and causes matrix degradation. It is possible that leptin requires the presence of other matrix degrading cytokines like interleukin 1β to exert its pro-inflammatory action [148]. However in this scenario, the use of leptin inhibitor alone will be insufficient in inhibiting interleukin 1β and preventing OA changes. This could be a reason for the ineffectiveness of leptin inhibitor in preventing the cartilage changes following the post-traumatic DMM model.

I demonstrate that mechanically stimulated osteoblasts are a source of local leptin secretion and the CM from FSS osteoblasts induce hypertrophic changes in the chondrocytes. Further studies are required to estimate the relative contribution of leptin as a subchondral bone-derived cytokine and to establish a link between the leptin in the FSS osteoblasts CM and the hypertrophic changes on chondrocytes. To

this end, current studies in the lab are focused on investigating the effect of using leptin inhibitor in counteracting the hypertrophic changes produced by the FSS osteoblasts on chondrocytes by using co-culture techniques. This is being conducted by shearing MC3T3-E1 cells on a rocker platform as this combination produced higher hypertrophic changes among the chondrocytes (as shown in chapter 3) than with primary osteoblasts.

Other joint tissues like the adipocytes present in the patellar fat pad are an obvious local source of leptin. Interestingly the leptin levels in the synovial fluid of OA patients are greater than the levels found in the plasma [153]. Similar to the white adipose tissue present elsewhere, the infra-patellar fat pad in knee joints are known to secrete several adipokines like leptin, visfatin, resistin, adiponectin and adipisin [182]. The CM from white adipose tissue of osteoarthritic knee joints is capable of degrading collagen matrix by secreting proteolytic enzymes like MMP1 and MMP13. Leptin alone or in coaction with Interleukin-1 β induces MMP1 and MMP13 in chondrocytes by activating several pathways including JNK, Erk, p38, Akt and NF-kB [165]. Similar to subchondral bone cells, adipocytes also secrete several inflammatory mediators. The infra-patellar fat pad in OA is known to secrete the major degradative enzymes implicated in OA like interleukin 1 β , TNF α and interleukin 6 [183]. Thus, the therapeutic strategy of using leptin inhibitor will serve to inhibit the proteolytic action of synovial leptin secreted from various sources.

Chondrocytes themselves act as a source of inflammatory mediators when subjected to altered loading and FSS can induce the release of several inflammatory mediators from chondrocytes [35]. Chondrocytes possess mechanosensors that include stretch-activated channels, integrins and CD44 [184]. These mechanosensors are

connected to the ECM proteins as well as the cytoskeleton and help relay intracellular signaling. Abnormal and high compressive forces stimulate the receptors that in turn activate various signaling pathways like mitogen-activated protein kinase and NF- κ B. This results in the secretion of various proteolytic cytokines, growth factors and inflammatory mediators like prostaglandins [148]. Chondrocytes in the obese OA patients exhibit higher expression of leptin mRNA levels and this correlates with the advance cartilage damage [153]. Therefore, it would be interesting to see if the FSS on normal chondrocytes secrete higher levels of leptin similar to the FSS osteoblasts. Higher amounts of leptin secretion from mechanically stimulated chondrocytes would serve as an additional validation for the use local leptin inhibitors for OA.

5.5 Studying the Association of T-VSCC Signaling and Leptin Secretion

The Ca_v3.2 T-VSCC KO mice display reduced bone mineral density that was accompanied by chondroprotection in a repetitive load-induced model of OA. Interestingly, leptin mutant mice also display decreased subchondral bone thickness [141]. Even though the leptin deficiency resulted in a 10-fold increase adiposity, there was no increase in the knee OA development [141]. These similar associations seen in the leptin-deficient and the T-VSCC KO mice not only validate the association between subchondral bone changes and chondroprotection but also the possibility of T-VSCC involvement in leptin signaling and release. Subsequently, it would be interesting to study whether the loss of T-VSCC interferes with normal signaling pathway of local leptin secretion. This can be investigated by performing ELISA for leptin levels with the CM collected after shearing osteoblasts extracted following T-

VSCC inhibition. A reduced leptin concentration in the CM obtained from the T-VSCC inhibited osteoblasts would suggest that the T-VSCC acts upstream to the secretion of leptin.

Even though the effect of leptin on bone mass is complex, studies show that leptin increases osteoblasts activity and reduces osteoclast function, thereby promoting anabolic effect on bone [185, 186]. Similarly, T-VSCC also is involved in the normal bone formation response by regulating the secretion of prostaglandins and other anabolic factors as shown in Chapter 3. Leptin deficiency can result in decreased bone mass of the cortical compartment by exerting actions through hypothalamic signals [142]. Inhibition of T-VSCC signaling reduces the early hypertrophic OA phenotype induced by the mechanically stimulated osteoblasts potentially by interfering with the release of the pro-inflammatory cytokines like leptin. To further investigate this possibility, the osteoblasts can be pre-treated with leptin inhibitor before FSS and the effect on chondrocyte should be studied by a co-culture experiment. If the use of the leptin inhibitor reversed the hypertrophic markers induced by the FSS CM, it would suggest that leptin has a major role as a subchondral bone-derived cytokine.

5.6 Final Conclusions

OA is the most common cause of chronic disability in United States and worldwide. It is primarily a disease of “wear and tear” of the joint structures with no promising interventions capable of reversing the disease process. For a successful management of OA, it is critical to intervene at an earlier stage of the disease when the damages are still reversible. I demonstrate that supplementing chondrogenic factor like BMP2 at initial stages of OA using PlnD1-HA delivery vehicle can help reduce the

progression of degradative changes. As OA is a disease of the synovial joint organ as a whole and not just cartilage, it is essential to target the surrounding structures and biochemical factors causing OA rather than the cartilage itself [51, 171]. Specifically, the mechanical factors associated with loading are strong contributors of OA etiopathology. Yet, the cellular pathways induced following mechanical stress are not fully understood. Here, I demonstrate that T-VSCC plays an important role in the subchondral bone-induced cartilage changes in OA and that chondro-protection result from the loss of T-VSCC. In order to develop efficient pharmacological interventions, it is crucial to understand and target the various biochemical factors involved in the etio-pathology of the disease [138]. To this end, I show that leptin, a well-established cytokine can be a therapeutic target to reduce the pro-inflammatory progression in OA. This can be applied as a patient-based approach for obese patients in addition to physical interventions such as weight reduction. Overall, further evaluation of the potential targets and therapeutics presented in this dissertation will help increase the quality of life and reduce the health care costs associated with the knee replacement surgeries for OA.

REFERENCES

1. Aigner T, Stöve J. Collagens--major component of the physiological cartilage matrix, major target of cartilage degeneration, major tool in cartilage repair. *Adv Drug Deliv Rev* 2003; 55: 1569-1593.
2. Gelse K, Pöschl E, Aigner T. Collagens--structure, function, and biosynthesis. *Adv Drug Deliv Rev* 2003; 55: 1531-1546.
3. Bruckner P, van der Rest M. Structure and function of cartilage collagens. *Microsc Res Tech* 1994; 28: 378-384.
4. Sophia Fox AJ, Bedi A, Rodeo SA. The basic science of articular cartilage: structure, composition, and function. *Sports Health* 2009; 1: 461-468.
5. Eyre DR, Weis MA, Wu JJ. Articular cartilage collagen: an irreplaceable framework? *Eur Cell Mater* 2006; 12: 57-63.
6. Masuda K, Sah RL, Hejna MJ, Thonar EJ. A novel two-step method for the formation of tissue-engineered cartilage by mature bovine chondrocytes: the alginate-recovered-chondrocyte (ARC) method. *J Orthop Res* 2003; 21: 139-148.
7. Martel-Pelletier J, Pelletier JP. Is osteoarthritis a disease involving only cartilage or other articular tissues? *Eklemler Hastalik Cerrahisi* 2010; 21: 2-14.
8. Madry H, van Dijk CN, Mueller-Gerbl M. The basic science of the subchondral bone. *Knee Surg Sports Traumatol Arthrosc* 2010; 18: 419-433.
9. Kwan Tat S, Lajeunesse D, Pelletier JP, Martel-Pelletier J. Targeting subchondral bone for treating osteoarthritis: what is the evidence? *Best Pract Res Clin Rheumatol* 2010; 24: 51-70.
10. Clarke B. Normal bone anatomy and physiology. *Clin J Am Soc Nephrol* 2008; 3 Suppl 3: S131-139.
11. Chen FH, Rousche KT, Tuan RS. Technology Insight: adult stem cells in cartilage regeneration and tissue engineering. *Nat Clin Pract Rheumatol* 2006; 2: 373-382.
12. Hall BK, Miyake T. All for one and one for all: condensations and the initiation of skeletal development. *Bioessays* 2000; 22: 138-147.
13. Michigami T. Current understanding on the molecular basis of chondrogenesis. *Clin Pediatr Endocrinol* 2014; 23: 1-8.
14. Nilsson O, Marino R, De Luca F, Phillip M, Baron J. Endocrine regulation of the growth plate. *Horm Res* 2005; 64: 157-165.
15. Goldring MB. Chondrogenesis, chondrocyte differentiation, and articular cartilage metabolism in health and osteoarthritis. *Ther Adv Musculoskelet Dis* 2012; 4: 269-285.
16. Kirn-Safran CB, Gomes RR, Brown AJ, Carson DD. Heparan sulfate proteoglycans: coordinators of multiple signaling pathways during chondrogenesis. *Birth Defects Res C Embryo Today* 2004; 72: 69-88.
17. Duncan RL, Turner CH. Mechanotransduction and the functional response of bone to mechanical strain. *Calcif Tissue Int* 1995; 57: 344-358.

18. Frost HM. From Wolff's law to the Utah paradigm: insights about bone physiology and its clinical applications. *Anat Rec* 2001; 262: 398-419.
19. Huang H, Kamm RD, Lee RT. Cell mechanics and mechanotransduction: pathways, probes, and physiology. *Am J Physiol Cell Physiol* 2004; 287: C1-11.
20. Smalt R, Mitchell FT, Howard RL, Chambers TJ. Induction of NO and prostaglandin E2 in osteoblasts by wall-shear stress but not mechanical strain. *Am J Physiol* 1997; 273: E751-758.
21. Mohtai M, Gupta MK, Donlon B, Ellison B, Cooke J, Gibbons G, et al. Expression of interleukin-6 in osteoarthritic chondrocytes and effects of fluid-induced shear on this expression in normal human chondrocytes in vitro. *J Orthop Res* 1996; 14: 67-73.
22. Prasadam I, van Gennip S, Friis T, Shi W, Crawford R, Xiao Y. ERK-1/2 and p38 in the regulation of hypertrophic changes of normal articular cartilage chondrocytes induced by osteoarthritic subchondral osteoblasts. *Arthritis Rheum* 2010; 62: 1349-1360.
23. Pavalko FM, Chen NX, Turner CH, Burr DB, Atkinson S, Hsieh YF, et al. Fluid shear-induced mechanical signaling in MC3T3-E1 osteoblasts requires cytoskeleton-integrin interactions. *Am J Physiol* 1998; 275: C1591-1601.
24. Reich KM, McAllister TN, Gudi S, Frangos JA. Activation of G proteins mediates flow-induced prostaglandin E2 production in osteoblasts. *Endocrinology* 1997; 138: 1014-1018.
25. Rawlinson SC, Pitsillides AA, Lanyon LE. Involvement of different ion channels in osteoblasts' and osteocytes' early responses to mechanical strain. *Bone* 1996; 19: 609-614.
26. Li J, Duncan RL, Burr DB, Turner CH. L-type calcium channels mediate mechanically induced bone formation in vivo. *J Bone Miner Res* 2002; 17: 1795-1800.
27. Ryder KD, Duncan RL. Parathyroid hormone enhances fluid shear-induced $[Ca^{2+}]_i$ signaling in osteoblastic cells through activation of mechanosensitive and voltage-sensitive Ca^{2+} channels. *J Bone Miner Res* 2001; 16: 240-248.
28. Hung CT, Pollack SR, Reilly TM, Brighton CT. Real-time calcium response of cultured bone cells to fluid flow. *Clin Orthop Relat Res* 1995; 256-269.
29. Duncan RL, Akanbi KA, Farach-Carson MC. Calcium signals and calcium channels in osteoblastic cells. *Semin Nephrol* 1998; 18: 178-190.
30. Rubin J, Rubin C, Jacobs CR. Molecular pathways mediating mechanical signaling in bone. *Gene* 2006; 367: 1-16.
31. Klein-Nulend J, Veldhuijzen JP, de Jong M, Burger EH. Increased bone formation and decreased bone resorption in fetal mouse calvaria as a result of intermittent compressive force in vitro. *Bone Miner* 1987; 2: 441-448.
32. Donahue TL, Haut TR, Yellowley CE, Donahue HJ, Jacobs CR. Mechanosensitivity of bone cells to oscillating fluid flow induced shear stress may be modulated by chemotransport. *J Biomech* 2003; 36: 1363-1371.

33. Heep H, Hilken G, Hofmeister S, Wedemeyer C. Osteoarthritis of leptin-deficient ob/ob mice in response to biomechanical loading in micro-CT. *Int J Biol Sci* 2009; 5: 265-275.
34. Hodge WA, Fijan RS, Carlson KL, Burgess RG, Harris WH, Mann RW. Contact pressures in the human hip joint measured in vivo. *Proc Natl Acad Sci U S A* 1986; 83: 2879-2883.
35. Lane Smith R, Trindade MC, Ikenoue T, Mohtai M, Das P, Carter DR, et al. Effects of shear stress on articular chondrocyte metabolism. *Biorheology* 2000; 37: 95-107.
36. Kiviranta I, Tammi M, Jurvelin J, Säämänen AM, Helminen HJ. Moderate running exercise augments glycosaminoglycans and thickness of articular cartilage in the knee joint of young beagle dogs. *J Orthop Res* 1988; 6: 188-195.
37. Säämänen AM, Tammi M, Kiviranta I, Helminen HJ. Running exercise as a modulatory of proteoglycan matrix in the articular cartilage of young rabbits. *Int J Sports Med* 1988; 9: 127-133.
38. Brama PA, Tekoppele JM, Bank RA, Barneveld A, Firth EC, van Weeren PR. The influence of strenuous exercise on collagen characteristics of articular cartilage in Thoroughbreds age 2 years. *Equine Vet J* 2000; 32: 551-554.
39. Vanwanseele B, Eckstein F, Knecht H, Stüssi E, Spaepen A. Knee cartilage of spinal cord-injured patients displays progressive thinning in the absence of normal joint loading and movement. *Arthritis Rheum* 2002; 46: 2073-2078.
40. Wolff KJ, Ramakrishnan PS, Brouillette MJ, Journot BJ, McKinley TO, Buckwalter JA, et al. Mechanical stress and ATP synthesis are coupled by mitochondrial oxidants in articular cartilage. *J Orthop Res* 2012.
41. Buckwalter JA, Martin JA, Brown TD. Perspectives on chondrocyte mechanobiology and osteoarthritis. *Biorheology* 2006; 43: 603-609.
42. Herzog W, Clark A, Longino D. Joint mechanics in osteoarthritis. *Novartis Found Symp* 2004; 260: 79-95; discussion 95-79, 100-104, 277-109.
43. Setton LA, Elliott DM, Mow VC. Altered mechanics of cartilage with osteoarthritis: human osteoarthritis and an experimental model of joint degeneration. *Osteoarthritis Cartilage* 1999; 7: 2-14.
44. Lawrence RC, Felson DT, Helmick CG, Arnold LM, Choi H, Deyo RA, et al. Estimates of the prevalence of arthritis and other rheumatic conditions in the United States. Part II. *Arthritis Rheum* 2008; 58: 26-35.
45. Hootman JM, Helmick CG. Projections of US prevalence of arthritis and associated activity limitations. *Arthritis Rheum* 2006; 54: 226-229.
46. Felson DT. The epidemiology of knee osteoarthritis: results from the Framingham Osteoarthritis Study. *Semin Arthritis Rheum* 1990; 20: 42-50.
47. Sarzi-Puttini P, Cimmino MA, Scarpa R, Caporali R, Parazzini F, Zaninelli A, et al. Osteoarthritis: an overview of the disease and its treatment strategies. *Semin Arthritis Rheum* 2005; 35: 1-10.

48. Goldring MB. The role of the chondrocyte in osteoarthritis. *Arthritis Rheum* 2000; 43: 1916-1926.
49. Girkontaite I, Frischholz S, Lammi P, Wagner K, Swoboda B, Aigner T, et al. Immunolocalization of type X collagen in normal fetal and adult osteoarthritic cartilage with monoclonal antibodies. *Matrix Biol* 1996; 15: 231-238.
50. Das SK, Farooqi A. Osteoarthritis. *Best Pract Res Clin Rheumatol* 2008; 22: 657-675.
51. Hunter DJ. Osteoarthritis. *Best Pract Res Clin Rheumatol* 2011; 25: 801-814.
52. Caron JP, Fernandes JC, Martel-Pelletier J, Tardif G, Mineau F, Geng C, et al. Chondroprotective effect of intraarticular injections of interleukin-1 receptor antagonist in experimental osteoarthritis. Suppression of collagenase-1 expression. *Arthritis Rheum* 1996; 39: 1535-1544.
53. Felson DT, Zhang Y. An update on the epidemiology of knee and hip osteoarthritis with a view to prevention. *Arthritis Rheum* 1998; 41: 1343-1355.
54. van der Kraan PM, Buma P, van Kuppevelt T, van den Berg WB. Interaction of chondrocytes, extracellular matrix and growth factors: relevance for articular cartilage tissue engineering. *Osteoarthritis Cartilage* 2002; 10: 631-637.
55. Jha AK, Yang W, Kirn-Safran CB, Farach-Carson MC, Jia X. Perlecan domain I-conjugated, hyaluronic acid-based hydrogel particles for enhanced chondrogenic differentiation via BMP-2 release. *Biomaterials* 2009; 30: 6964-6975.
56. Blaney Davidson EN, Vitters EL, van Lent PL, van de Loo FA, van den Berg WB, van der Kraan PM. Elevated extracellular matrix production and degradation upon bone morphogenetic protein-2 (BMP-2) stimulation point toward a role for BMP-2 in cartilage repair and remodeling. *Arthritis Res Ther* 2007; 9: R102.
57. Quintana L, Muinos TF, Genove E, Del Mar Olmos M, Borros S, Semino CE. Early tissue patterning recreated by mouse embryonic fibroblasts in a three-dimensional environment. *Tissue Eng Part A* 2009; 15: 45-54.
58. Ducy P, Karsenty G. The family of bone morphogenetic proteins. *Kidney Int* 2000; 57: 2207-2214.
59. Schmitt B, Ringe J, Haupl T, Notter M, Manz R, Burmester GR, et al. BMP2 initiates chondrogenic lineage development of adult human mesenchymal stem cells in high-density culture. *Differentiation* 2003; 71: 567-577.
60. Valentin-Opran A, Wozney J, Csimma C, Lilly L, Riedel GE. Clinical evaluation of recombinant human bone morphogenetic protein-2. *Clin Orthop Relat Res* 2002: 110-120.
61. Rosen V. BMP and BMP inhibitors in bone. *Ann N Y Acad Sci* 2006; 1068: 19-25.
62. Bessa PC, Casal M, Reis RL. Bone morphogenetic proteins in tissue engineering: the road from laboratory to clinic, part II (BMP delivery). *J Tissue Eng Regen Med* 2008; 2: 81-96.

63. Blaney Davidson EN, Vitters EL, van der Kraan PM, van den Berg WB. Expression of transforming growth factor-beta (TGFbeta) and the TGFbeta signalling molecule SMAD-2P in spontaneous and instability-induced osteoarthritis: role in cartilage degradation, chondrogenesis and osteophyte formation. *Ann Rheum Dis* 2006; 65: 1414-1421.
64. Dell'Accio F, De Bari C, El Tawil NM, Barone F, Mitsiadis TA, O'Dowd J, et al. Activation of WNT and BMP signaling in adult human articular cartilage following mechanical injury. *Arthritis Res Ther* 2006; 8: R139.
65. Nimni ME. Polypeptide growth factors: targeted delivery systems. *Biomaterials* 1997; 18: 1201-1225.
66. Babensee JE, McIntire LV, Mikos AG. Growth factor delivery for tissue engineering. *Pharm Res* 2000; 17: 497-504.
67. Kirn-Safran C, Farach-Carson MC, Carson DD. Multifunctionality of extracellular and cell surface heparan sulfate proteoglycans. *Cell Mol Life Sci* 2009; 66: 3421-3434.
68. Farach-Carson MC, Carson DD. Perlecan--a multifunctional extracellular proteoglycan scaffold. *Glycobiology* 2007; 17: 897-905.
69. Rodgers KD, Sasaki T, Aszodi A, Jacenko O. Reduced perlecan in mice results in chondrodysplasia resembling Schwartz-Jampel syndrome. *Hum Mol Genet* 2007; 16: 515-528.
70. Arikawa-Hirasawa E, Watanabe H, Takami H, Hassell JR, Yamada Y. Perlecan is essential for cartilage and cephalic development. *Nat Genet* 1999; 23: 354-358.
71. Costell M, Gustafsson E, Aszodi A, Morgelin M, Bloch W, Hunziker E, et al. Perlecan maintains the integrity of cartilage and some basement membranes. *J Cell Biol* 1999; 147: 1109-1122.
72. French MM, Gomes RR, Jr., Timpl R, Hook M, Czymmek K, Farach-Carson MC, et al. Chondrogenic activity of the heparan sulfate proteoglycan perlecan maps to the N-terminal domain I. *J Bone Miner Res* 2002; 17: 48-55.
73. Yang WD, Gomes RR, Jr., Alicknavitch M, Farach-Carson MC, Carson DD. Perlecan domain I promotes fibroblast growth factor 2 delivery in collagen I fibril scaffolds. *Tissue Eng* 2005; 11: 76-89.
74. Takada T, Katagiri T, Ifuku M, Morimura N, Kobayashi M, Hasegawa K, et al. Sulfated polysaccharides enhance the biological activities of bone morphogenetic proteins. *J Biol Chem* 2003; 278: 43229-43235.
75. Ruppert R, Hoffmann E, Sebald W. Human bone morphogenetic protein 2 contains a heparin-binding site which modifies its biological activity. *Eur J Biochem* 1996; 237: 295-302.
76. Yang W, Gomes RR, Brown AJ, Burdett AR, Alicknavitch M, Farach-Carson MC, et al. Chondrogenic differentiation on perlecan domain I, collagen II, and bone morphogenetic protein-2-based matrices. *Tissue Eng* 2006; 12: 2009-2024.

77. Knudson CB, Knudson W. Cartilage proteoglycans. *Semin Cell Dev Biol* 2001; 12: 69-78.
78. Kirchner M, Marshall D. A double-blind randomized controlled trial comparing alternate forms of high molecular weight hyaluronan for the treatment of osteoarthritis of the knee. *Osteoarthritis Cartilage* 2006; 14: 154-162.
79. van der Kraan PM, Vitters EL, van de Putte LB, van den Berg WB. Development of osteoarthritic lesions in mice by "metabolic" and "mechanical" alterations in the knee joints. *Am J Pathol* 1989; 135: 1001-1014.
80. Costell M, Mann K, Yamada Y, Timpl R. Characterization of recombinant perlecan domain I and its substitution by glycosaminoglycans and oligosaccharides. *Eur J Biochem* 1997; 243: 115-121.
81. Kang QK, LaBreck JC, Gruber HE, An YH. Histological Techniques for Decalcified Bone and Cartilage. In: *Handbook of Histology Methods for Bone and Cartilage*, An YH, Martin KL Eds. Totowa: Humana Press Inc. 2003:209-219.
82. Glasson SS, Blanchet TJ, Morris EA. The surgical destabilization of the medial meniscus (DMM) model of osteoarthritis in the 129/SvEv mouse. *Osteoarthritis Cartilage* 2007; 15: 1061-1069.
83. Nagase H, Kashiwagi M. Aggrecanases and cartilage matrix degradation. *Arthritis Res Ther* 2003; 5: 94-103.
84. Kiani C, Chen L, Wu YJ, Yee AJ, Yang BB. Structure and function of aggrecan. *Cell Res* 2002; 12: 19-32.
85. McDonald J. *Handbook of Biological Statistics. Second Edition.* Baltimore, Sparky House Publishing 2009.
86. Vandesompele J, De Preter K, Pattyn F, Poppe B, Van Roy N, De Paepe A, et al. Accurate normalization of real-time quantitative RT-PCR data by geometric averaging of multiple internal control genes. *Genome Biol* 2002; 3: RESEARCH0034.
87. Venkatesan N, Barre L, Magdalou J, Mainard D, Netter P, Fournel-Gigleux S, et al. Modulation of xylosyltransferase I expression provides a mechanism regulating glycosaminoglycan chain synthesis during cartilage destruction and repair. *Faseb J* 2009; 23: 813-822.
88. Blaney Davidson EN, Vitters EL, van Beuningen HM, van de Loo FA, van den Berg WB, van der Kraan PM. Resemblance of osteophytes in experimental osteoarthritis to transforming growth factor beta-induced osteophytes: limited role of bone morphogenetic protein in early osteoarthritic osteophyte formation. *Arthritis Rheum* 2007; 56: 4065-4073.
89. Glasson SS, Askew R, Sheppard B, Carito B, Blanchet T, Ma HL, et al. Deletion of active ADAMTS5 prevents cartilage degradation in a murine model of osteoarthritis. *Nature* 2005; 434: 644-648.
90. van Beuningen HM, Glansbeek HL, van der Kraan PM, van den Berg WB. Differential effects of local application of BMP-2 or TGF-beta 1 on both

- articular cartilage composition and osteophyte formation. *Osteoarthritis Cartilage* 1998; 6: 306-317.
91. Bakker AC, van de Loo FA, van Beuningen HM, Sime P, van Lent PL, van der Kraan PM, et al. Overexpression of active TGF-beta-1 in the murine knee joint: evidence for synovial-layer-dependent chondro-osteophyte formation. *Osteoarthritis Cartilage* 2001; 9: 128-136.
 92. Vlodavsky I, Miao HQ, Medalion B, Danagher P, Ron D. Involvement of heparan sulfate and related molecules in sequestration and growth promoting activity of fibroblast growth factor. *Cancer Metastasis Rev* 1996; 15: 177-186.
 93. Whitelock JM, Melrose J, Iozzo RV. Diverse cell signaling events modulated by perlecan. *Biochemistry* 2008; 47: 11174-11183.
 94. Li S, Shimono C, Norioka N, Nakano I, Okubo T, Yagi Y, et al. Activin A binds to perlecan through its pro-region that has heparin/heparan sulfate binding activity. *J Biol Chem*; 285: 36645-36655.
 95. Ohkawara B, Iemura S, ten Dijke P, Ueno N. Action range of BMP is defined by its N-terminal basic amino acid core. *Curr Biol* 2002; 12: 205-209.
 96. Otto TC, Bowers RR, Lane MD. BMP-4 treatment of C3H10T1/2 stem cells blocks expression of MMP-3 and MMP-13. *Biochem Biophys Res Commun* 2007; 353: 1097-1104.
 97. Maroudas A, Palla G, Gilav E. Racemization of aspartic acid in human articular cartilage. *Connect Tissue Res* 1992; 28: 161-169.
 98. Lohmander LS, Englund PM, Dahl LL, Roos EM. The long-term consequence of anterior cruciate ligament and meniscus injuries: osteoarthritis. *Am J Sports Med* 2007; 35: 1756-1769.
 99. Hayami T, Pickarski M, Wesolowski GA, McLane J, Bone A, Destefano J, et al. The role of subchondral bone remodeling in osteoarthritis: reduction of cartilage degeneration and prevention of osteophyte formation by alendronate in the rat anterior cruciate ligament transection model. *Arthritis Rheum* 2004; 50: 1193-1206.
 100. Goldring MB, Goldring SR. Articular cartilage and subchondral bone in the pathogenesis of osteoarthritis. *Ann N Y Acad Sci* 2010; 1192: 230-237.
 101. Genetos DC, Geist DJ, Liu D, Donahue HJ, Duncan RL. Fluid shear-induced ATP secretion mediates prostaglandin release in MC3T3-E1 osteoblasts. *J Bone Miner Res* 2005; 20: 41-49.
 102. Chen CC, Lamping KG, Nuno DW, Barresi R, Prouty SJ, Lavoie JL, et al. Abnormal coronary function in mice deficient in alpha1H T-type Ca²⁺ channels. *Science* 2003; 302: 1416-1418.
 103. Shao Y, Alicknavitch M, Farach-Carson MC. Expression of voltage sensitive calcium channel (VSCC) L-type Cav1.2 (alpha1C) and T-type Cav3.2 (alpha1H) subunits during mouse bone development. *Dev Dyn* 2005; 234: 54-62.
 104. Catterall WA. Structure and function of voltage-gated ion channels. *Annu Rev Biochem* 1995; 64: 493-531.

105. Kronbergs A. T-TYPE CaV3.2 ($\alpha 1H$) VOLTAGE SENSITIVE CALCIUM CHANNEL DEFICIENCY NEGATIVELY IMPACTS SKELETAL PROPERTIES AND REDUCES BONE FORMATION IN A RODENT MODEL. *Biological Sciences*, vol. PhD. UMI Dissertation Publishing: University of Delaware 2011:226.
106. Huang L, Keyser BM, Tagmose TM, Hansen JB, Taylor JT, Zhuang H, et al. NNC 55-0396 [(1S,2S)-2-(2-(N-[(3-benzimidazol-2-yl)propyl]-N-methylamino)ethyl)-6-fluoro-1,2,3,4-tetrahydro-1-isopropyl-2-naphthyl cyclopropanecarboxylate dihydrochloride]: a new selective inhibitor of T-type calcium channels. *J Pharmacol Exp Ther* 2004; 309: 193-199.
107. Poulet B, Hamilton RW, Shefelbine S, Pitsillides AA. Characterizing a novel and adjustable noninvasive murine joint loading model. *Arthritis Rheum* 2011; 63: 137-147.
108. Herman BC, Cardoso L, Majeska RJ, Jepsen KJ, Schaffler MB. Activation of bone remodeling after fatigue: differential response to linear microcracks and diffuse damage. *Bone* 2010; 47: 766-772.
109. Kennedy OD, Herman BC, Laudier DM, Majeska RJ, Sun HB, Schaffler MB. Activation of resorption in fatigue-loaded bone involves both apoptosis and active pro-osteoclastogenic signaling by distinct osteocyte populations. *Bone* 2012; 50: 1115-1122.
110. Ko FC, Dragomir C, Plumb DA, Goldring SR, Wright TM, Goldring MB, et al. In vivo cyclic compression causes cartilage degeneration and subchondral bone changes in mouse tibiae. *Arthritis Rheum* 2013; 65: 1569-1578.
111. Robling AG, Turner CH. Mechanotransduction in bone: genetic effects on mechanosensitivity in mice. *Bone* 2002; 31: 562-569.
112. Srinivasan PP, McCoy SY, Jha AK, Yang W, Jia X, Farach-Carson MC, et al. Injectable perlecan domain 1-hyaluronan microgels potentiate the cartilage repair effect of BMP2 in a murine model of early osteoarthritis. *Biomed Mater* 2012; 7: 024109.
113. Zhou X, Liu D, You L, Wang L. Quantifying fluid shear stress in a rocking culture dish. *J Biomech* 2010; 43: 1598-1602.
114. McDonald JH. *Handbook of Biological Statistics*. <st1:city w:st="on"><st1:place w:st="on">Baltimore: Sparky House Publishing 2009.
115. Bergink AP, Uitterlinden AG, Van Leeuwen JP, Hofman A, Verhaar JA, Pols HA. Bone mineral density and vertebral fracture history are associated with incident and progressive radiographic knee osteoarthritis in elderly men and women: the Rotterdam Study. *Bone* 2005; 37: 446-456.
116. Radin EL, Rose RM. Role of subchondral bone in the initiation and progression of cartilage damage. *Clin Orthop Relat Res* 1986: 34-40.
117. Hunter DJ, Spector TD. The role of bone metabolism in osteoarthritis. *Curr Rheumatol Rep* 2003; 5: 15-19.

118. Ohba S, Lanigan TM, Roessler BJ. Leptin receptor JAK2/STAT3 signaling modulates expression of Frizzled receptors in articular chondrocytes. *Osteoarthritis Cartilage*; 18: 1620-1629.
119. Li J, Duncan RL, Burr DB, Turner CH. L-type calcium channels mediate mechanically induced bone formation in vivo. *J Bone Miner Res* 2002; 17: 1795-1800.
120. Duncan R, Misler S. Voltage-activated and stretch-activated Ba²⁺ conducting channels in an osteoblast-like cell line (UMR 106). *FEBS Lett* 1989; 251: 17-21.
121. Suzuki T, Notomi T, Miyajima D, Mizoguchi F, Hayata T, Nakamoto T, et al. Osteoblastic differentiation enhances expression of TRPV4 that is required for calcium oscillation induced by mechanical force. *Bone* 2013; 54: 172-178.
122. Muramatsu S, Wakabayashi M, Ohno T, Amano K, Ooishi R, Sugahara T, et al. Functional gene screening system identified TRPV4 as a regulator of chondrogenic differentiation. *J Biol Chem* 2007; 282: 32158-32167.
123. Abed E, Labelle D, Martineau C, Loghin A, Moreau R. Expression of transient receptor potential (TRP) channels in human and murine osteoblast-like cells. *Mol Membr Biol* 2009; 26: 146-158.
124. Krakow D, Vriens J, Camacho N, Luong P, Deixler H, Funari TL, et al. Mutations in the gene encoding the calcium-permeable ion channel TRPV4 produce spondylometaphyseal dysplasia, Kozlowski type and metatropic dysplasia. *Am J Hum Genet* 2009; 84: 307-315.
125. Phan MN, Leddy HA, Votta BJ, Kumar S, Levy DS, Lipshutz DB, et al. Functional characterization of TRPV4 as an osmotically sensitive ion channel in porcine articular chondrocytes. *Arthritis Rheum* 2009; 60: 3028-3037.
126. Clark AL, Votta BJ, Kumar S, Liedtke W, Guilak F. Chondroprotective role of the osmotically sensitive ion channel transient receptor potential vanilloid 4: age- and sex-dependent progression of osteoarthritis in Trpv4-deficient mice. *Arthritis Rheum* 2010; 62: 2973-2983.
127. Westacott C. Interactions between subchondral bone and cartilage in OA. Cells from osteoarthritic bone can alter cartilage metabolism. *J Musculoskelet Neuronal Interact* 2002; 2: 507-509.
128. Pan J, Wang B, Li W, Zhou X, Scherr T, Yang Y, et al. Elevated cross-talk between subchondral bone and cartilage in osteoarthritic joints. *Bone* 2011.
129. Truong LH, Kuliwaba JS, Tsangari H, Fazzalari NL. Differential gene expression of bone anabolic factors and trabecular bone architectural changes in the proximal femoral shaft of primary hip osteoarthritis patients. *Arthritis Res Ther* 2006; 8: R188.
130. Pavalko FM, Chen NX, Turner CH, Burr DB, Atkinson S, Hsieh YF, et al. Fluid shear-induced mechanical signaling in MC3T3-E1 osteoblasts requires cytoskeleton-integrin interactions. *Am J Physiol* 1998; 275: C1591-1601.

131. Alford AI, Jacobs CR, Donahue HJ. Oscillating fluid flow regulates gap junction communication in osteocytic MLO-Y4 cells by an ERK1/2 MAP kinase-dependent mechanism. *Bone* 2003; 33: 64-70.
132. Lu XL, Huo B, Chiang V, Guo XE. Osteocytic network is more responsive in calcium signaling than osteoblastic network under fluid flow. *J Bone Miner Res* 2012; 27: 563-574.
133. Pitsillides AA, Beier F. Cartilage biology in osteoarthritis--lessons from developmental biology. *Nat Rev Rheumatol* 2011; 7: 654-663.
134. D'Angelo M, Yan Z, Nooreyazdan M, Pacifici M, Sarment DS, Billings PC, et al. MMP-13 is induced during chondrocyte hypertrophy. *J Cell Biochem* 2000; 77: 678-693.
135. Todorovic SM, Jevtovic-Todorovic V. T-type voltage-gated calcium channels as targets for the development of novel pain therapies. *Br J Pharmacol* 2011; 163: 484-495.
136. Todorovic SM, Jevtovic-Todorovic V, Mennerick S, Perez-Reyes E, Zorumski CF. Ca(v)3.2 channel is a molecular substrate for inhibition of T-type calcium currents in rat sensory neurons by nitrous oxide. *Mol Pharmacol* 2001; 60: 603-610.
137. Choi S, Na HS, Kim J, Lee J, Lee S, Kim D, et al. Attenuated pain responses in mice lacking Ca(V)3.2 T-type channels. *Genes Brain Behav* 2007; 6: 425-431.
138. Issa SN, Sharma L. Epidemiology of osteoarthritis: an update. *Curr Rheumatol Rep* 2006; 8: 7-15.
139. Presle N, Pottie P, Dumond H, Guillaume C, Lopicque F, Pallu S, et al. Differential distribution of adipokines between serum and synovial fluid in patients with osteoarthritis. Contribution of joint tissues to their articular production. *Osteoarthritis Cartilage* 2006; 14: 690-695.
140. Houseknecht KL, Baile CA, Matteri RL, Spurlock ME. The biology of leptin: a review. *J Anim Sci* 1998; 76: 1405-1420.
141. Griffin TM, Huebner JL, Kraus VB, Guilak F. Extreme obesity due to impaired leptin signaling in mice does not cause knee osteoarthritis. *Arthritis Rheum* 2009; 60: 2935-2944.
142. Sandell LJ. Obesity and osteoarthritis: is leptin the link? *Arthritis Rheum* 2009; 60: 2858-2860.
143. Gabay O, Hall DJ, Berenbaum F, Henrotin Y, Sanchez C. Osteoarthritis and obesity: experimental models. *Joint Bone Spine* 2008; 75: 675-679.
144. Griffin TM, Guilak F. Why is obesity associated with osteoarthritis? Insights from mouse models of obesity. *Biorheology* 2008; 45: 387-398.
145. Cicuttini FM, Baker JR, Spector TD. The association of obesity with osteoarthritis of the hand and knee in women: a twin study. *J Rheumatol* 1996; 23: 1221-1226.
146. Bradley RL, Cleveland KA, Cheatham B. The adipocyte as a secretory organ: mechanisms of vesicle transport and secretory pathways. *Recent Prog Horm Res* 2001; 56: 329-358.

147. Mutabaruka MS, Aoulad Aissa M, Delalandre A, Lavigne M, Lajeunesse D. Local leptin production in osteoarthritis subchondral osteoblasts may be responsible for their abnormal phenotypic expression. *Arthritis Res Ther* 2010; 12: R20.
148. Pottie P, Presle N, Terlain B, Netter P, Mainard D, Berenbaum F. Obesity and osteoarthritis: more complex than predicted! *Ann Rheum Dis* 2006; 65: 1403-1405.
149. Kapur S, Amoui M, Kesavan C, Wang X, Mohan S, Baylink DJ, et al. Leptin receptor (*Lepr*) is a negative modulator of bone mechanosensitivity and genetic variations in *Lepr* may contribute to the differential osteogenic response to mechanical stimulation in the C57BL/6J and C3H/HeJ pair of mouse strains. *J Biol Chem* 2010; 285: 37607-37618.
150. Presle N, Pottie P, Dumond H, Guillaume C, Lopicque F, Pallu S, et al. Differential distribution of adipokines between serum and synovial fluid in patients with osteoarthritis. Contribution of joint tissues to their articular production. *Osteoarthritis Cartilage* 2006; 14: 690-695.
151. Dumond H, Presle N, Terlain B, Mainard D, Loeuille D, Netter P, et al. Evidence for a key role of leptin in osteoarthritis. *Arthritis Rheum* 2003; 48: 3118-3129.
152. Koskinen A, Vuolteenaho K, Nieminen R, Moilanen T, Moilanen E. Leptin enhances MMP-1, MMP-3 and MMP-13 production in human osteoarthritic cartilage and correlates with MMP-1 and MMP-3 in synovial fluid from OA patients. *Clin Exp Rheumatol* 2011; 29: 57-64.
153. Simopoulou T, Malizos KN, Iliopoulos D, Stefanou N, Papatheodorou L, Ioannou M, et al. Differential expression of leptin and leptin's receptor isoform (*Ob-Rb*) mRNA between advanced and minimally affected osteoarthritic cartilage; effect on cartilage metabolism. *Osteoarthritis Cartilage* 2007; 15: 872-883.
154. Ley K, Lundgren E, Berger E, Arfors KE. Shear-dependent inhibition of granulocyte adhesion to cultured endothelium by dextran sulfate. *Blood* 1989; 73: 1324-1330.
155. Worton LE, Ausk BJ, Downey LM, Bain SD, Gardiner EM, Srinivasan S, et al. Systems-based identification of temporal processing pathways during bone cell mechanotransduction. *PLoS One* 2013; 8: e74205.
156. Young SR, Hum JM, Rodenberg E, Turner CH, Pavalko FM. Non-overlapping functions for *Pyk2* and *FAK* in osteoblasts during fluid shear stress-induced mechanotransduction. *PLoS One* 2011; 6: e16026.
157. Glasson SS, Blanchet TJ, Morris EA. The surgical destabilization of the medial meniscus (DMM) model of osteoarthritis in the 129/SvEv mouse. *Osteoarthritis Cartilage* 2007; 15: 1061-1069.
158. Ma HL, Blanchet TJ, Peluso D, Hopkins B, Morris EA, Glasson SS. Osteoarthritis severity is sex dependent in a surgical mouse model. *Osteoarthritis Cartilage* 2007; 15: 695-700.

159. Teichtahl AJ, Wluka AE, Proietto J, Cicuttini FM. Obesity and the female sex, risk factors for knee osteoarthritis that may be attributable to systemic or local leptin biosynthesis and its cellular effects. *Med Hypotheses* 2005; 65: 312-315.
160. Gandhi R, Takahashi M, Smith H, Rizek R, Mahomed NN. The synovial fluid adiponectin-leptin ratio predicts pain with knee osteoarthritis. *Clin Rheumatol* 2010; 29: 1223-1228.
161. Ku JH, Lee CK, Joo BS, An BM, Choi SH, Wang TH, et al. Correlation of synovial fluid leptin concentrations with the severity of osteoarthritis. *Clin Rheumatol* 2009; 28: 1431-1435.
162. Otero M, Gomez Reino JJ, Gualillo O. Synergistic induction of nitric oxide synthase type II: in vitro effect of leptin and interferon-gamma in human chondrocytes and ATDC5 chondrogenic cells. *Arthritis Rheum* 2003; 48: 404-409.
163. Tong KM, Shieh DC, Chen CP, Tzeng CY, Wang SP, Huang KC, et al. Leptin induces IL-8 expression via leptin receptor, IRS-1, PI3K, Akt cascade and promotion of NF-kappaB/p300 binding in human synovial fibroblasts. *Cell Signal* 2008; 20: 1478-1488.
164. Otero M, Lago R, Gomez R, Dieguez C, Lago F, Gómez-Reino J, et al. Towards a pro-inflammatory and immunomodulatory emerging role of leptin. *Rheumatology (Oxford)* 2006; 45: 944-950.
165. Hui W, Litherland GJ, Elias MS, Kitson GI, Cawston TE, Rowan AD, et al. Leptin produced by joint white adipose tissue induces cartilage degradation via upregulation and activation of matrix metalloproteinases. *Ann Rheum Dis* 2012; 71: 455-462.
166. Srinivasan PP, McCoy SY, Jha AK, Yang W, Jia X, Farach-Carson MC, et al. Injectable perlecan domain 1-hyaluronan microgels potentiate the cartilage repair effect of BMP2 in a murine model of early osteoarthritis. *Biomed Mater* 2012; 7: 024109.
167. Tanamas SK, Wluka AE, Davies-Tuck M, Wang Y, Strauss BJ, Proietto J, et al. Association of weight gain with incident knee pain, stiffness, and functional difficulties: a longitudinal study. *Arthritis Care Res (Hoboken)* 2013; 65: 34-43.
168. Zhai G, Blizzard L, Srikanth V, Ding C, Cooley H, Cicuttini F, et al. Correlates of knee pain in older adults: Tasmanian Older Adult Cohort Study. *Arthritis Rheum* 2006; 55: 264-271.
169. McCoy SY, Falgowski KA, Srinivasan PP, Thompson WR, Selva EM, Kirn-Safran CB. Serum xylosyltransferase 1 level increases during early posttraumatic osteoarthritis in mice with high bone forming potential. *Bone* 2012; 51: 224-231.
170. van der Kraan PM, Buma P, van Kuppevelt T, van den Berg WB. Interaction of chondrocytes, extracellular matrix and growth factors: relevance for articular cartilage tissue engineering. *Osteoarthritis Cartilage* 2002; 10: 631-637.

171. Buchanan WW. William Hunter (1718–1783). vol. 42:1260–1: Rheumatology 2003.
172. Shi S, Mercer S, Eckert GJ, Trippel SB. Growth factor regulation of growth factors in articular chondrocytes. *J Biol Chem* 2009; 284: 6697-6704.
173. Sekiya I, Tang T, Hayashi M, Morito T, Ju YJ, Mochizuki T, et al. Periodic knee injections of BMP-7 delay cartilage degeneration induced by excessive running in rats. *J Orthop Res* 2009; 27: 1088-1092.
174. Hurtig M, Chubinskaya S, Dickey J, Rueger D. BMP-7 protects against progression of cartilage degeneration after impact injury. *J Orthop Res* 2009; 27: 602-611.
175. Buckwalter JA, Mankin HJ. Articular cartilage repair and transplantation. *Arthritis Rheum* 1998; 41: 1331-1342.
176. Gazzero E, Gangji V, Canalis E. Bone morphogenetic proteins induce the expression of noggin, which limits their activity in cultured rat osteoblasts. *J Clin Invest* 1998; 102: 2106-2114.
177. Pereira RC, Economides AN, Canalis E. Bone morphogenetic proteins induce gremlin, a protein that limits their activity in osteoblasts. *Endocrinology* 2000; 141: 4558-4563.
178. Sowers M. Epidemiology of risk factors for osteoarthritis: systemic factors. *Curr Opin Rheumatol* 2001; 13: 447-451.
179. Mesallati T, Buckley CT, Nagel T, Kelly DJ. Scaffold architecture determines chondrocyte response to externally applied dynamic compression. *Biomech Model Mechanobiol* 2013; 12: 889-899.
180. Zhu F, Wang P, Lee NH, Goldring MB, Konstantopoulos K. Prolonged application of high fluid shear to chondrocytes recapitulates gene expression profiles associated with osteoarthritis. *PLoS One* 2010; 5: e15174.
181. Kishida Y, Hirao M, Tamai N, Nampei A, Fujimoto T, Nakase T, et al. Leptin regulates chondrocyte differentiation and matrix maturation during endochondral ossification. *Bone* 2005; 37: 607-621.
182. Ioan-Facsinay A, Kloppenburg M. An emerging player in knee osteoarthritis: the infrapatellar fat pad. *Arthritis Res Ther* 2013; 15: 225.
183. Distel E, Cadoudal T, Durant S, Poignard A, Chevalier X, Benelli C. The infrapatellar fat pad in knee osteoarthritis: an important source of interleukin-6 and its soluble receptor. *Arthritis Rheum* 2009; 60: 3374-3377.
184. Mobasheri A, Lewis R, Maxwell JE, Hill C, Womack M, Barrett-Jolley R. Characterization of a stretch-activated potassium channel in chondrocytes. *J Cell Physiol* 2010; 223: 511-518.
185. Hamrick MW. Leptin, bone mass, and the thrifty phenotype. *J Bone Miner Res* 2004; 19: 1607-1611.
186. Steppan CM, Crawford DT, Chidsey-Frink KL, Ke H, Swick AG. Leptin is a potent stimulator of bone growth in ob/ob mice. *Regul Pept* 2000; 92: 73-78.

Appendix
PERMISSIONS

IOP Publishing



AUTHOR RIGHTS

Named Authors of subscription access Articles who submitted an *Assignment of copyright and publication agreement* (the Agreement) linking to this document after 1st June 2014 are granted, in addition to those rights set out in the Agreement, the following additional rights:

- The right to include the **Accepted Manuscript** on their personal website, immediately upon publication.
- Following the **Embargo Period**, the right to include the **Accepted Manuscript**, accompanied by a **statement of provenance**, on the website of their institution or employer.
- Following the **Embargo Period**, the right to include the **Accepted Manuscript**, accompanied by a **statement of provenance**, on non-commercial third party websites but not on the websites of other publishers.

Named Authors of Articles published in *Journal of Physics A*, *Journal of Physics G*, and *Classical and Quantum Gravity* **only** shall have the following right:

- The right, at any time, to include the **Accepted Manuscript** on arXiv.org subject to a nonexclusive, perpetual licence (the first option available on the submission page).

The terms used in this document shall, unless otherwise defined, have the meanings ascribed to them in the Agreement. The key definitions are as follows:

Accepted Manuscript	The author's own version of the Article, including changes made during the peer review process but excluding editing or typesetting by IOP and/or any relevant partner.
Embargo Period	A period of 12 months from the date of first online publication of the Article.
Statement of provenance	"This is an author-created, un-copyedited version of an article accepted for publication in [insert name of journal]. The publisher is not responsible for any errors or omissions in this version of the manuscript or any version derived from it. The Version of Record is available online at [insert DOI]."

Version of Record The final version of the Article, as published in the Journal.

In the case of any discrepancy between the definitions contained on this page and those in the Agreement, the definition in the Agreement will prevail.

If you have any questions about the content of this page, please contact permissions@iop.org.

These terms apply to articles submitted to *Nanotechnology* after 1st June 2014; to *J. Phys. A: Math. Theor.*, *J. Phys. B: At. Mol. Opt. Phys.*, *J. Phys.: Condens. Matter*, *J. Phys. D: Appl. Phys.*, *Smart Mater. Struct.*, *J. Micromech. Microeng.*, and *Meas. Sci. Technol.* after 1st July 2014; and to *2D Mater.*, *Biofabrication*, *Bioinspir. Biomim.*, *Biomed. Mater.*, *Class. Quantum Grav.*, *Comput. Sci. Disc.*, *Inverse Problems*, *J. Breath Res.*, *J. Neural Eng.*, *J. Opt.*, *J. Phys. G: Nucl. Part. Phys.*, *Mater. Res. Express*, *Methods Appl. Fluoresc.*, *Modelling Simul. Mater. Sci. Eng.*, *Phys. Biol.*, *Phys. Educ.*, *Plasma Phys. Control. Fusion*, *Plasma Sources Sci. Technol.*, *Semicond. Sci. Technol.*, *Surf. Topogr.: Metrol. Prop.*, *Supercond. Sci. Technol.* and *Transl. Mater. Res.* after 21st July 2014.

This page last updated July 2014

NATURE PUBLISHING GROUP LICENSE
TERMS AND CONDITIONS

Sep 10, 2014

This is a License Agreement between Padma Pradeepa Srinivasan ("You") and Nature Publishing Group ("Nature Publishing Group") provided by Copyright Clearance Center ("CCC"). The license consists of your order details, the terms and conditions provided by Nature Publishing Group, and the payment terms and conditions.

All payments must be made in full to CCC. For payment instructions, please see information listed at the bottom of this form.

License Number	3465521066774
License date	Sep 10, 2014
Licensed content publisher	Nature Publishing Group
Licensed content publication	Nature Reviews Rheumatology
Licensed content title	Technology Insight: adult stem cells in cartilage regeneration and tissue engineering
Licensed content author	Faye H Chen, Kathleen T Rousche and Rocky S Tuan
Licensed content date	Jul 1, 2006
Volume number	2
Issue number	7
Type of Use	reuse in a dissertation / thesis
Requestor type	academic/educational
Format	print and electronic
Portion	figures/tables/illustrations
Number of figures/tables/illustrations	1
High-res required	no
Figures	Figure 1 Extracellular matrix of cartilage
Author of this NPG article	no
Your reference number	None

Title of your thesis / dissertation	Novel Preclinical Targets and Therapies for Treatment of Osteoarthritis
Expected completion date	Jan 2015
Estimated size (number of pages)	180
Total	0.00 USD
Terms and Conditions	

Terms and Conditions for Permissions

Nature Publishing Group hereby grants you a non-exclusive license to reproduce this material for this purpose, and for no other use, subject to the conditions below:

1. NPG warrants that it has, to the best of its knowledge, the rights to license reuse of this material. However, you should ensure that the material you are requesting is original to Nature Publishing Group and does not carry the copyright of another entity (as credited in the published version). If the credit line on any part of the material you have requested indicates that it was reprinted or adapted by NPG with permission from another source, then you should also seek permission from that source to reuse the material.
2. Permission granted free of charge for material in print is also usually granted for any electronic version of that work, provided that the material is incidental to the work as a whole and that the electronic version is essentially equivalent to, or substitutes for, the print version. Where print permission has been granted for a fee, separate permission must be obtained for any additional, electronic reuse (unless, as in the case of a full paper, this has already been accounted for during your initial request in the calculation of a print run). NB: In all cases, web-based use of full-text articles must be authorized separately through the 'Use on a Web Site' option when requesting permission.
3. Permission granted for a first edition does not apply to second and subsequent editions and for editions in other languages (except for signatories to the STM Permissions Guidelines, or where the first edition permission was granted for free).
4. Nature Publishing Group's permission must be acknowledged next to the figure, table or abstract in print. In electronic form, this acknowledgement must be visible at the same time as the figure/table/abstract, and must be hyperlinked to the journal's homepage.

5. The credit line should read:

Reprinted by permission from Macmillan Publishers Ltd: [JOURNAL NAME] (reference citation), copyright (year of publication) For AOP papers, the credit line should read:

Reprinted by permission from Macmillan Publishers Ltd: [JOURNAL NAME], advance online publication, day month year (doi: 10.1038/sj.[JOURNAL ACRONYM].XXXXX)

Note: For republication from the British Journal of Cancer, the following credit lines apply.

Reprinted by permission from Macmillan Publishers Ltd on behalf of Cancer Research UK: [JOURNAL NAME] (reference citation), copyright (year of publication) For AOP papers, the credit line should read:

Reprinted by permission from Macmillan Publishers Ltd on behalf of Cancer Research UK:

[JOURNAL NAME], advance online publication, day month year (doi: 10.1038/sj.[JOURNAL ACRONYM].XXXXX)

6. Adaptations of single figures do not require NPG approval. However, the adaptation should be credited as follows:

Adapted by permission from Macmillan Publishers Ltd: [JOURNAL NAME] (reference citation), copyright (year of publication)

Note: For adaptation from the British Journal of Cancer, the following credit line applies.

Adapted by permission from Macmillan Publishers Ltd on behalf of Cancer Research UK: [JOURNAL NAME] (reference citation), copyright (year of publication)

7. Translations of 401 words up to a whole article require NPG approval. Please visit <http://www.macmillanmedicalcommunications.com> for more information. Translations of up to a 400 words do not require NPG approval.

The translation should be credited as follows:

Translated by permission from Macmillan Publishers Ltd: [JOURNAL NAME] (reference citation), copyright (year of publication).

Note: For translation from the British Journal of Cancer, the following credit line applies.

Translated by permission from Macmillan Publishers Ltd on behalf of Cancer Research UK:
[JOURNAL NAME] (reference citation), copyright (year of publication)

We are certain that all parties will benefit from this agreement and wish you the best in the use of this material. Thank you.

Special Terms:

v1.1

You will be invoiced within 48 hours of this transaction date. You may pay your invoice by credit card upon receipt of the invoice for this transaction. Please follow instructions provided at that time.

To pay for this transaction now; please remit a copy of this document along with your payment. Payment should be in the form of a check or money order referencing your account number and this invoice number RLNK501399640. Make payments to "COPYRIGHT CLEARANCE CENTER" and send to:

Copyright Clearance Center
Dept 001
P.O. Box 843006
Boston, MA 02284-3006

Please disregard electronic and mailed copies if you remit payment in advance.

Questions? customercare@copyright.com or +1-855-239-3415 (toll free in the US) or +1-978-646-2777.

Gratis licenses (referencing \$0 in the Total field) are free. Please retain this printable license for your reference. No payment is required.

ELSEVIER LICENSE
TERMS AND CONDITIONS

Sep 04, 2014

This is a License Agreement between Padma Pradeepa Srinivasan ("You") and Elsevier ("Elsevier") provided by Copyright Clearance Center ("CCC"). The license consists of your order details, the terms and conditions provided by Elsevier, and the payment terms and conditions.

All payments must be made in full to CCC. For payment instructions, please see information listed at the bottom of this form.

Supplier	Elsevier Limited The Boulevard, Langford Lane Kidlington, Oxford, OX5 1GB, UK
Registered Company Number	1982084
Customer name	Padma Pradeepa Srinivasan
Customer address	12 Meghan Lane BEAR, DE 19701
License number	3462000084158
License date	Sep 04, 2014
Licensed content publisher	Elsevier
Licensed content publication	Advanced Drug Delivery Reviews
Licensed content title	Collagens—major component of the physiological cartilage matrix, major target of cartilage degeneration, major tool in cartilage repair
Licensed content author	T Aigner, J Stöve
Licensed content date	28 November 2003
Licensed content volume number	55
Licensed content issue number	12
Number of pages	25
Start Page	1569
End Page	1593
Type of Use	reuse in a thesis/dissertation

Portion	figures/tables/illustrations
Number of figures/tables/illustrations	2
Format	both print and electronic
Are you the author of this Elsevier article?	No
Will you be translating?	No
Title of your thesis/dissertation	Novel Preclinical Targets and Therapies for Treatment of Osteoarthritis
Expected completion date	Jan 2015
Estimated size (number of pages)	180
Elsevier VAT number	GB 494 6272 12
Permissions price	0.00 USD
VAT/Local Sales Tax	0.00 USD / 0.00 GBP
Total	0.00 USD
Terms and Conditions	

INTRODUCTION

1. The publisher for this copyrighted material is Elsevier. By clicking "accept" in connection with completing this licensing transaction, you agree that the following terms and conditions apply to this transaction (along with the Billing and Payment terms and conditions established by Copyright Clearance Center, Inc. ("CCC"), at the time that you opened your Rightslink account and that are available at any time at <http://myaccount.copyright.com>).

GENERAL TERMS

2. Elsevier hereby grants you permission to reproduce the aforementioned material subject to the terms and conditions indicated.

3. Acknowledgement: If any part of the material to be used (for example, figures) has appeared in our publication with credit or acknowledgement to another source, permission must also be sought from that source. If such permission is not obtained then that material may not be included in your publication/copies. Suitable acknowledgement to the source must be made, either as a footnote or in a reference list at the end of your publication, as follows:

“Reprinted from Publication title, Vol /edition number, Author(s), Title of article / title of chapter, Pages No., Copyright (Year), with permission from Elsevier [OR APPLICABLE

SOCIETY COPYRIGHT OWNER].” Also Lancet special credit - “Reprinted from The Lancet, Vol. number, Author(s), Title of article, Pages No., Copyright (Year), with permission from Elsevier.”

4. Reproduction of this material is confined to the purpose and/or media for which permission is hereby given.
5. Altering/Modifying Material: Not Permitted. However figures and illustrations may be altered/adapted minimally to serve your work. Any other abbreviations, additions, deletions and/or any other alterations shall be made only with prior written authorization of Elsevier Ltd. (Please contact Elsevier at permissions@elsevier.com)
6. If the permission fee for the requested use of our material is waived in this instance, please be advised that your future requests for Elsevier materials may attract a fee.
7. Reservation of Rights: Publisher reserves all rights not specifically granted in the combination of (i) the license details provided by you and accepted in the course of this licensing transaction, (ii) these terms and conditions and (iii) CCC's Billing and Payment terms and conditions.
8. License Contingent Upon Payment: While you may exercise the rights licensed immediately upon issuance of the license at the end of the licensing process for the transaction, provided that you have disclosed complete and accurate details of your proposed use, no license is finally effective unless and until full payment is received from you (either by publisher or by CCC) as provided in CCC's Billing and Payment terms and conditions. If full payment is not received on a timely basis, then any license preliminarily granted shall be deemed automatically revoked and shall be void as if never granted. Further, in the event that you breach any of these terms and conditions or any of CCC's Billing and Payment terms and conditions, the license is automatically revoked and shall be void as if never granted. Use of materials as described in a revoked license, as well as any use of the materials beyond the scope of an unrevoked license, may constitute copyright infringement and publisher reserves the right to take any and all action to protect its copyright in the materials.
9. Warranties: Publisher makes no representations or warranties with respect to the licensed material.
10. Indemnity: You hereby indemnify and agree to hold harmless publisher and CCC, and their respective officers, directors, employees and agents, from and against any and all claims arising out of your use of the licensed material other than as specifically authorized pursuant to this license.

11. **No Transfer of License:** This license is personal to you and may not be sublicensed, assigned, or transferred by you to any other person without publisher's written permission.
12. **No Amendment Except in Writing:** This license may not be amended except in a writing signed by both parties (or, in the case of publisher, by CCC on publisher's behalf).
13. **Objection to Contrary Terms:** Publisher hereby objects to any terms contained in any purchase order, acknowledgment, check endorsement or other writing prepared by you, which terms are inconsistent with these terms and conditions or CCC's Billing and Payment terms and conditions. These terms and conditions, together with CCC's Billing and Payment terms and conditions (which are incorporated herein), comprise the entire agreement between you and publisher (and CCC) concerning this licensing transaction. In the event of any conflict between your obligations established by these terms and conditions and those established by CCC's Billing and Payment terms and conditions, these terms and conditions shall control.
14. **Revocation:** Elsevier or Copyright Clearance Center may deny the permissions described in this License at their sole discretion, for any reason or no reason, with a full refund payable to you. Notice of such denial will be made using the contact information provided by you. Failure to receive such notice will not alter or invalidate the denial. In no event will Elsevier or Copyright Clearance Center be responsible or liable for any costs, expenses or damage incurred by you as a result of a denial of your permission request, other than a refund of the amount(s) paid by you to Elsevier and/or Copyright Clearance Center for denied permissions.

LIMITED LICENSE

The following terms and conditions apply only to specific license types:

15. **Translation:** This permission is granted for non-exclusive world English rights only unless your license was granted for translation rights. If you licensed translation rights you may only translate this content into the languages you requested. A professional translator must perform all translations and reproduce the content word for word preserving the integrity of the article. If this license is to re-use 1 or 2 figures then permission is granted for non-exclusive world rights in all languages.
16. **Posting licensed content on any Website:** The following terms and conditions apply as follows: Licensing material from an Elsevier journal: All content posted to the web site must maintain the copyright information line on the bottom of each image; A hyper-text must be included to the Homepage of the journal from which you are licensing at <http://www.sciencedirect.com/science/journal/xxxxx> or the Elsevier homepage for books at <http://www.elsevier.com>; Central Storage: This license does not include

permission for a scanned version of the material to be stored in a central repository such as that provided by Heron/XanEdu.

Licensing material from an Elsevier book: A hyper-text link must be included to the Elsevier homepage at <http://www.elsevier.com> . All content posted to the web site must maintain the copyright information line on the bottom of each image.

Posting licensed content on Electronic reserve: In addition to the above the following clauses are applicable: The web site must be password-protected and made available only to bona fide students registered on a relevant course. This permission is granted for 1 year only. You may obtain a new license for future website posting.

For journal authors: the following clauses are applicable in addition to the above: Permission granted is limited to the author accepted manuscript version* of your paper.

*Accepted Author Manuscript (AAM) Definition: An accepted author manuscript (AAM) is the author's version of the manuscript of an article that has been accepted for publication and which may include any author-incorporated changes suggested through the processes of submission processing, peer review, and editor-author communications. AAMs do not include other publisher value-added contributions such as copy-editing, formatting, technical enhancements and (if relevant) pagination. You are not allowed to download and post the published journal article (whether PDF or HTML, proof or final version), nor may you scan the printed edition to create an electronic version. A hyper-text must be included to the Homepage of the journal from which you are licensing at <http://www.sciencedirect.com/science/journal/xxxxx>. As part of our normal production process, you will receive an e-mail notice when your article appears on Elsevier's online service ScienceDirect (www.sciencedirect.com). That e-mail will include the article's Digital Object Identifier (DOI). This number provides the electronic link to the published article and should be included in the posting of your personal version. We ask that you wait until you receive this e-mail and have the DOI to do any posting.

Posting to a repository: Authors may post their AAM immediately to their employer's institutional repository for internal use only and may make their manuscript publically available after the journal-specific embargo period has ended.

Please also refer to [Elsevier's Article Posting Policy](#) for further information.

18. For book authors the following clauses are applicable in addition to the above: Authors are permitted to place a brief summary of their work online only.. You are not allowed to download and post the published electronic version of your chapter, nor may you scan the printed edition to create an electronic version. Posting to a repository: Authors are permitted to post a summary of their chapter only in their institution's repository.

20. Thesis/Dissertation: If your license is for use in a thesis/dissertation your thesis may be submitted to your institution in either print or electronic form. Should your thesis be published commercially, please reapply for permission. These requirements include permission for the Library and Archives of Canada to supply single copies, on demand, of the complete thesis and include permission for UMI to supply single copies, on demand, of the complete thesis. Should your thesis be published commercially, please reapply for permission.

Elsevier Open Access Terms and Conditions

Elsevier publishes Open Access articles in both its Open Access journals and via its Open Access articles option in subscription journals.

Authors publishing in an Open Access journal or who choose to make their article Open Access in an Elsevier subscription journal select one of the following Creative Commons user licenses, which define how a reader may reuse their work: Creative Commons

Attribution License (CC BY), Creative Commons Attribution – Non Commercial ShareAlike (CC BY NC SA) and Creative Commons Attribution – Non Commercial – No Derivatives (CC BY NC ND)

Terms & Conditions applicable to all Elsevier Open Access articles:

Any reuse of the article must not represent the author as endorsing the adaptation of the article nor should the article be modified in such a way as to damage the author's honour or reputation.

The author(s) must be appropriately credited.

If any part of the material to be used (for example, figures) has appeared in our publication with credit or acknowledgement to another source it is the responsibility of the user to ensure their reuse complies with the terms and conditions determined by the rights holder.

Additional Terms & Conditions applicable to each Creative Commons user license:

CC BY: You may distribute and copy the article, create extracts, abstracts, and other revised versions, adaptations or derivative works of or from an article (such as a translation), to include in a collective work (such as an anthology), to text or data mine the article, including for commercial purposes without permission from Elsevier

CC BY NC SA: For non-commercial purposes you may distribute and copy the article, create extracts, abstracts and other revised versions, adaptations or derivative works of or from an article (such as a translation), to include in a collective work

(such as an anthology), to text and data mine the article and license new adaptations or creations under identical terms without permission from Elsevier

CC BY NC ND: For non-commercial purposes you may distribute and copy the article and include it in a collective work (such as an anthology), provided you do not alter or modify the article, without permission from Elsevier
Any commercial reuse of Open Access articles published with a CC BY NC SA or CC

BY NC ND license requires permission from Elsevier and will be subject to a fee.

Commercial reuse includes:

- Promotional purposes (advertising or marketing)
- Commercial exploitation (e.g. a product for sale or loan)
- Systematic distribution (for a fee or free of charge)

Please refer to [Elsevier's Open Access Policy](#) for further information.

21. Other Conditions:

v1.6

You will be invoiced within 48 hours of this transaction date. You may pay your invoice by credit card upon receipt of the invoice for this transaction. Please follow instructions provided at that time.

To pay for this transaction now; please remit a copy of this document along with your payment. Payment should be in the form of a check or money order referencing your account number and this invoice number RLNK501394675. Make payments to "COPYRIGHT CLEARANCE CENTER" and send to:

Copyright Clearance Center

Dept 001

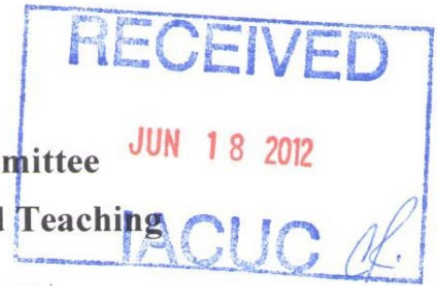
P.O. Box 843006

Boston, MA 02284-3006

Please disregard electronic and mailed copies if you remit payment in advance. Questions? customercare@copyright.com or +1-855-239-3415 (toll free in the US) or +1-978-646-2777.

Gratis licenses (referencing \$0 in the Total field) are free. Please retain this printable license for your reference. No payment is required.

**University of Delaware
Institutional Animal Care and Use Committee**
Application to Use Animals in Research and Teaching

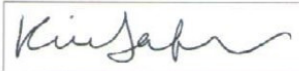


(Please complete below using Arial, size 12 Font.)

Title of Protocol: Transgenic Models of Skeletal and Metabolic Diseases	
AUP Number: 1204-2012-0	← (4 digits only — if new, leave blank)
Principal Investigator: Catherine B. Kirn-Safran	
Common Name: Mice	
Genus Species: Mus musculus	
Pain Category: (please mark one)	
USDA PAIN CATEGORY: (Note change of categories from previous form)	
Category	Description
<input type="checkbox"/> B	Breeding or holding where NO research is conducted
<input checked="" type="checkbox"/> C	Procedure involving momentary or no pain or distress
<input type="checkbox"/> D	Procedure where pain or distress is alleviated by appropriate means (analgesics, tranquilizers, euthanasia etc.)
<input type="checkbox"/> E	Procedure where pain or distress cannot be alleviated, as this would adversely affect the procedures, results or interpretation

Official Use Only	
IACUC Approval Signature:	
Date of Approval:	7/1/12

Principal Investigator Assurance

1. I agree to abide by all applicable federal, state, and local laws and regulations, and UD policies and procedures.
2. I understand that deviations from an approved protocol or violations of applicable policies, guidelines, or laws could result in immediate suspension of the protocol and may be reportable to the Office of Laboratory Animal Welfare (OLAW).
3. I understand that the Attending Veterinarian or his/her designee must be consulted in the planning of any research or procedural changes that may cause more than momentary or slight pain or distress to the animals.
4. I declare that all experiments involving live animals will be performed under my supervision or that of another qualified scientist. All listed personnel will be trained and certified in the proper humane methods of animal care and use prior to conducting experimentation.
5. I understand that emergency veterinary care will be administered to animals showing evidence of discomfort, ailment, or illness.
6. I declare that the information provided in this application is accurate to the best of my knowledge. If this project is funded by an extramural source, I certify that this application accurately reflects all currently planned procedures involving animals described in the proposal to the funding agency.
7. I assure that any modifications to the protocol will be submitted to by the UD-IACUC and I understand that they must be approved by the IACUC prior to initiation of such changes.
8. I understand that the approval of this project is for a maximum of one year from the date of UD-IACUC approval and that I must re-apply to continue the project beyond that period.
9. I understand that any unanticipated adverse events, morbidity, or mortality must be reported to the UD-IACUC immediately.
10. I assure that the experimental design has been developed with consideration of the three Rs: reduction, refinement, and replacement, to reduce animal pain and/or distress and the number of animals used in the laboratory.
11. I assure that the proposed research does not unnecessarily duplicate previous experiments. <i>(Teaching Protocols Exempt)</i>
12. I understand that by signing, I agree to these assurances.
<div style="display: flex; justify-content: space-between; align-items: center;"><div style="text-align: center;"> _____ Signature of Principal Investigator</div><div style="text-align: center;"><u>05-07-2012</u> _____ Date</div></div>

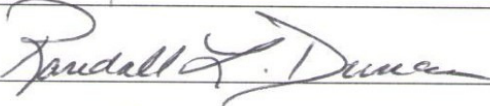
NAMES OF ALL PERSONS WORKING ON THIS PROTOCOL

I certify that I have read this protocol, accept my responsibility and will perform only those procedures that have been approved by the IACUC.

Name	Signature
1. Padma Pradeepa Srinivasan	
2. Randall L. Duncan	
3. Mary E. Boggs	
4.	
5.	
6.	
7.	
8.	
9.	
10.	
11.	
12.	
13.	
14.	

NAMES OF ALL PERSONS WORKING ON THIS PROTOCOL

I certify that I have read this protocol, accept my responsibility and will perform only those procedures that have been approved by the IACUC.

Name	Signature
1. Padma Pradeepa Srinivasan	
2. Randall L. Duncan	
3. Mary E. Boggs	
4.	
5.	
6.	
7.	
8.	
9.	
10.	
11.	
12.	
13.	
14.	

The Animal Use Protocol form has been developed to facilitate review of requests for specific research, teaching, or biological testing projects. The review process has been designed to communicate methods and materials for using animals through administrative officials and attending veterinarians to the Institutional Animal Care and Use Committee (IACUC). This process will help assure that provisions are made for compliance with the Animal Welfare Act, the Public Health Service Policy on Humane Care and Use of Laboratory Animals and the Guide for the Care and Use of Laboratory Animals.

Please read this form carefully and fill out all sections. Failure to do so may delay the review of this application. Sections that do not apply to your research must be marked “NA” for “Not Applicable.”

This application form must be used for all NEW or THREE-YEAR RENEWAL protocols.

All answers are to be completed using Arial 12 size font.

All questions must be answered in their respective boxes and NOT as attachments at the end of this form.

Please complete any relevant addenda:

Hybridoma/Monoclonal Antibodies (“B”)

Polyclonal Antibodies (“C”)

Survival Surgery (“D”)

Non-Survival Surgery (“E”)

Wildlife Research (“F”)

If help is needed with these forms, contact the IACUC Coordinator at extension 2616, the Facility Manager at extension 2400 or the Attending Veterinarian at extension 2980.

1. Principal Investigator Information:	
a. Name:	Catherine B. Kirn-Safran
b. University/Company:	University of Delaware
c. Department:	Biological Sciences
d. Building/Room:	Wolf 310
e. Office Phone:	302-831-3249
f. Lab Phone(s):	N/A
g. Home Phone:	302-836-4272
h. Mobile Phone:	302-981-8967
i. E-Mail Address:	ckirn@udel.edu
2. Protocol Status:	
a. <input type="checkbox"/> New Protocol OR × Re-submission due to three (3) completed years. If re-submission, enter Protocol Number: 1204	
b. × Research OR <input type="checkbox"/> Teaching	
c. × Laboratory Animals OR <input type="checkbox"/> Wildlife If "Wildlife" please complete Addendum "F"	
d. Proposed Start Date: July 22, 2012	
e. Proposed Completion Date: ongoing (standard breeding protocol)	
f. Funding Source: BISC322236 (no cost extension)	
g. Award Number: NIH COBRE P20RR016458	
3. Personnel involved in Protocol (Include Principal Investigator):	
Status: Indicate Prof, Post-Doc, Grad Student, Lab Manager, Research Assistant, Technician, etc.	

Qualifications: Include **procedures this person is proficient in performing** on proposed species and the time they have been doing the procedure.

Be specific (e.g. sub-mandibular bleeding on mice-2yrs, performing castrations on mice and rats-1yr, tail-vein injections on mice-2yrs, etc.) **(If no experience, list who will train.)**

Responsibilities: Include **all responsibilities** this person will have with live animals on this protocol, including euthanizing animals.

Name	E-mail	Office Phone Number	Home/Cell Phone Number	Received Animal Facility Training	
				Yes	No
a. Catherine Kirn-Safran	ckirn@udel.edu	302-831-3249	302-981-8967	×	

Status: Principal Investigator, faculty advisor, UD Research Assistant Professor Dept. Biological Sciences

Qualifications: Dr. Kirn-Safran has over 15 years of experience with mouse handling, breeding, and mineralized tissue collection for organ culture or histological processing; over 10 years with administration of hormones, drug, or anesthetic intraperitoneally, and 6 years with animal surgeries under anesthesia. Dr. Kirn-Safran has been studying effects of genetic mutations, growth factors, and hormones on bone/cartilage physiology and embryonic development in mouse models for over 15 years.

Responsibilities: Dr. Kirn-Safran will design, perform, and supervise personnel. Dr. Kirn-Safran will comply with any training program required by OLAM for her staff.

Name	E-mail	Office Phone Number	Home/Cell Phone Number	Received Animal Facility Training	
				Yes	No
b. Padma Srinivasan	padma@udel.edu	302-831-2017	716-568-7152 or 302-482-5558	×	

Status: Graduate Student Researcher

Qualifications: Three years experience with breeding animal mouse models of osteoarthritis and knee surgeries performing intra-articular knee injections and meniscus destabilization under anesthesia (isoflurane, AUP#1170). Ms. Srinivasan has experience sacrificing mice. **She will receive training from Jillian Hash to collect blood samples.**

Responsibilities: Padma will perform research studies under the supervision of Dr. Catherine Kirn-Safran. Padma will maintain/breed transgenic mouse lines (genotyping), sacrifice animals, collect blood ante-mortem, collect cells/tissue samples post-mortem.

Name	E-mail	Office Phone Number	Home/Cell Phone Number	Received Animal Facility Training	
				Yes	No
c. Randall L. Duncan	rlduncan@udel.edu	302-831-4296	(302) 379-8244	×	

Status: Faculty advisor, mentor, Professor and Chairman UD Dept. of Biological Sciences

Qualifications: Dr. Duncan has over 30 years experience working with animal models and over 17 years working with rat and mouse models. Experience over the past 30 years includes live animal survival surgery (nephrectomy), intraperitoneal or intravenous administration of drugs or anesthetics, mechanical loading experiments of both tibial four point bending and ulnar loading and animal sacrifice. Dr. Duncan has been studying the effects of mechanical loading and hormone regulation of bone/cartilage physiology in rodent models for over 17 years.

Responsibilities: Dr. Duncan will train his research staff for participation in these breeding procedures and co-supervise with Dr. Kirn-Safran personnel for completion of the proposed studies.

Name	E-mail	Office Phone Number	Home/Cell Phone Number	Received Animal Facility Training	
				Yes	No
d. Mary E. Boggs	mboggs@udel.edu	x3238	(302) 222-3269	×	

Status: Post-doctoral researcher, UD Research Associate.

Qualifications: Dr. Boggs has taken animal training and has 3 years of experience working with animals. Her animal work includes isolation of dorsal root ganglion from mice and rats following CO2 euthanasia (AUP# 1205). Dr. Boggs will receive training from Dr. Kirn-Safran on breeding procedures.

Responsibilities: Dr. Boggs will perform the breeding and genotyping according to the protocol, euthanize animals, and harvest tissue post-mortem.

4. Non-Scientific Summary: In language understandable to a *high-school senior, very briefly describe* the goals and significance of this study.

- a. Specific Scientific Goals: Maintenance and breeding of transgenic and control lines for *ex vivo* comparative studies. Most experiments will use tissues from sacrificed animals except when blood will be taken from live animals for biochemical assays. This project serves several projects in our laboratory that all look at various aspects of bone and

cartilage cell function. Perlecan/Hspg2 mutant (C1532Yneo line) mice are affected by a mild short stature and skeletal bone phenotype (Rodgers et al., 2007) and were obtained in the past through a collaboration with Dr. Kathryn Rodgers. Breeding pairs of the homozygous *Cacna1h* (calcium channel, voltage-dependent, T type, alpha 1H subunit; also called α_1 Cav3.2) targeted mutant mice were purchased from the Jackson Laboratory (Stock number: 013770) and bred in-house to establish a colony. They display a short stature phenotype and have mild cardiovascular defects (increased vasoconstriction of the vessels in the heart). These two mice lines and control C57BL6/J wild type mice are currently housed under AUP1204.

- b. Significance of this Research (including the possible benefits to human and/or animal health, the advancement of scientific knowledge, or the betterment of society): Establishment of mouse colonies to understand the molecular mechanisms leading to osteoporosis, osteoarthritis and other bone-related diseases for the discovery of novel therapeutics.

5. Experimental Design: Explain the experimental design. This description should allow the IACUC to understand fully the experimental course of an animal or group of animals from its entry into the experiment to the endpoint of the study.

The inclusion of flow charts, diagrams, and/or tables are greatly encouraged to explain experimental design or sequential events.

Be sure to include all animal events and related details, i.e.,

- **All Procedures**—bleedings, injections, surgical procedures, euthanasia, etc.
- **Procedural details**—number of animals involved in procedure, approximate animal weight, if relevant (for injections, bleeding, etc.), route, frequency, volume, etc.
- **Names of surgical procedures** (but reserve the surgical details for the proper Surgical Addenda)
- **Monitoring**—observations, measurements (animal weight, tumor size, etc)
- **Monitoring details**—criteria, frequency, names of personnel monitoring, conditions for removing an animal from the study, etc.
- **Endpoints**—include endpoints for the animals/study and how will they be determined.

(Describe):

- Design 1) Natural breeding** will be performed to maintain the perlecan (C1532Yneo) mutant and Cav3.2 knock-out lines on the C57BL6/J background and generate age-matched controls of the same background. The C1532Yneo line was created at the University of Pennsylvania and is not commercially available.
- Design 2) Tail biopsies** Genotypes of mutant mice will be determined by DNA analysis of tail tissue. Tail biopsies will be performed on mice at three weeks of age. Sampling will be done by OLAM staff according to SOP #PRO-001. If for any reason a second biopsy is required, it will be done under isoflurane anesthesia.
- Design 3) Dissection of embryonic, postnatal, and adult mouse bones and**

control organs. Mice will be euthanized by CO₂ asphyxiation followed by cervical dislocation to collect bone and other organs for macroscopic and microscopic analyses. Bone and control organs will be mostly collected after weaning age. Certain studies will require the use of embryonic and postnatal tissues. In this case, the female if still pregnant will be sacrificed prior to pup collection from the uterine horns. Embryos or pups (age ≤ 10 days) will be rapidly decapitated with sharp scissors in one stroke and their skull bones or long bones harvested for *in vitro* culture or specimen storage.

- iv. **Design 4) Collection of blood.** Blood will be collected from live animals after weaning age through retro-orbital route by OLAM staff. No more than 10% of the mouse body weight will be collected every other week according to the NIH guidelines for survival bleeding of mice:
http://oacu.od.nih.gov/ARAC/documents/Rodent_Bleeding.pdf

REFINEMENT, REDUCTION & REPLACEMENT

When using animals for research, it is important to consider the three Rs: reduction, refinement, and replacement to reduce both animal distress and the number of animals used in the laboratory.

Reduction: Minimizing the number of animals used

Refinement: Using techniques and procedures to reduce pain and distress

Replacement: Using non-animal methods or lower phylogenetic organisms

6. **Justification for the Use of Animals** (instead of *in vitro* methods)
(*Check all that apply and explain*):

a. The complexity of the processes being studied cannot be duplicated or modeled in simpler systems: (*Explain*): It is necessary to use animals because the tissue architecture of the bone and the organization of the different responsive cell types can only be found in animals not in dissociated cell cultures

b. There is not enough information known about the processes being studied to design non-living models: (*Explain*): The sequence of molecular events leading to osteoarthritis and osteoporosis are unknown and cannot be recapitulated in non-living systems.

c. Other: (*Explain*):

7. **Justification for Species Appropriateness:**

(Check all that apply and explain):

a. A large database exists, allowing comparisons with previous data: ***(Explain):***

b. The anatomy or physiology is uniquely suited to the study proposed: ***(Explain):***

c. This is the lowest species on the phylogenic scale suitable to the proposed study: ***(Explain):***
Mouse is the lowest phylogenic species that has bones similar to humans. Availability of transgenic lines in mice provides the opportunity to gain insight into the function of individual genes in bone and cartilage physiology.

d. Other: ***(Explain):***

8. Justification for Number of Animals Requested:

a. Pilot study or preliminary project where group variances are unknown at the present time. Describe the information used to estimate how many animals will be needed: (Only a limited number of animals will be permitted.)
(Explain):

b. Group sizes are determined statistically. Describe the statistical analysis used to estimate the number (N) of animals needed: N may be estimated from a power analysis for the most important measurement in the study, usually based on the expected size of the treatment effect, the standard error associated with the measurement, and the desired statistical power (e.g. $P < 0.05$). Data analysis methods should not be submitted unless directly applicable to the estimate of N.

*An online calculator may be found at: <http://www.math.uiowa.edu/~rlenth/Power/>
or a stand-alone calculator that can be downloaded from
<http://www.psych.uni-duesseldorf.de/abteilungen/aap/gpower3>*

(Explain):

c. Group sizes are based on the quantity of harvested cells or the amount of tissue required for *in vitro* studies. Explain how much tissue is needed based on the number of experiments to be conducted and the amount of tissue you expect to obtain from each animal (e.g., 10g of tissues are needed: Each animal can provide 2g. $10g / 2g \text{ per animal} = 5 \text{ animals needed.}$)
(Explain):

d. Teaching protocol. Specify the number of students in the class, the student to animal ratio and how that ratio was determined: Animal numbers should be minimized to the fullest extent possible without compromising the quality of the hands-on teaching experience for students or the health and welfare of the animals. (*Explain*):

e. Study involving feral or wild animals. Animals will be captured and released in an attempt to maximize the sample size within logistical constraints. Describe the process by which you estimate these numbers and estimate the precision needed: (*Explain*):

f. Observational, non-manipulative study. Animals will not be captured, their behavior will not be interfered with, and exact animal numbers cannot be predicted: (*Explain*):

g. Product testing. The number of animals needed is based on FDA guidelines. Provide the citation from the regulations, the IND tracking number, or relevant FDA correspondence: (*Explain*):

h. × Other. Elaborate, indicating the method used to determine the group size. (*Explain*):
Mice of the C57BL6/J inbred strains will be used to generate perlecan mutant, Cav3.2 knock-out and control bone/cartilage specimens. Thus, at all time we will maintain sexually mature mutant animals of each line. The C1532Yneo line is not commercially available and the Cav3.2 knockout line is classified as a low demand strain by the Jackson Laboratory and each purchase is considered a custom order (\$172.00/individual animal). Thus, both lines have to be bred in-house. After six months, breeding pairs are retired and replaced by new breeders.
C1532Yneo line: This line can be maintained through homozygous breeding and will be used to analyze the molecular mechanisms involved in perlecan function as a modulator of heterotopic calcification. Bone progenitor cell lines will be generated from newborn and adult tissues post-mortem.
An average of 3 stud males and 15 breeding females will be maintained year round. The average litter size for this strain is small (approximately 5 pups/litter) and will require a large number of pregnancies to obtain a reasonable amount of bone specimens. Since we will replace animals after six months, we will need 6 males and 30 females for breeding purpose to generate embryonic and postnatal tissue for cell isolation. In summary, we will need $36 \times 3 \text{ year} = 108$ **animals** over the 3-year period for the C1532Yneo line.

Cav3.2 knockout line: This line will be used to generate bone cell lines to analyze their responsiveness to mechanical stress. Additionally, we plan to test the hypothesis that deletion of this Ca²⁺ channel is chondroprotective for cartilage progression and need to generate 2.5 month-old animals for a study proposed under a pending NIH proposal using our AUP1170 knee surgery protocol. This experiments will require 48 mutant males (24 animals at two time points) as delineated in Table 1.

2.5 month-old mice; 4 wks post-knee surgery								2.5 month-old mice; 8 wks post-knee surgery							
WT (n=24)				KO (n=24)				WT (n=24)				KO (n=24)			
Surgery (n=12♂)		Sham (n=12♂)		Surgery (n=12♂)		Sham (n=12♂)		Surgery (n=12♂)		Sham (n=12♂)		Surgery (n=12♂)		Sham (n=12♂)	
OA score,IIF (n=6)	Histomorph. (n=6)	OA score,IIF (n=6)	Histomorph. (n=6)	OA score,IIF (n=6)	Histomorph. (n=6)	OA score,IIF (n=6)	Histomorph. (n=6)	OA score,IIF (n=6)	Histomorph. (n=6)	OA score,IIF (n=6)	Histomorph. (n=6)	OA score,IIF (n=6)	Histomorph. (n=6)	OA score,IIF (n=6)	Histomorph. (n=6)

Table 1: Groups for *in vivo* experimental knee osteoarthritis (OA) studies under AUP1170 IIF, immunohistochemistry. Previous experiments performed in our laboratory determined that a sample size of 6 is appropriate to determine changes in articular cartilage architecture via histological scoring (Srinivasan et al., 2012).

The Cav3.2 line may be maintained through homozygous breeding. We observed, however, a 50% rate of perinatal death due to subfertility in Cav3.2^{-/-} females as a result of short stature and cardiovascular defects. Hence, this line will require maintenance either through the breeding of Cav3.2 knockout male to heterozygous females or through fostering of Cav3.2 null pups with C57BL6/J control females. An average of 5 stud males and 20 breeding females will be maintained year round. Since we will replace breeders after six months, we will need 10 males and 40 females/year for breeding purpose and approximately 50 mutant males for experimental osteoarthritis experiments. In summary, we will need 50×3 years + 50 male=**200 animals** for the 3-year period for the Cav3.2 knockout line.

C57BL6/J controls: An average of 2 stud males and 6 breeding females will be maintained year round. Since we will replace breeders after six months, we will need 4 males and 12 females/year for fostering purpose. In summary, we will need 16×3 years=**48 animals** for the 3-year period for the C57BL6/J control line.

**Total number of animals requested for the 3-year period is:
108+200+48=356 animals**

Reference:

Srinivasan PP, McCoy SY, Jha AK, Yang W, Jia X, Farach-Carson MC, and Kirn-Safran CB. Injectable perlecan domain 1-hyaluronan microgels potentiate the cartilage repair effect of BMP2 in a murine model of early osteoarthritis. Biomed Mater. 2012 Mar 29;7(2):024109.

9. Animals Requested:

Common Name	Genus and Species	Total Number of Animals for Three Years
1. Mouse	Mus musculus	356
2.		
3.		
4.		
5.		

10. Where will animals be housed (or captured for wildlife)?

OLAM

11. Where will the experiments take place?

Wolf Hall room 334 and OLAM

12. Will any animals be humanely killed, without treatment or manipulations, to be used to obtain tissue, cells, etc.? Yes No

If Yes, list types of tissue, etc: Calvaria and limbs for newborn and embryos. Spleen and long bones for adult animals.

13. Physiological Measurements Yes No

If Yes, list and explain:

<p>14. Dietary Manipulations <input type="checkbox"/> Yes <input checked="" type="checkbox"/> No</p> <p>If Yes, list and explain:</p>
<p>15. Environmental Stress (e.g. cold, restraint, forced exercise) <input type="checkbox"/> Yes <input checked="" type="checkbox"/> No</p> <p>If Yes, list and explain:</p>
<p>16. Trauma or Burn Injury <input type="checkbox"/> Yes <input checked="" type="checkbox"/> No</p> <p>If Yes, list and explain:</p>
<p>17. Production of Hybridoma/Monoclonal Antibodies <input type="checkbox"/> Yes <input checked="" type="checkbox"/> No</p> <p>If Yes, please complete Addendum "B".</p>
<p>18. Production of Polyclonal Antibodies <input type="checkbox"/> Yes <input checked="" type="checkbox"/> No</p> <p>If Yes, please complete Addendum "C".</p>
<p>19. Study of the effects of drugs or toxins <i>in vivo</i> <input type="checkbox"/> Yes <input checked="" type="checkbox"/> No</p> <p>If Yes, list and explain:</p>
<p>20. Administration of hazardous or biological materials (e.g. pathogens, carcinogens, radioactive materials) <input type="checkbox"/> Yes <input checked="" type="checkbox"/> No</p> <p>a. Type to be used:</p>
<p>b. Describe the practices and procedures for the handling and disposal of contaminated materials associated with this study:</p> <p><i>(For radioactive materials, include the methods for removal of radioactive wastes and monitoring for radioactivity, if applicable.)</i></p>
<p>c. Approval received from UD- Environmental Health and Safety? <input type="checkbox"/> Yes <input type="checkbox"/> No</p>
<p>21. Study of Irradiation <i>in vivo</i>? <input type="checkbox"/> Yes <input checked="" type="checkbox"/> No</p> <p>a. Type to be used:</p>

b. Approval received from UD- Environmental Health and Safety? Yes No

22. Any other procedures? Yes No
If Yes, explain:

23. Will this study involve surgery? Yes No
If Yes, and it is "Survival Surgery," please complete Addendum "D".
If Yes, and it is "Terminal Surgery," please complete Addendum "E".

24. Will any animal undergo anesthesia for any reason other than surgery? Yes No
If Yes,
a. List Procedures and Reason(s) for using anesthesia:
If tail biopsy has to be repeated
b. Check the type of anesthesia to be used.
 Isoflurane
 Injectable (*For injectable, complete the following*):

Drug:
Dose:
Route:

25. **Animal Use and Pain Distress.** If you have indicated that **animals in your study will experience pain or distress**, even if it will be fully alleviated, please mark the appropriate check boxes below and fill in the requested information for each item marked.

You must conduct at least two (2) searches.

I have considered alternatives to the use of animals in my study. Alternatives refer to methods or approaches which result in refinement of procedures which lessen pain and/or distress; reduction in numbers of animals required; or replacement of animals with non-whole-animal systems or replacement of one animal species with another, particularly if the substituted species is non-mammalian or invertebrate. I have used the following methods and sources to search for alternatives:

Note: You may need to do more than one search per database to look for alternatives if there are multiple procedures that may cause pain and/or distress.

Database Used:
 Medline Agricola

<input type="checkbox"/> Toxline	<input type="checkbox"/> CAB Abstracts
<input type="checkbox"/> Biosis	<input type="checkbox"/> Other (Specify):
Date of Search:	
Years Covered:	
Keywords Used (must include the word <i>alternative</i>):	
Number of Papers Found:	
Discussion of the Relevancy of the Papers Found:	

Database Used:	
<input type="checkbox"/> Medline	<input type="checkbox"/> Agricola
<input type="checkbox"/> Toxline	<input type="checkbox"/> CAB Abstracts
<input type="checkbox"/> Biosis	<input type="checkbox"/> Other (Specify):
Date of Search:	
Years Covered:	
Keywords Used (must include the word <i>alternative</i>):	
Number of Papers Found:	
Discussion of the Relevancy of the Papers Found:	

26. Unnecessary Duplication of Work. Activities involving animals must not unnecessarily duplicate previous experiments performed by you or others. Provide a written narrative that assures that the activities of this project comply with this requirement and support this assurance by performing a literature search.

The search should return, at minimum, the related previous work from your laboratory.

You must conduct at least two (2) searches.

(NOT REQUIRED FOR TEACHING PROTOCOLS)

Note: You may need to do more than one search per database to look for duplication of work, especially if you are doing more than one experiment.

Database Used:	
<input checked="" type="checkbox"/> Medline	<input type="checkbox"/> Agricola
<input type="checkbox"/> Toxline	<input type="checkbox"/> CAB Abstracts
<input type="checkbox"/> Biosis	<input type="checkbox"/> Other (Specify):
Date of Search: 5/08/12	
Years Covered: unrestricted	

Keywords Used: Search #1:Cav 3.2 and bone

Search #2: Hspg2 and bone

Number of Papers Found: Search #1: no hit; Search #2 :5 hits

Discussion of the Relevancy of the Papers Found:

Search #1 N/A

Search #2: one paper is from our collaborator Dr. Rodgers who donated the mouse line; three papers are from our group and one paper studies the effect of prolactin (a protein produced during pregnancy) on the expression of Hspg2 in an established clonal cell line (ATDC5) different from the primary cell culture system proposed in our studies.

Database Used:

Medline

Agricola

Toxline

CAB Abstracts

Biosis

Other (*Specify*):

Date of Search: 5/08/12

Years Covered: unrestricted

Keywords Used: Search #1:Cav 3.2 and bone: 2 hits

Search #2: Hspg2 and bone: 4 hits

Number of Papers Found:

Discussion of the Relevancy of the Papers Found:

Search #1: The first paper tests the effect of an anticonvulsant drug in mice overexpressing a protein involved in bone resorbing cell activity and demonstrated that topical application of this drug may help reduce bone loss via Cav3.2 calcium channel. This paper shows that Cav3.2 channel activity can affect the differentiation of bone resorbing cell progenitors in the bone marrow. This studies differs from our study since it focuses on the function of Cav3.2 in bone resorbing cells rather than bone forming cells. The second paper is from our group and published the initial observation of the expression of Cav3.2 by terminally differentiated bone cells.

Search #2: Paper 1 describes the lethal phenotype of mice in which Hspg2 is totally absent. The mouse model used in our study is viable because small amounts of Hspg2 are expressed. Paper 2 is a paper describing expression of all heparan sulfate proteoglycans in rat bone and is not targeting Hspg2 which is the molecule of interest for part of the studies described under this protocol. Paper 3&4 are entirely unrelated to Hspg2 function in bone.

27. What is the expected disposition of animals at the end of the experiments?

(Check all that apply):

Euthanized

Maintained

Released (*Wildlife Only*)

Other (*Specify*):

28. Euthanasia*

Select methods that will be used in case of emergency and/or at the end of the procedure/experiment.

***NOTE:**

- Methods must be approved by the AVMA or must be scientifically justified.
- A “Primary” and “Secondary” method must be selected (UD Double Kill Policy).
- **If different methods will be used for different groups** of animals, indicate the group after the procedure (e.g., write “Neonates” after Decapitation, “Adults” after CO₂, “Terminal Surgery Animals” after Isoflurane Anesthesia Overdose, etc.).

Animals will NOT be under anesthesia when euthanasia is performed.

Animals will be under anesthesia when euthanasia is performed. (*Check drug used below*):

Isoflurane

Injectable (*Complete the following*):

Drug:

Dose:

Route:

PRIMARY method(s) of euthanasia

CO₂ by compressed gas cylinder (*Not for animals already under anesthesia or neonates*)

Barbiturate Euthanasia Solution - Injectable $\geq 150\text{mg/kg}$ (*Check route below*):

IV

IP

IC

Isoflurane Anesthesia Overdose - Inhalant

Cervical Dislocation (*only under anesthesia*)

Decapitation (*only under anesthesia or neonates*)

Exsanguination or Perfusion (*only under anesthesia*)

Incision of Chest Cavity – Bilateral Pneumothorax (*only under anesthesia*)

Pithing – Double pithing required (*fish, amphibians, reptiles only*)

Thoracic Compression (*small birds only*)

**University of Delaware
Institutional Animal Care and Use Committee
Annual Review**



(Please complete below using Arial, size 12 Font.)

Title of Protocol: Transgenic Models of Skeletal and Metabolic Diseases	
AUP Number: 1204-2014-1	← (4 digits only)
Principal Investigator: Catherine B. Kirn-Safran	
Common Name: Mice	
Genus Species: Mus musculus	
Pain Category: <i>(please mark one)</i>	
USDA PAIN CATEGORY: <i>(Note change of categories from previous form)</i>	
Category	Description
<input type="checkbox"/> B	Breeding or holding where NO research is conducted
× C	Procedure involving momentary or no pain or distress
<input type="checkbox"/> D	Procedure where pain or distress is alleviated by appropriate means (analgesics, tranquilizers, euthanasia etc.)
<input type="checkbox"/> E	Procedure where pain or distress cannot be alleviated, as this would adversely affect the procedures, results or interpretation

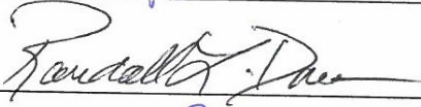
Official Use Only	
IACUC Approval Signature:	
Date of Approval:	

Principal Investigator Assurance

1. I agree to abide by all applicable federal, state, and local laws and regulations, and UD policies and procedures.	
2. I understand that deviations from an approved protocol or violations of applicable policies, guidelines, or laws could result in immediate suspension of the protocol and may be reportable to the Office of Laboratory Animal Welfare (OLAW).	
3. I understand that the Attending Veterinarian or his/her designee must be consulted in the planning of any research or procedural changes that may cause more than momentary or slight pain or distress to the animals.	
4. I declare that all experiments involving live animals will be performed under my supervision or that of another qualified scientist listed on this AUP. All listed personnel will be trained and certified in the proper humane methods of animal care and use prior to conducting experimentation.	
5. I understand that emergency veterinary care will be administered to animals showing evidence of discomfort, ailment, or illness.	
6. I declare that the information provided in this application is accurate to the best of my knowledge. If this project is funded by an extramural source, I certify that this application accurately reflects all currently planned procedures involving animals described in the proposal to the funding agency.	
7. I assure that any modifications to the protocol will be submitted to the UD-IACUC and I understand that they must be approved by the IACUC prior to initiation of such changes.	
8. I understand that the approval of this project is for a maximum of one year from the date of UD-IACUC approval and that I must re-apply to continue the project beyond that period.	
9. I understand that any unanticipated adverse events, morbidity, or mortality must be reported to the UD-IACUC immediately.	
10. I assure that the experimental design has been developed with consideration of the three Rs: reduction, refinement, and replacement, to reduce animal pain and/or distress and the number of animals used in the laboratory.	
11. I assure that the proposed research does not unnecessarily duplicate previous experiments. <i>(Teaching Protocols Exempt)</i>	
12. I understand that by signing, I agree to these assurances.	
 <hr style="width: 40%; margin-left: 0;"/>	<u>05/03/10</u> Date
Signature of Principal Investigator	

SIGNATURE(S) OF ALL PERSONS LISTED ON THIS PROTOCOL

I certify that I have read this protocol, accept my responsibility and will perform only the procedures that have been approved by the IACUC.

Name	Signature
1. Catherine Kirn-Safran	
2. Padma Pradeepa Srinivasan	
3. Randall L. Duncan	
4. Mary E. Boggs	
5.	
6.	
7.	
8.	
9.	
10.	
11.	
12.	
13.	
14.	
15.	

IACUC approval of animal protocols must be renewed on an annual basis.

1. Previous Approval Date: 7/01/12

Is Funding Source the same as on original, approved AUP?

Yes No

If no, please state Funding Source and Award Number: NIH COBRE
P30GM103333 (no cost extension)

2. Record of Animal Use:

Common Name	Genus Species	Total Number Previously Approved	Number Used To Date
1. Mouse	Mus musculus	356	24
2.			
3.			
4.			
5.			

3. Protocol Status: *(Please indicate by check mark the status of project.)*

Request for Protocol Continuance:

- A. Active: Project ongoing
- B. Currently inactive: Project was initiated but is presently inactive
- C. Inactive: Project never initiated but anticipated starting date is:

Request for Protocol Termination:

- D. Inactive: Project never initiated
- E. Completed: No further activities with animals will be done.

4. Project Personnel: Have there been any personnel changes since the last IACUC approval? Yes No

If Yes, fill out the Amendment to Add/Delete Personnel form to "Add" Personnel.

Project Personnel Deletions:

Name	Effective Date
1.	
2.	

5. Progress Report: If the status of this project is 3.A or 3.B, please provide a brief update on the progress made in achieving the aims of the protocol.

This protocol is a maintenance and breeding of transgenic and control lines for ex-vivo comparative studies and for in vivo studies approved under AUP1170. This protocol serves several project in our laboratory that all look at various aspects of bone and cartilage function. Currently, we are housing three lines:

- 1) The Hspg2 mutant (C1532Yneo) line obtained from Dr. Rodgers
- 2) The T-VSCC knock-out line purchased from the Jackson Lab (Stock#013770)
- 3) The C57BL6/J line purchased from the Jackson Lab (Stock#000664)

6. Problems or Adverse Effects: If the status of this project is 3.A or 3.B, please describe any unanticipated adverse events, morbidity, or mortality, the cause if known, and how these problems were resolved. If there were none, this should be indicated.

No problems or adverse effects were observed to this date.

<input type="checkbox"/> Removal of Vital Organ(s) (<i>only under anesthesia</i>) (<i>Check all that apply</i>): <table style="margin-left: 20px; width: 80%;"> <tr> <td><input type="checkbox"/> Brain</td> <td><input type="checkbox"/> Kidneys</td> </tr> <tr> <td><input type="checkbox"/> Heart</td> <td><input type="checkbox"/> GI Tract</td> </tr> <tr> <td><input type="checkbox"/> Liver</td> <td><input type="checkbox"/> Lungs</td> </tr> <tr> <td colspan="2"><input type="checkbox"/> Other Vital Organ(s) – (<i>Specify</i>):</td> </tr> </table>	<input type="checkbox"/> Brain	<input type="checkbox"/> Kidneys	<input type="checkbox"/> Heart	<input type="checkbox"/> GI Tract	<input type="checkbox"/> Liver	<input type="checkbox"/> Lungs	<input type="checkbox"/> Other Vital Organ(s) – (<i>Specify</i>):	
<input type="checkbox"/> Brain	<input type="checkbox"/> Kidneys							
<input type="checkbox"/> Heart	<input type="checkbox"/> GI Tract							
<input type="checkbox"/> Liver	<input type="checkbox"/> Lungs							
<input type="checkbox"/> Other Vital Organ(s) – (<i>Specify</i>):								
<input type="checkbox"/> Other Method of Euthanasia: (<i>Describe and Scientifically Justify</i>):								
SECONDARY method(s) of euthanasia that will be used to ensure that the animal does not survive:								
<input checked="" type="checkbox"/> Cervical Dislocation								
<input type="checkbox"/> Decapitation								
<input type="checkbox"/> Exsanguination or Perfusion								
<input type="checkbox"/> Incision of Chest Cavity – Bilateral Pneumothorax								
<input type="checkbox"/> Barbiturate Euthanasia Solution - Injectable $\geq 150\text{mg/kg}$ (<i>Check route below</i>): <table style="margin-left: 20px; width: 80%;"> <tr> <td><input type="checkbox"/> IV</td> <td><input type="checkbox"/> IP</td> <td><input type="checkbox"/> IC</td> </tr> </table>	<input type="checkbox"/> IV	<input type="checkbox"/> IP	<input type="checkbox"/> IC					
<input type="checkbox"/> IV	<input type="checkbox"/> IP	<input type="checkbox"/> IC						
<input type="checkbox"/> Pithing – Double pithing required (<i>fish, amphibians, reptiles only</i>)								
<input type="checkbox"/> Removal of Vital Organ(s): (<i>Check all that apply</i>): <table style="margin-left: 20px; width: 80%;"> <tr> <td><input type="checkbox"/> Brain</td> <td><input type="checkbox"/> Kidneys</td> </tr> <tr> <td><input type="checkbox"/> Heart</td> <td><input type="checkbox"/> GI Tract</td> </tr> <tr> <td><input type="checkbox"/> Liver</td> <td><input type="checkbox"/> Lungs</td> </tr> <tr> <td colspan="2"><input type="checkbox"/> Other Vital Organ(s) – (<i>Specify</i>):</td> </tr> </table>	<input type="checkbox"/> Brain	<input type="checkbox"/> Kidneys	<input type="checkbox"/> Heart	<input type="checkbox"/> GI Tract	<input type="checkbox"/> Liver	<input type="checkbox"/> Lungs	<input type="checkbox"/> Other Vital Organ(s) – (<i>Specify</i>):	
<input type="checkbox"/> Brain	<input type="checkbox"/> Kidneys							
<input type="checkbox"/> Heart	<input type="checkbox"/> GI Tract							
<input type="checkbox"/> Liver	<input type="checkbox"/> Lungs							
<input type="checkbox"/> Other Vital Organ(s) – (<i>Specify</i>):								
<input type="checkbox"/> Other Method of Euthanasia: (<i>Describe and Scientifically Justify</i>):								